

## Technical Report Documentation Page

**1. REPORT No.**

FHWA/CA/TL-84/10

**2. GOVERNMENT ACCESSION No.****3. RECIPIENT'S CATALOG No.****4. TITLE AND SUBTITLE**

Dynamic Approach to Embankment Construction Control

**5. REPORT DATE**

June 1984

**6. PERFORMING ORGANIZATION****7. AUTHOR(S)**

John Vrymoed

**8. PERFORMING ORGANIZATION REPORT No.**

57322-632304

**9. PERFORMING ORGANIZATION NAME AND ADDRESS**

Office of Transportation Laboratory  
California Department of Transportation  
Sacramento, California 95819

**10. WORK UNIT No.****11. CONTRACT OR GRANT No.**

F72322-632304

**12. SPONSORING AGENCY NAME AND ADDRESS**

California Department of Transportation  
Sacramento, California 95807

**13. TYPE OF REPORT & PERIOD COVERED**

Final

**14. SPONSORING AGENCY CODE****15. SUPPLEMENTARY NOTES**

This study was conducted in cooperation with the U.S. Department of Transportation, Federal Highway Administration.

**16. ABSTRACT**

A research proposal was written in March 1972 to investigate a dynamic approach to embankment compaction control. The research objective was to determine a soil's elastic parameters by geophysical means and incorporate these parameters in a static finite element analysis. The information gained from this could then lead to an understanding of embankment performance relative to the measured elastic parameters. The research was not completed due to higher priority assignments.

The information contained in this report puts the concepts stated in the research proposal in perspective with the current state of the art in geotechnical engineering. The results of a finite element analysis are reported relating embank stresses and movements to compactive effort and moisture content. Conclusions and recommendations are made regarding further research in the area of compaction and embankment performance.

**17. KEYWORDS**

Embankment, compaction, finite element, stresses, movements, shear modulus, shear wave velocity, compressional wave velocity

**18. No. OF PAGES:**

198

**19. DRI WEBSITE LINK**

<http://www.dot.ca.gov/hq/research/researchreports/1981-1988/84-10.pdf>

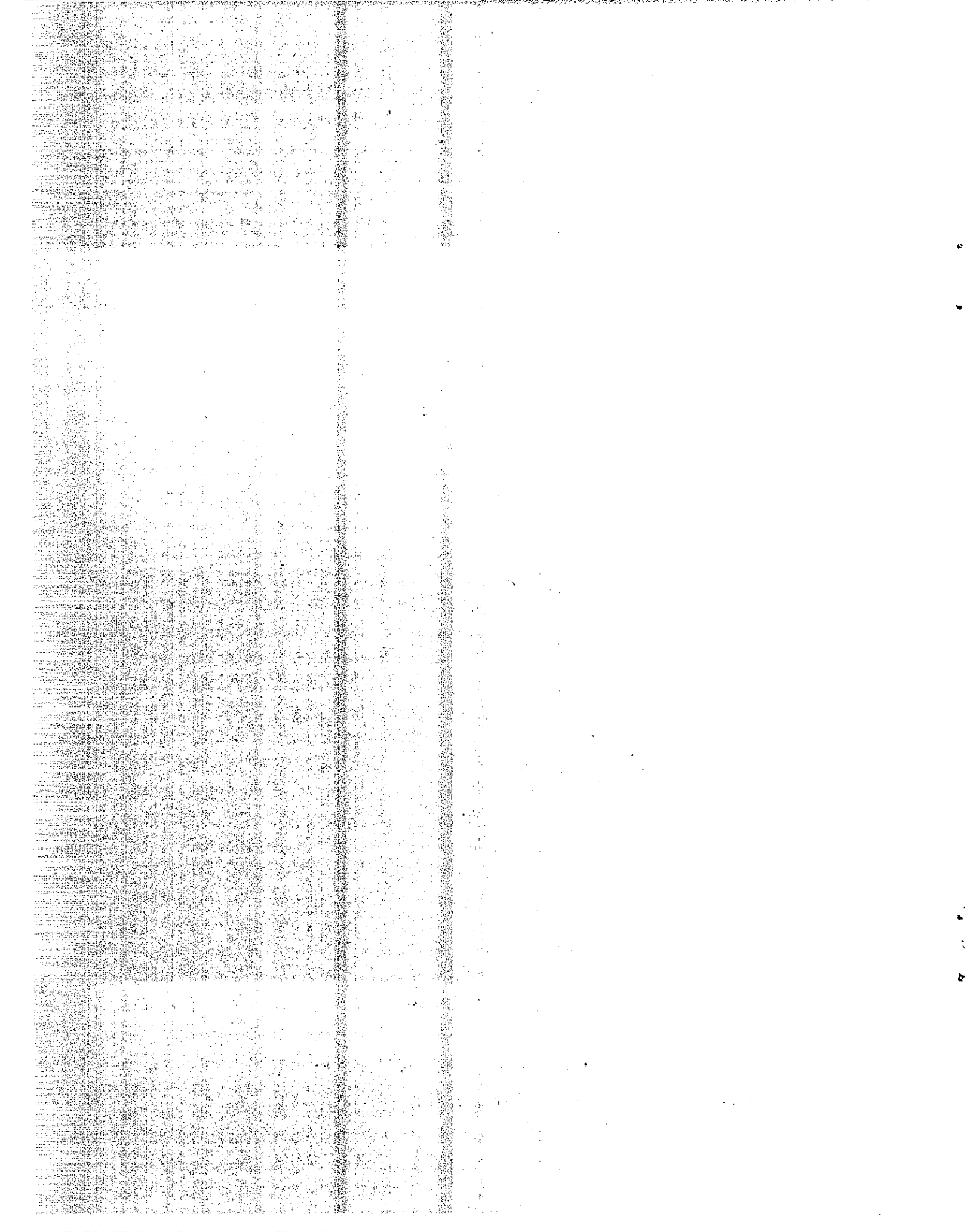
**20. FILE NAME**

84-10.pdf

**TRANSPORTATION  
LABORATORY**

**Dynamic Approach  
to Embankment  
Construction Control**

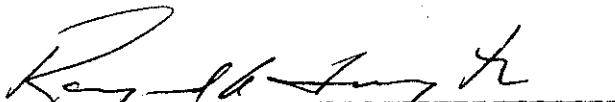
***ET Caltrans***



STATE OF CALIFORNIA  
DEPARTMENT OF TRANSPORTATION  
DIVISION OF ENGINEERING SERVICES  
OFFICE OF TRANSPORTATION LABORATORY

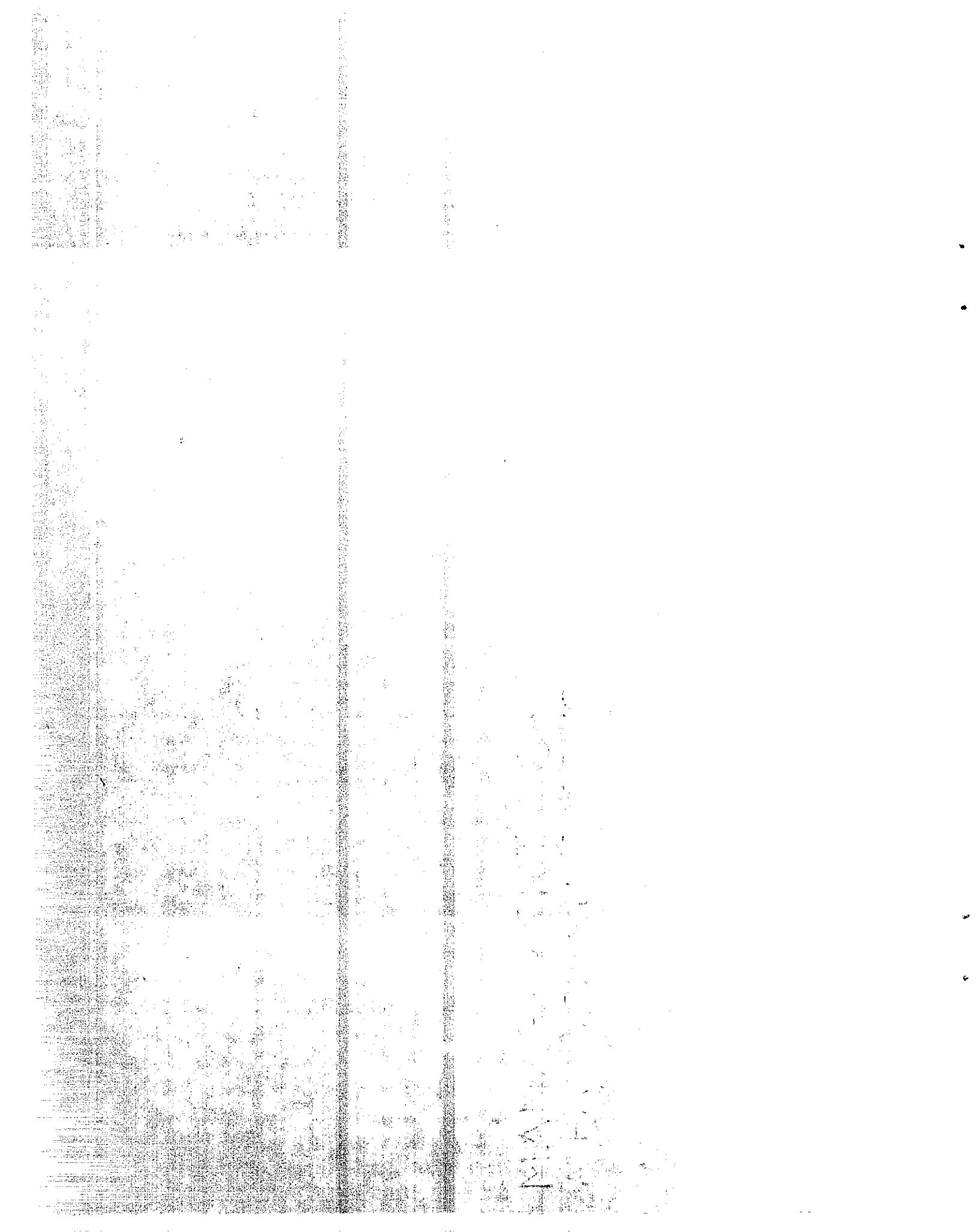
DYNAMIC APPROACH TO EMBANKMENT  
CONSTRUCTION CONTROL

Study Supervised by ..... Raymond A. Forsyth, P.E.  
Principal Investigator ..... John Vrymoed, P.E.  
Co-Investigator ..... Jerry Chang, P.E.  
Report Prepared by ..... John Vrymoed, P.E.



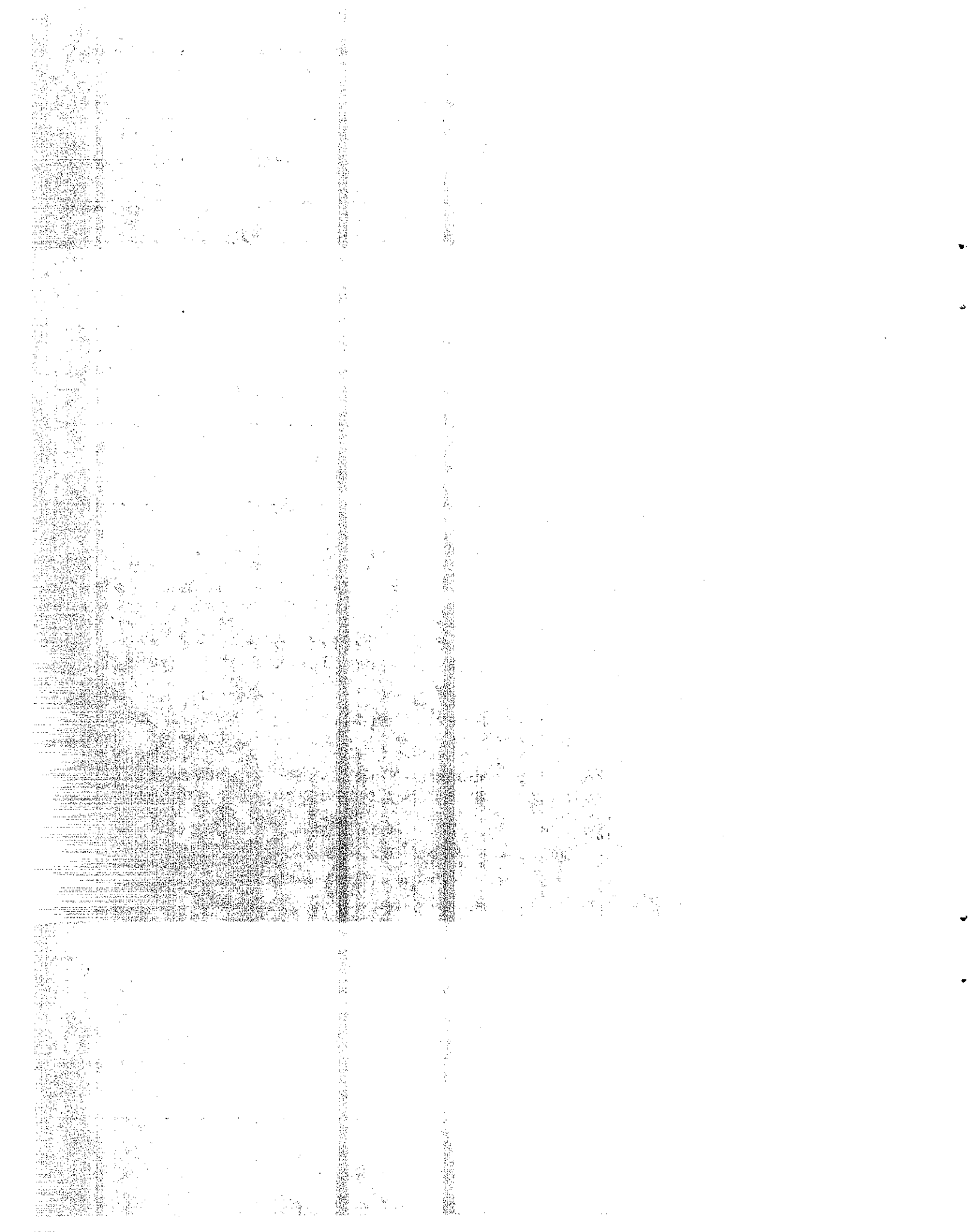
RAYMOND A. FORSYTH, P.E.

Chief, Office of Transportation Laboratory



TECHNICAL REPORT STANDARD TITLE PAGE

1. REPORT NO FHWA/CA/TL-84/10		2. GOVERNMENT ACCESSION NO.		3. RECIPIENT'S CATALOG NO.	
4. TITLE AND SUBTITLE DYNAMIC APPROACH TO EMBANKMENT CONSTRUCTION CONTROL				5. REPORT DATE June 1984	
				6. PERFORMING ORGANIZATION CODE	
7. AUTHOR(S) John Vrymoed				8. PERFORMING ORGANIZATION REPORT NO. 57322-632304	
9. PERFORMING ORGANIZATION NAME AND ADDRESS Office of Transportation Laboratory California Department of Transportation Sacramento, California 95819				10. WORK UNIT NO.	
				11. CONTRACT OR GRANT NO. F72TL11	
12. SPONSORING AGENCY NAME AND ADDRESS California Department of Transportation Sacramento, California 95807				13. TYPE OF REPORT & PERIOD COVERED Final	
				14. SPONSORING AGENCY CODE	
15. SUPPLEMENTARY NOTES This study was conducted in cooperation with the U.S. Department of Transportation, Federal Highway Administration.					
16. ABSTRACT <p>A research proposal was written in March 1972 to investigate a dynamic approach to embankment compaction control. The research objective was to determine a soil's elastic parameters by geophysical means and incorporate these parameters in a static finite element analysis. The information gained from this could then lead to an understanding of embankment performance relative to the measured elastic parameters. The research was not completed due to higher priority assignments.</p> <p>The information contained in this report puts the concepts stated in the research proposal in perspective with the current state of the art in geotechnical engineering. The results of a finite element analysis are reported relating embankment stresses and movements to compactive effort and moisture content. Conclusions and recommendations are made regarding further research in the area of compaction and embankment performance.</p>					
17. KEY WORDS Embankment, compaction, finite element, stresses, movements, shear modulus, shear wave velocity, compressional wave velocity.				18. DISTRIBUTION STATEMENT No restrictions. This document is available to the public through the National Technical Information Service, Springfield, VA 22161.	
19. SECURITY CLASSIF. (OF THIS REPORT) Unclassified		20. SECURITY CLASSIF. (OF THIS PAGE) Unclassified		21. NO. OF PAGES	
				22. PRICE	



## NOTICE

The contents of this report reflect the views of the Office of Transportation Laboratory which is responsible for the facts and the accuracy of the data presented herein. The contents do not necessarily reflect the official views or policies of the State of California or the Federal Highway Administration. This report does not constitute a standard, specification, or regulation.

Neither the State of California nor the United States Government endorse products or manufacturers. Trade or manufacturers' names appear herein only because they are considered essential to the object of this document.

5

4

CONVERSION FACTORS

English to Metric System (SI) of Measurement

Quantity	English unit	Multiply by	To get metric equivalent
Length	inches (in) or (")	25.40 .02540	millimetres (mm) metres (m)
	feet (ft) or (')	.3048	metres (m)
	miles (mi)	1.609	kilometres (km)
Area	square inches (in <sup>2</sup> )	6.432 x 10 <sup>-4</sup>	square metres (m <sup>2</sup> )
	square feet (ft <sup>2</sup> )	.09290	square metres (m <sup>2</sup> )
	acres	.4047	hectares (ha)
Volume	gallons (gal)	3.785	litres (l)
	cubic feet (ft <sup>3</sup> )	.02832	cubic metres (m <sup>3</sup> )
	cubic yards (yd <sup>3</sup> )	.7646	cubic metres (m <sup>3</sup> )
Volume/Time (Flow)	cubic feet per second (ft <sup>3</sup> /s)	28.317	litres per second (l/s)
	gallons per minute (gal/min)	.06309	litres per second (l/s)
Mass	pounds (lb)	.4536	kilograms (kg)
Velocity	miles per hour (mph)	.4470	metres per second (m/s)
	feet per second (fps)	.3048	metres per second (m/s)
Acceleration	feet per second squared (ft/s <sup>2</sup> )	.3048	metres per second squared (m/s <sup>2</sup> )
	acceleration due to force of gravity (G)	9.807	metres per second squared (m/s <sup>2</sup> )
Weight Density	pounds per cubic (lb/ft <sup>3</sup> )	16.02	kilograms per cubic metre (kg/m <sup>3</sup> )
Force	pounds (lbs)	4.448	newtons (N)
	kips (1000 lbs)	4448	newtons (N)
Thermal Energy	British thermal unit (BTU)	1055	joules (J)
Mechanical Energy	foot-pounds (ft-lb)	1.356	joules (J)
	foot-kips (ft-k)	1356	joules (J)
Bending Moment or Torque	inch-pounds (ft-lbs)	.1130	newton-metres (Nm)
	foot-pounds (ft-lbs)	1.356	newton-metres (Nm)
Pressure	pounds per square inch (psi)	6895	pascals (Pa)
	pounds per square foot (psf)	47.88	pascals (Pa)
Stress Intensity	kips per square inch square root inch (ksi √in)	1.0988	mega pascals √metre (MPa √m)
	pounds per square inch square root inch (psi √in)	1.0988	kilo pascals √metre (KPa √m)
Plane Angle	degrees (°)	0.0175	radians (rad)
Temperature	degrees fahrenheit (F)	$\frac{tF - 32}{1.8} = tC$	degrees celsius (°C)



## TABLE OF CONTENTS

	<u>Page</u>
INTRODUCTION	1
RESEARCH PROPOSAL	3
SCOPE OF THIS REPORT	5
COMPACTION CORRELATED WITH SURFACE GEO- PHYSICAL MEANS	7
EMBANKMENT PERFORMANCE PREDICTED BY THE FINITE ELEMENT METHOD	18
USAGE OF ELASTIC MODULUS AT $10^{-4}$ PERCENT STRAIN	30
EFFECTS OF VARIATION IN MOISTURE CONTENT AND COMPACTIVE EFFORT ON EMBANKMENT STRESSES AND MOVEMENTS	35
SUMMARY AND CONCLUSIONS	53
RECOMMENDATIONS FOR FUTURE STUDY	55
REFERENCES	56
APPENDICES	60

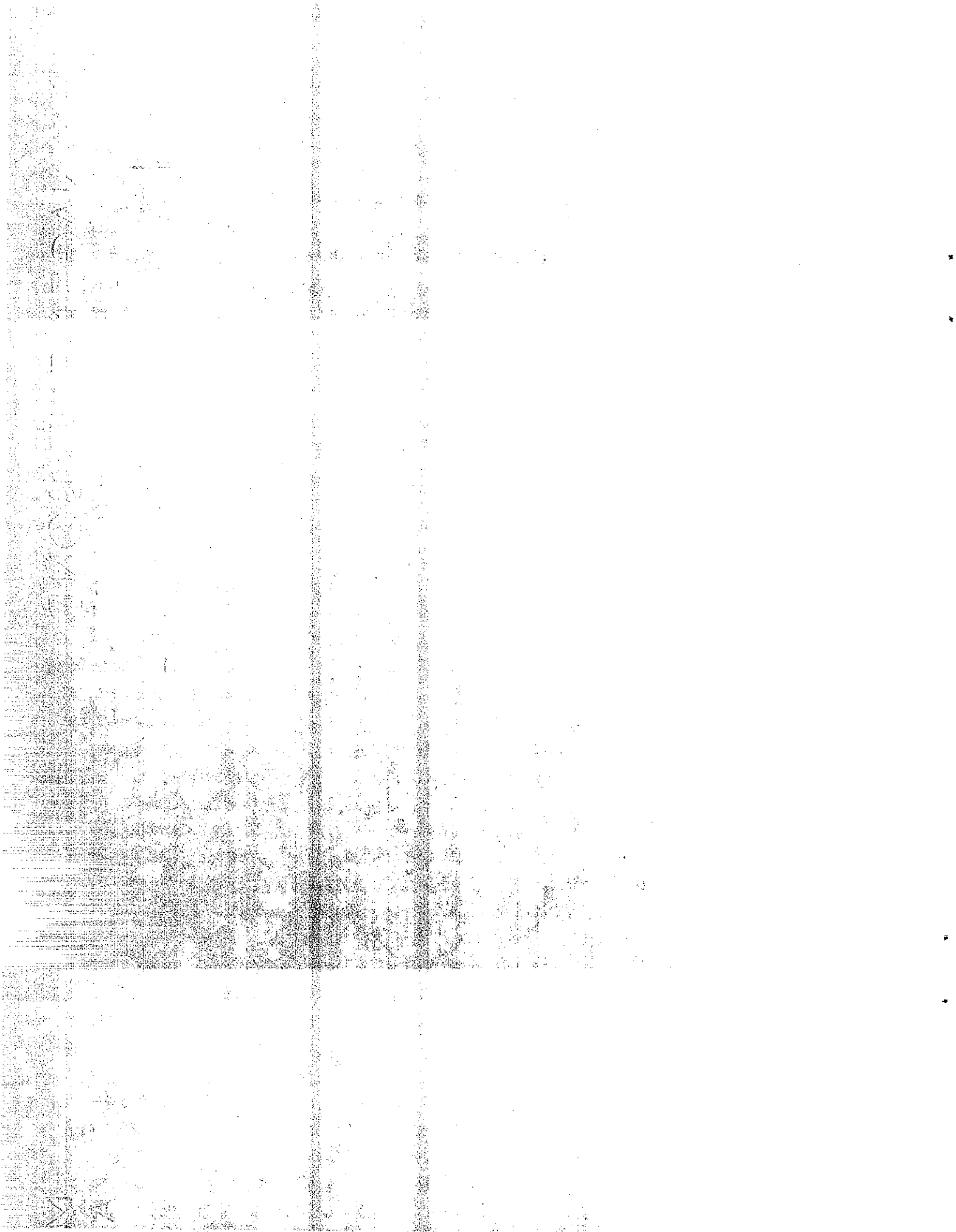
1950

1950

1950

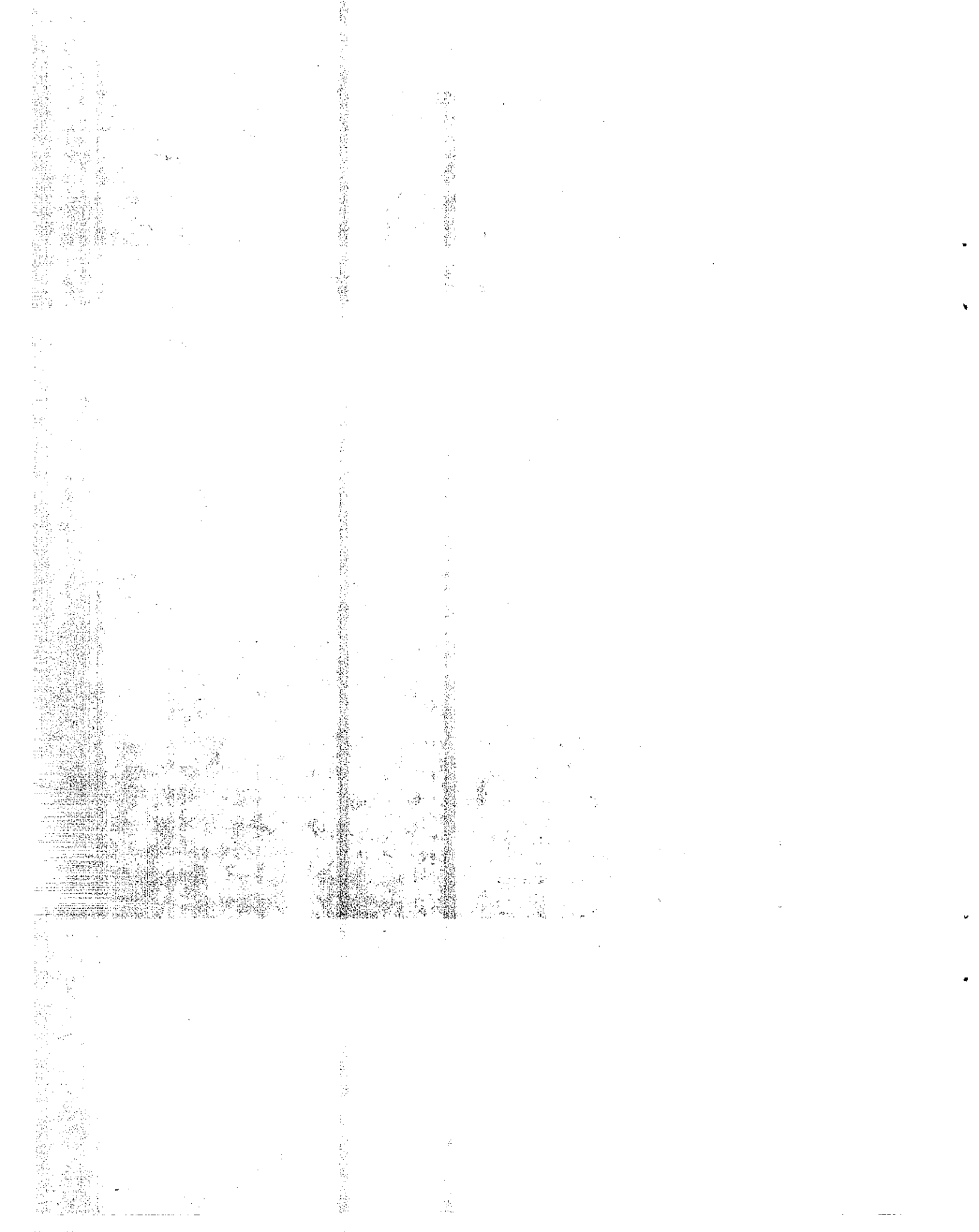
## LIST OF TABLES

<u>Table No.</u>	<u>Title</u>	<u>Page</u>
1	Gradation, Class 4 Aggregate Subbase (Type I)	10
2	Quality, Class 4 Aggregate Subbase (Type I)	11
3	Values of Stress-Strain Parameters for Analysis of Oroville Dam	19
4	Static Stress Comparison	26
5	Comparison of Elastic Moduli	34
6	Hyperbolic Stress-Strain Parameters	39
7	Maximum Vertical Movements	50
8	Maximum Lateral Movements	51
9	Minimum Factors of Safety	49



## LIST OF FIGURES

<u>Figure No.</u>	<u>Title</u>	<u>Page</u>
1	Resonant Footing Apparatus	9
2	MD-1 Seismic Equipment	13
3	Relation of Seismic Wave Velocity (compression) to Density of Compacted Soil Layers	14
4	Oroville Dam Maximum Section	20
5	Horizontal Displacements at Elevation 355 in Oroville Dam	22
6	Horizontal Displacements at Elevation 540 in Oroville Dam	23
7	Crossarm Settlements in Oroville Dam	24
8	Osito Canyon Embankment	27
9	No Name Canyon Embankment	28
10	San Luis Reservoir Embankment	29
11	Behavior of Shear Modulus with Shear Strain	30
12	Initial Elastic Modulus	32
13	FEM Mesh Used in Analyses	36
14	Moisture-Density Relationship for Compacted Pittsburg Sandy Clay	37
15	Strength Parameters For Compacted Pittsburg Sandy Clay Tested Under UU Test Conditions	40
16	Modulus Parameters For Compacted Pittsburg Sandy Clay Tested Under UU Test Conditions	41



LIST OF FIGURES (Continued)

<u>Figure No.</u>	<u>Title</u>	<u>Page</u>
17	Poisson's Ratio Parameters for Compacted Pittsburg Sandy Clay Tested Under UU Test Conditions	42
18	Vertical Stress at Midheight of 100 ft Embankment, 1.5:1 Slopes	43
19	Lateral Stress at Midheight of 100 ft Embankment, 1.5:1 Slopes	44
20	Horizontal Shear Stress at Midheight of 100 ft Embankment, 1.5:1 Slopes	45
21	Horizontal Movements, 100 ft Embankment 1.5:1 Slopes	47
22	Vertical Movements, 100 ft Embankment 1.5:1 Slopes	48

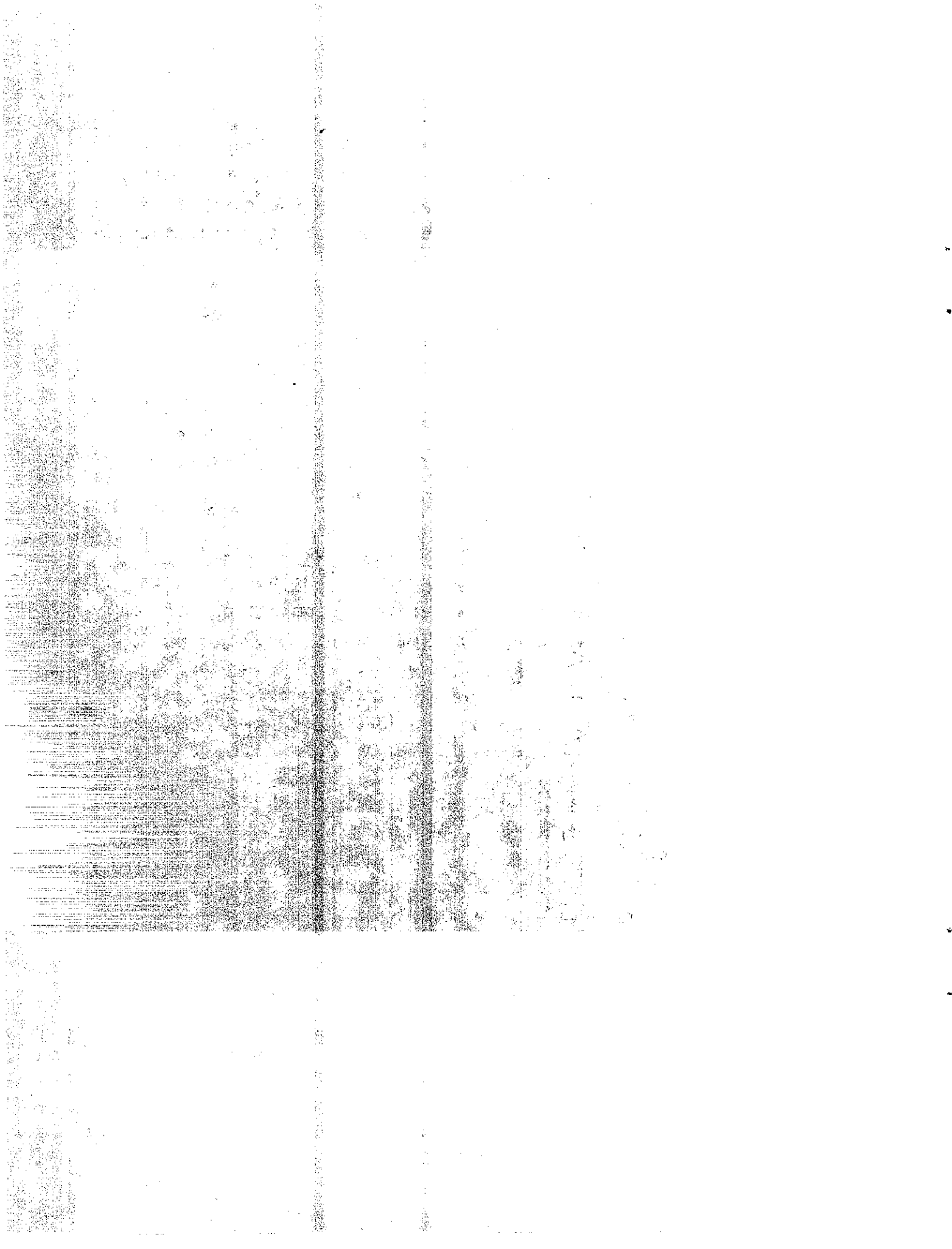
THE STEINER ENDORSE  
MILK MILLS PRODUCT

## IMPLEMENTATION

This report presents a method whereby the required level of compaction for an embankment can be evaluated. This method can now be implemented and possibly reduce the cost of placement of fill by requiring less compactive effort than the compactive effort mentioned in standard specifications.

The method demonstrated in this report considered only one soil type and four embankment geometries. An appropriate and safe level of compaction for a highway embankment can similarly be determined by incorporating any given set of foundation, embankment and soil type conditions. Depending on these conditions, the reduction in cost per cubic yard of material could vary from 0 to 25 cents.

The report also discusses the evaluation of compaction in the field by surface geophysical means. Further research would be required before a new method of compaction control can be implemented using geophysical means.



## INTRODUCTION

One of the many endeavors within geotechnical engineering is the construction of embankments. As Sowers (1981) points out, the construction of embankments dates back to the times of Roman and Incan civilizations. The purpose to which these embankments have served mankind has changed little since those early days. The requirements of travel, the irrigation of fields, the conveyance of goods to the marketplace all have gained an increasing importance in the functioning of today's society. What has changed dramatically over the years is the ability to construct embankments in terms of quantity and speed. With the increased size and sophistication of construction equipment, embankments of record height and volume have been constructed in the last two decades.

Quantitative terms are easily defined when describing embankment construction, qualitative terms are more difficult to define, however. In assessing qualitative terms, one has to judge the adequacy of performance of an embankment vis-a-vis the intended use. From this perspective, one would certainly have to give credit to the early geotechnical engineers of the Roman and Incan times. Some of their roadways endure to this day and still adequately serve their original intended purpose having withstood all of the elements that nature has inflicted over the many centuries.

Methods used to achieve a level of adequacy of performance of an embankment have evolved more from traditional rather than analytical means. The traditional means have mainly relied upon compaction as the construction mechanism

providing satisfactory performance. A proper selection of graded materials along with compaction has been used to provide satisfactory performance when embankments are acted upon by seepage forces. Focusing on compaction, a simplistic conclusion that can be drawn from observing construction practices is that little or no compactive effort will result in the poorest embankment performance and the greatest compactive effort will result in the best performance. And so the questions that arise are what level of compaction will give adequate performance with respect to the embankment's intended use and is that level of compaction necessarily related to adequate performance?

## RESEARCH PROPOSAL (March 1972)

A research proposal was written in March 1972 to address some of these questions. A copy of the proposal can be found in Appendix A of this report. The primary objective of the research proposal was to develop a standard procedure evaluating and directly controlling the quality of a compacted fill in terms of its elastic properties.

The proposal divided the research into three phases. Phase I was to include a literature review, the purchase of laboratory test equipment and the testing of laboratory specimens. Phase II was to consider field testing of embankments and correlate the results with the results from Phase I. Phase III would, having the conclusions from the first two phases, select a test embankment under construction and install instrumentation. The elastic properties of the fill would be measured by surface geophysical means and the data from field instrumentation recorded. A study would then be undertaken using the measured elastic properties in a finite element analysis and compare the predicted results to the observed field behavior. Subsequent to this, a comprehensive correlation study of elastic constants would be made for each type of soil. Having done this, a final report was to be issued in June 1976 along with a standard procedure of field tests and compaction control for embankment construction.

In the intervening years, this research has unfortunately received a limited amount of attention and effort due to other projects requiring immediate attention. In the intervening years, however, other researchers have contributed in areas directly and indirectly related to the

subject of compaction and embankment performance. It is, therefore, the intent of this report to consider aspects new to geotechnical engineering since the research proposal was first written in March 1972 and to consider aspects that should have been considered and were not. Also, areas requiring further investigation are identified which would hopefully bring the subject of compaction and embankment performance into sharper focus.

## SCOPE OF THIS REPORT

To address the research proposal's primary objective of developing a procedure controlling the quality of a compacted fill in terms of its elastic parameters, this report will consider and attempt to demonstrate the following:

1. Consider the evaluation of compaction by surface geophysical means.
2. Demonstrate that the theoretical determination of stresses and construction movements can, at this time, best be done with the use of appropriate constitutive relationships and the incremental construction technique.
3. Demonstrate that the use of elastic moduli at strains ranging from  $10^{-5}$  to  $10^{-4}$  percent is inappropriate for computing construction movements in embankments.
4. Demonstrate the effect of changing water content and percent compaction on computed stresses and movements in embankments.
5. List conclusions and recommend areas for further research in the field of embankment construction control.

To meet the primary objective, the research proposal postulated the use of elastic parameters as measured in the field by surface geophysical means to determine embankment stresses and strains. This postulation neglected the fact that a soil's elastic modulus is a strain-dependent property and that strain level needs to be considered and appropriately accounted for.

The measurement of elastic moduli values by geophysical means is generally considered to occur at strain levels ranging from  $10^{-5}$  to  $10^{-4}$  percent. This low level of strain is contrary to the large and variable embankment strains which occur during construction. Furthermore, a soil's elastic modulus is also a function of confining pressure and therefore needs to be included in any model predicting stress-strain behavior. In March of 1972, when the research proposal was written, these aspects of soil behavior were not widely known or understood.

The first four items therefore, when taken collectively, are an attempt to address the research proposal's primary objective. Item 1 discusses the correlation of compaction with surface geophysical means. Items 2 and 3 demonstrate that the theoretical determination of stresses and construction movements can best be done by using elastic moduli values determined at large strain levels as opposed to the low strain levels considered in geophysical methods. Item 4 is included to suggest a method by which an adequate level of compaction can be selected. The method involves a determination of the effects on embankment stresses, movements and traditional factors of safety due to variations in elastic and conventional soil strength parameters. The variations of these parameters are due to variations in percent relative compaction and moisture content.

## COMPACTION CORRELATED WITH SURFACE GEOPHYSICAL MEANS

As part of this research a resonant footing and resonant column apparatus were purchased in 1975 to measure elastic parameters in the field and laboratory, respectively. The resonant footing technique used for measuring shear modulus was first developed in 1950 by the Engineering Research and Development Laboratories (ERDL), U.S. Army, Fort Belvoir, Virginia.

The technique, as used in this research, involved the preparation of a three square foot area sufficiently large for the 12-inch diameter footing. Attached to this footing is a beam that is put into motion by action of sinusoidal voltage applied to coils at the ends of the beam. The frequency of the voltage is varied until resonancy is observed on an oscilloscope. The system resonant frequency is used in the following equation to determine the apparent shear modulus, "G", of the soil;

$$"G" = 3/16 \frac{K}{r_0^3} \left( \frac{f_n}{f_{app}} - 1 \right) \quad \text{Eq. 1}$$

where K,  $f_{app}$  and  $r_0^3$  are the spring constant, the resonant frequency, and the footing radius of the apparatus, respectively;  $f_n$  is the resonant frequency determined by the test.

To determine the actual shear modulus, a slippage factor (SF) is determined and is related to the shear moduli values as follows:

$$SF = \frac{"G"}{G} \quad \text{Eq. 2}$$

$$\text{where } SF = \frac{0.5\theta}{p \tan \phi} \quad \text{Eq. 3}$$

In this equation,  $\theta$  is the peak-to-peak rotational amplitude as determined in the test,  $p$  is the bearing pressure exerted by the footing and  $\phi$  is the angle of internal friction of the soil.

A photograph of the resonant footing apparatus is shown in Figure 1. A complete description of the test procedure is given in Appendix E.

The resonant column test, as used in this research, was developed by Hardin (1970). A cylindrical specimen is held fixed at the base and excited by torsional oscillation at the upper free end. The torsional oscillation is produced by application of a sinusoidal voltage to the coils, exciting the mass which, in turn, excites the soil sample. The frequency of the oscillation is varied until resonance is obtained. Knowing the resonant frequency allows for a determination of the shear modulus by application of the theory of wave propagation in prismatic rods.

Resonant column tests were carried out for the following projects:

1. Soil Cement, Behavior of
2. I-15, San Diego
3. Dunsuir, Reinforced Earthen Wall
4. Pasadena, 7-11 Interchange

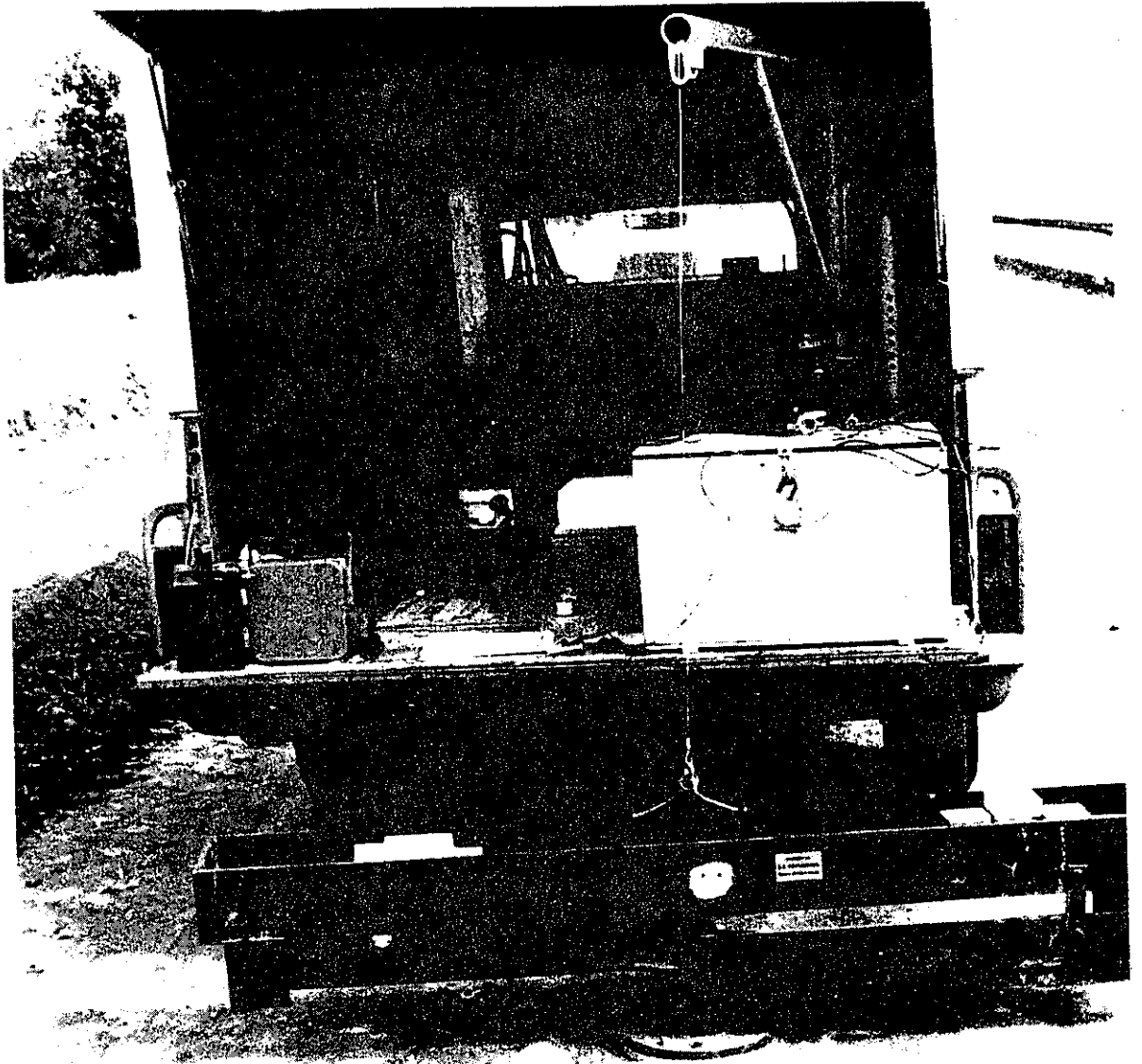


Figure 1. RESONANT FOOTING APPARATUS

5. I-5, 56th Avenue, Sacramento
6. State Capitol, Sacramento

Shear moduli and damping values of materials for all of the above projects are reported in Appendix B. The resonant column test procedure, as used in this research, is reported in Appendix F.

Field resonant footing tests were conducted on the surface of compacted backfill material for both a reinforced earth wall and a mechanically stabilized embankment on Interstate 5 at Dunsmuir. The backfill material is a Class 4 aggregate subbase (Type I). Tables 1 and 2 show the gradation and quality requirements of Class 4 aggregate subbase.

Table 1

Gradation, Class 4 Aggregate Subbase (Type I)

Sieve Sizes	Percentage Passing	
	Individual Test Results	Moving Average
4"	100	100
No. 4	30-94	35-90
No. 200	0-29	0-25

Table 2

## Quality, Class 4 Aggregate Subbase (Type I)

Item	Test Method No. Calif.	Individual Test Results	Moving Average
Sand Equivalent	217	18 min	20 min
Resistance (R-value)	301	50 min	--

Test results indicated average shear modulus values of  $6.3 \times 10^5$  psf for the mechanically stabilized embankment and  $15.8 \times 10^5$  psf for the reinforced earth wall. A shear modulus of  $6.6 \times 10^5$  psf was determined when samples were taken from the backfill material of the reinforced earth wall and tested to determine the shear modulus by the resonant column device.

The value of  $15.8 \times 10^5$  psf appears to be anomalous while the shear modulus determined by the resonant column appears to corroborate the field resonant test results for the mechanically stabilized embankment. The anomalous result is possibly due to seating problems of the footing. Caltrans' brief experience at this site and others verified this finding. It is therefore concluded that the use of the resonant footing is of questionable value for some soils because of the need to provide a satisfactory seating at the contact surface between the device and the ground surface. For this reason, it may be limited only to fine grained compact soils. It also has a limited depth of influence.

Moore (1973) conducted a study comparing the compressional wave velocities for embankment, base course and pavement layers to their respective compacted in-place densities. Data for the compression wave velocity line were obtained by placing a detector firmly on the surface of the layer to be studied. Impact blows were made with a two pound hammer on a small steel bar (3/4" x 3/4" x 4"). The time of wave travel was measured at 0.5 foot intervals over a 1.5 foot distance. A contact on the hammer closed a circuit upon striking the plate starting a timer measuring in units of 1/8 millisecond. A photograph of this equipment is shown in Figure 2.

Results from 254 tests indicated an essentially straight line relationship between the measured in-place density and the compressional wave velocity. Standard deviations from a straight line were 2.30 percent and 2.20 percent of maximum dry density for tests made on granular and subgrade materials, respectively. A compilation of the test results is shown in Figure 3.

Comparing the techniques employed as a part of this research and as employed by Moore (1973) for determination of elastic parameters, it is clear that the technique used by Moore is more advantageous. The main reasons are as follows:

1. The technique has a greater volume of influence
2. The equipment needed is much less complicated
3. The test is less time consuming
4. And the seating problem is less critical.

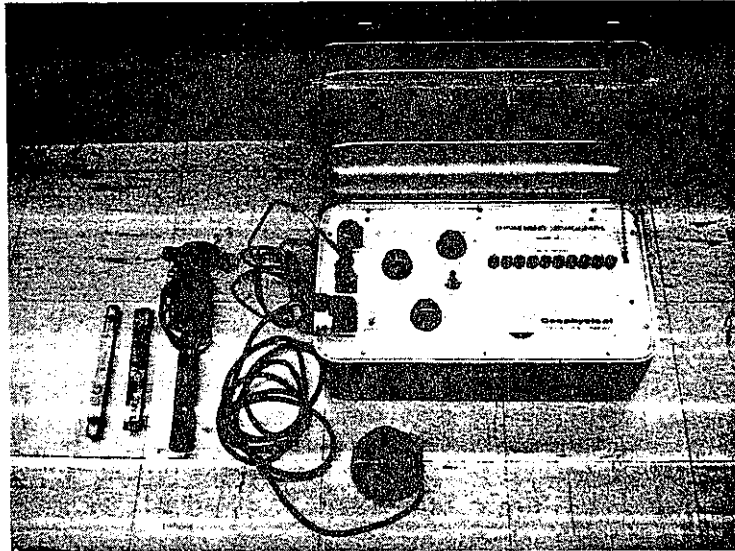


**Figure 2. MD-1 SEISMIC EQUIPMENT**

**From Moore, "Seismic Test for Compaction of Embankment,  
Base Course and Pavement Layers"**

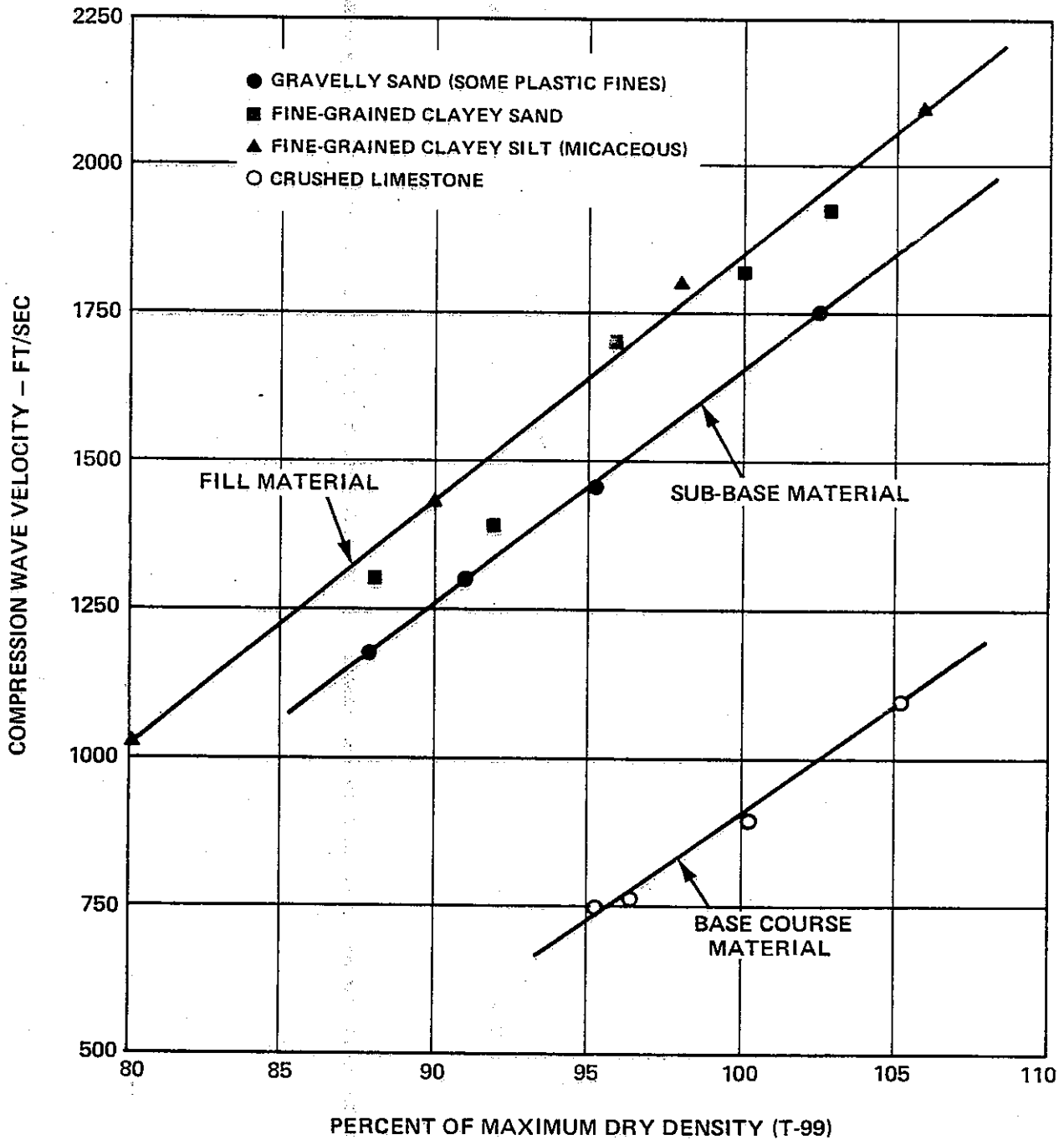


**Figure 3. RELATION OF SEISMIC WAVE VELOCITY (COMPRESSION) TO DENSITY OF COMPACTED SOIL LAYERS**

From Moore, "Seismic Test for Compaction of Embankment, Base Course and Pavement Layers"

It is important to note that measuring the shear modulus by the resonant footing method neglects the effect of aging. It has been demonstrated by a number of investigators (1,2,3,4,6,10,14,) that the shear modulus of a soil is a time-dependent property. Aging a sample under a confining pressure increases the shear modulus. This effect is very predominant in finer grained soils and less so in the coarser grained soils. Afifi and Woods (1971) showed a 5 to 10 percent increase in shear modulus for an Ottawa Sand when confined for a period of 24 hours without showing an increase in density.

The aging effect on the shear modulus is an important factor accounting for a difference in shear modulus determined by subsurface geophysical means compared to the shear modulus determined from undisturbed samples tested in the laboratory. It is postulated that the aging of a (undisturbed) sample is a phenomenon whereby a sample regains some of its strength lost during the sampling and extrusion process.

Studies determining the effect of aging on the compressional wave velocity of soils were not found in the literature. The relationships between the shear and compressional wave velocities and the elastic modulus are as follows:

$$V_p^2 = V_s^2 \left( \frac{2\mu-2}{2\mu-1} \right) \quad \text{Eq. 4}$$

$$V_p^2 = \frac{E(1-\mu)}{\rho(1+\mu)(1-2\mu)} \quad \text{Eq. 5}$$

where  $V_p$  and  $V_s$  are the compressional and shear wave velocities, respectively,  $\mu$  is Poisson's ratio,  $\rho$  is the material's mass density, and  $E$  is the elastic modulus.

It is usually assumed that Poisson's ratio is not affected by aging. By examination of Equation 4, it can likewise be assumed that  $V_p$  is equally increased as  $V_s$  is increased with time.

Consideration should therefore be given to the aging effect on either compressional wave velocities or shear moduli determinations of an embankment fill with time. Moore (1973) did indeed find a 20 percent increase in compressional wave velocity of bituminous pavement 13 days after completion of rolling.

Studies recently published by Floss, et al (1983) and Schwab, et al (1983) describe a new dynamic test method used on a number of test fills to assess compaction. The method consists of using a light vibratory roller mounted with an accelerometer to measure the vibration characteristics of the roller and the fill. Although this method can probably not be considered as a surface geophysical test, it does attempt to measure the same property, namely stiffness.

In their studies, the stiffness of a newly placed lift was assessed by noting the compactometer value (CMV) which is the ratio of amplitudes of the first and second modes of vibration as measured by the accelerometer. The studies compared the CMV as a function of the number of passes with results from mechanical tests which included plate load, pressuremeter, dynamic sounding and density tests. Comparisons indicated a general increase in CMV with an increase in values determined by the mechanical tests. The comparisons did, however, indicate a large amount of scatter for all the mechanical test results. Although the initial results appear to be promising, the following areas

remain to be studied before much reliance can be placed upon this new method; frequency of the roller, roller speed during compaction, direction of travel, boundary condition of the fill, type of material, moisture content, lift thickness, subsurface condition and excess pore water pressure in the fine grained soils.

This method of assessing compaction of an embankment fill would be very advantageous. The operator would continuously receive information with each pass of the roller and would therefore know which areas require additional rolling and which areas of the fill are sufficiently compacted.



## EMBANKMENT PERFORMANCE PREDICTED BY THE FINITE ELEMENT METHOD

The finite element method has seen a dramatic increase in usage within the geotechnical community during the last decade. The method has been demonstrated to be a powerful tool in estimating stresses, strains and movements within embankments. Studies have been carried out and reported in the literature demonstrating the validity of the method and the appropriateness of the stress-strain characterizations employed.

In their report on stresses and movements in Oroville Dam, Kulhawy and Duncan (1970), demonstrated good agreement between computed and measured stresses and movements throughout the embankment. At the time of their report, Oroville Dam was the world's highest embankment and was therefore, a significant test of the finite element method and the use of the incremental construction technique along with the use of hyperbolic stress-strain parameters.

The hyperbolic stress-strain parameters used in the study were derived from standard triaxial tests run on embankment materials set up at the same density and water content as the different materials comprising the dam. The values used in the analysis are shown in Table 3.

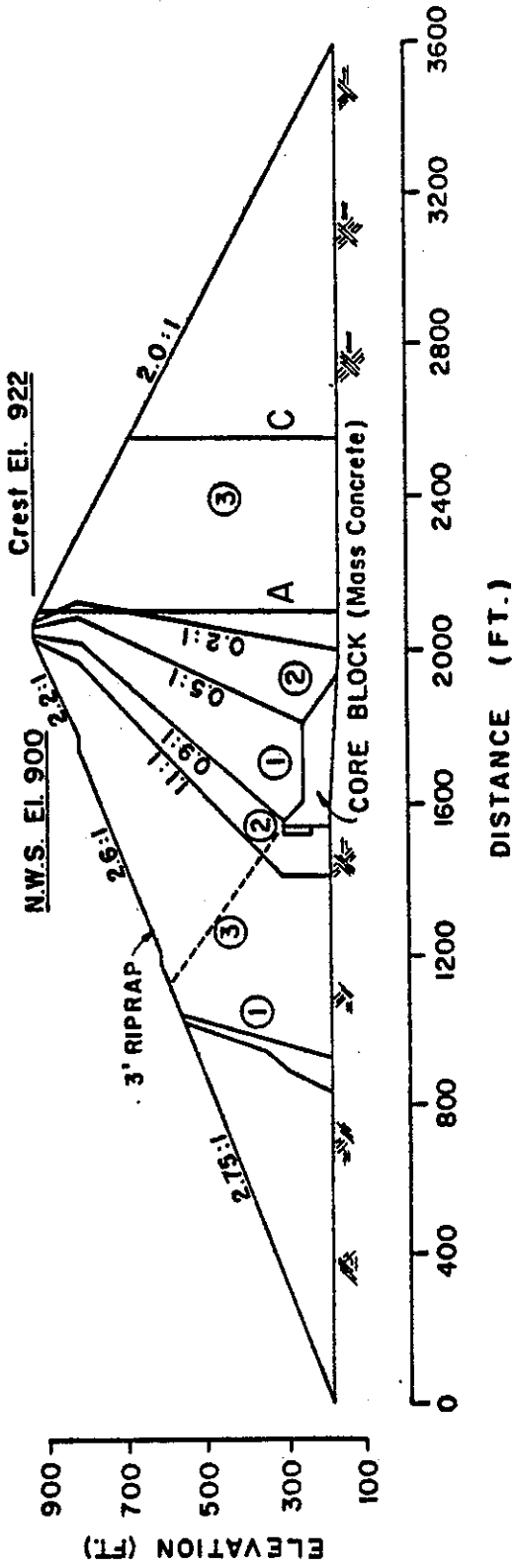
The maximum cross section of Oroville Dam is shown in Figure 4. The dam was modeled by first simulating the construction of the core block, secondly, the upstream cofferdam and finally the full embankment.

Table 3. Values of Stress-Strain Parameters for Analysis of Oroville Dam

Parameter	Symbol	Values Employed in Analyses				
		Shell	Transition	Core	Soft Clay <sup>a</sup>	Concrete
Unit Weight (lb/ft <sup>3</sup> )		150	150	150	125	162
Cohesion (tons/ft <sup>2</sup> )	C	0	0	1.32 <sup>b</sup>	0.3	216 <sup>c</sup>
Friction angle (degrees)		43.5	43.5	25.1 <sup>b</sup>	13.0	0
Modulus Number	K	3780	3350	345	150	137,500
Modulus Exponent	n	0.19	0.19	0.76	1.0	0
Failure Ratio	Rf	0.76	0.76	0.88	0.9	1.0
Poisson's Ratio	G	0.43	0.43	0.30	0.49	0.15
Ratio	F	0.19	0.19	-0.05	0	0
Parameters	d	14.8	14.8	3.83	0	0

- a. Zone of soft clay at upstream end of core block.
- b. C and  $\phi$  for  $(\sigma_1 + \sigma_3) < 50$  tons/ft<sup>2</sup>; C = 10.2 tons/ft<sup>2</sup>,  $\phi = 4$  degrees for  $(\sigma_1 + \sigma_3) > 50$  tons/ft<sup>2</sup>.
- c. Tensile strength of concrete = 14 tons/ft<sup>2</sup> (200 psi).

From Kulhawy & Duncan, "Nonlinear Finite Element Analysis of Stresses and Movements in Oroville Dam"



ZONE 1	-	9,000,000	YD <sup>3</sup>	-	Impervious
ZONE 2	-	9,500,000	YD <sup>3</sup>	-	Transition
ZONE 3	-	61,100,000	YD <sup>3</sup>	-	Pervious
RIPRAP		-	413,000	YD <sup>3</sup>	
CONCRETE		-	291,000	YD <sup>3</sup>	

A	-	CROSS ARM DEVICE
C	-	CROSS ARM DEVICE

Figure 4. OROVILLE DAM MAXIMUM SECTION

From Kulhawy & Duncan, "Nonlinear Finite Element Analysis of Stresses and Movements in Oroville Dam"

A comparison of the computed and measured horizontal movements at two different elevations within the downstream portion of the embankment are shown in Figures 5 and 6. Cross arm devices shown in Figure 4 were installed within the maximum section for the purpose of measuring settlements. Comparisons of the measured and computed settlements are shown in Figure 7.

It is important to note that before the development of the incremental construction technique, the settlement behavior shown in Figure 7 was impossible to predict. If the analysis were conducted using "gravity-turn on" (instant full embankment load) techniques, even with hyperbolic stress-strain parameters, the maximum settlement would have occurred at the top instead of approximately midheight of the embankment. The incremental construction technique does not, however, address post-construction or secondary consolidation of any of the materials within an embankment.

Although gravity-turn on analyses do not model construction movements, they do adequately quantify stresses within an embankment.

In comparing computed and measured stresses, it should not be assumed that stress cells correctly identify the actual stress in an embankment. Weiler, et al (1982) list 15 factors which, if not carefully considered, could lead to very erroneous measurements. Vrymoed (1981), in a gravity-turn on analysis of Oroville Dam, compared the measured and computed stresses as shown in Table 4.

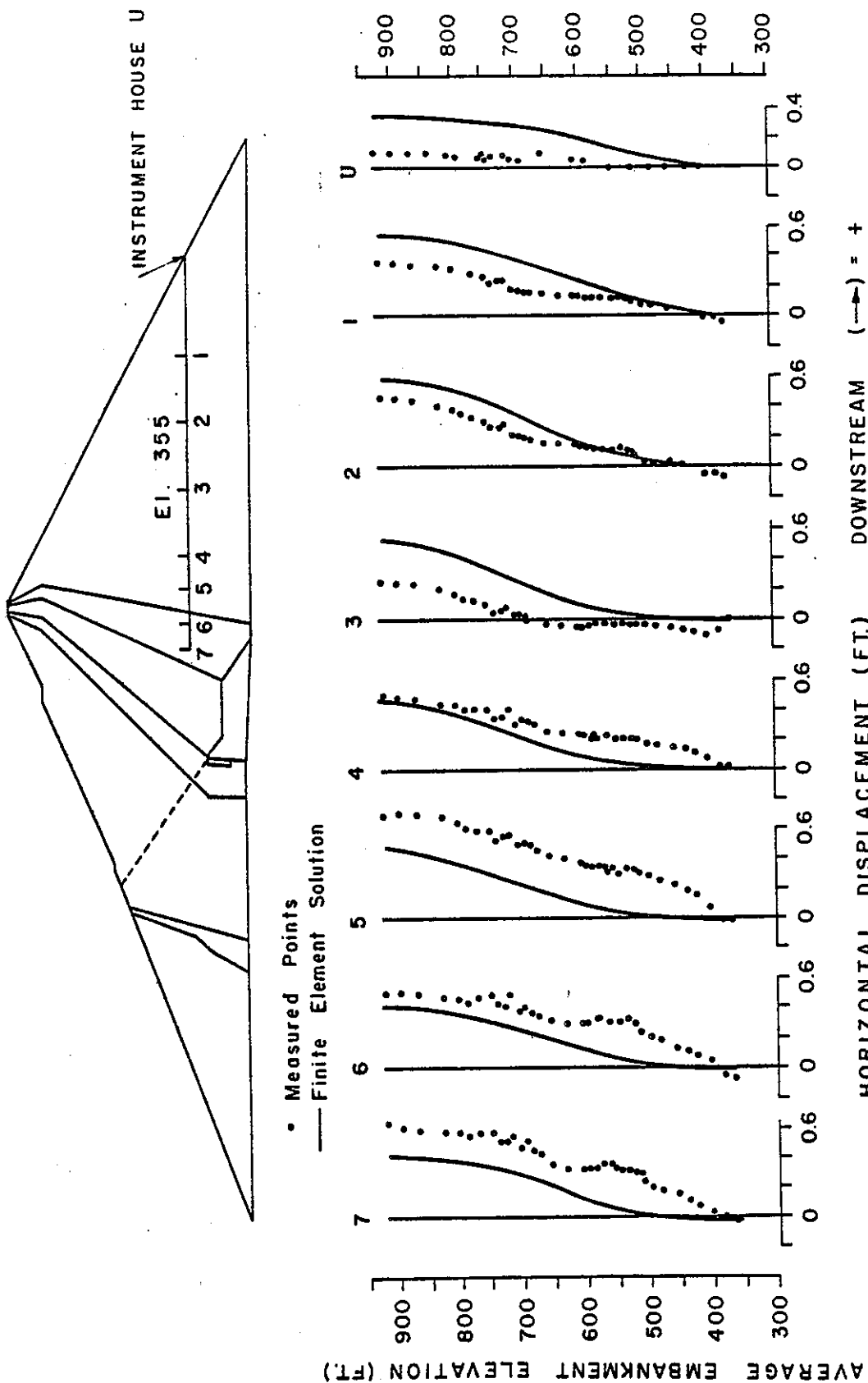


**Figure 5. HORIZONTAL DISPLACEMENTS AT ELEVATION 355 IN OROVILLE DAM**  
 From Kulhawy & Duncan, "Nonlinear Finite Element Analysis of Stresses and Movements in Oroville Dam"

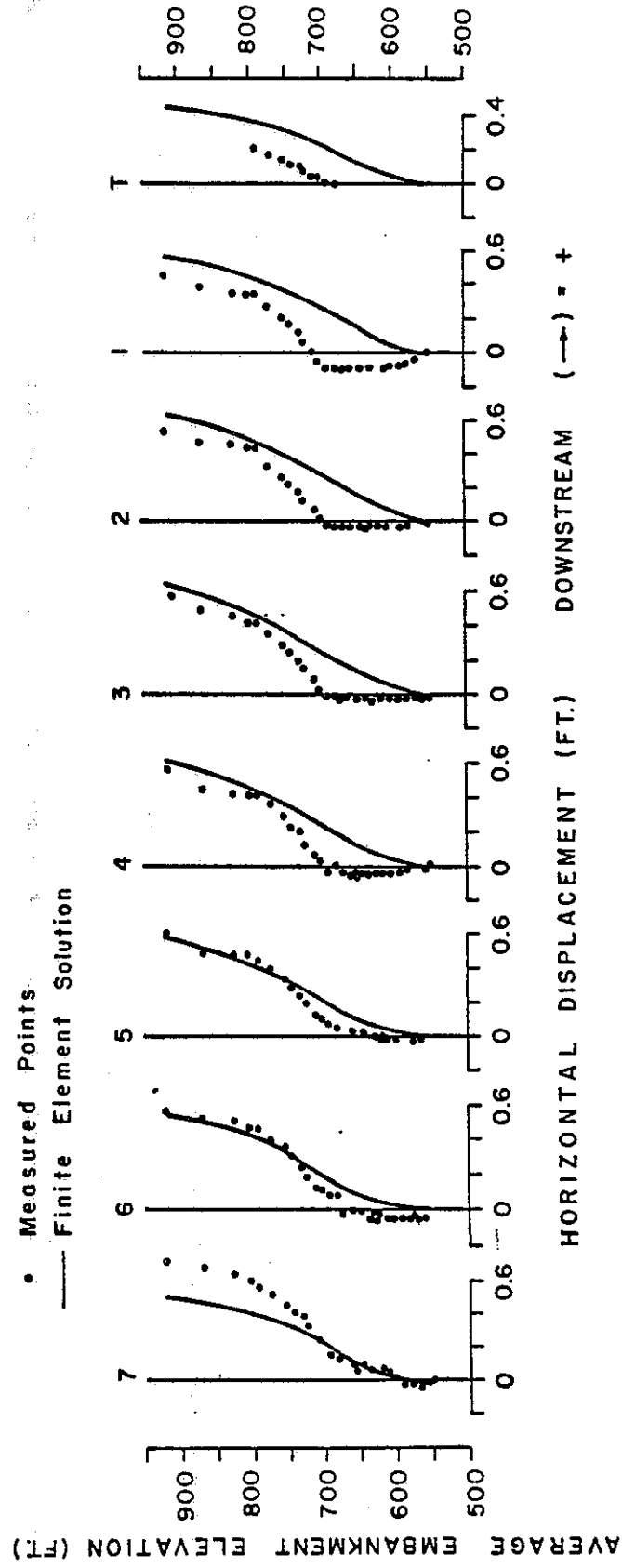
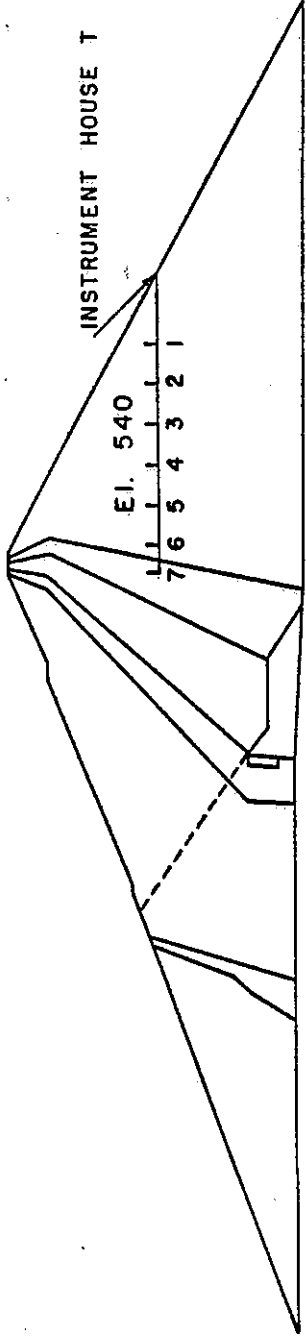


**Figure 6. HORIZONTAL DISPLACEMENTS AT ELEVATION 540 IN OROVILLE DAM**

From Kulhawy & Duncan, "Nonlinear Finite Element Analysis of Stresses and Movements in Oroville Dam"

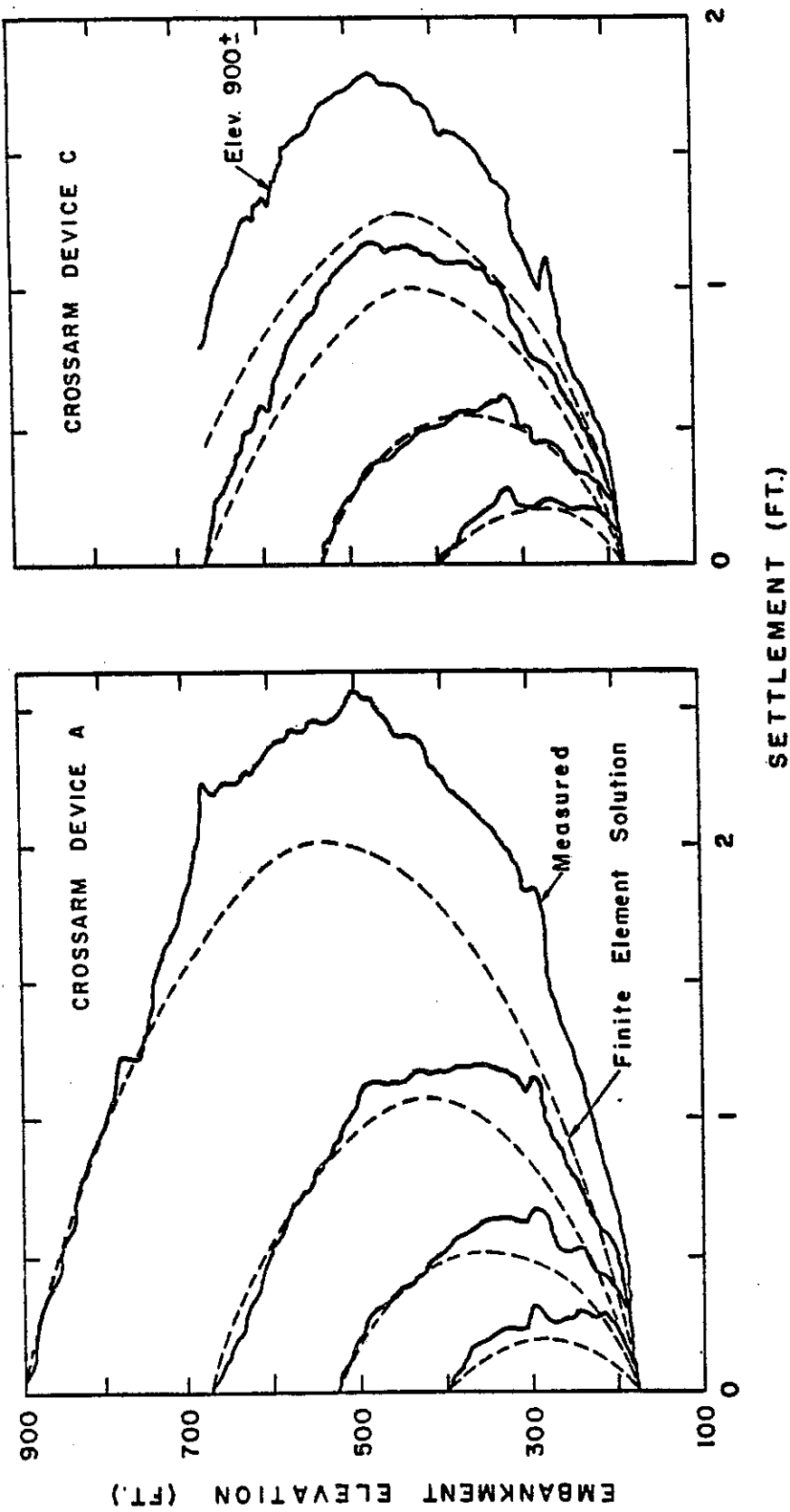


Figure 7. CROSSARM SETTLEMENTS IN OROVILLE DAM

From Kulhawy & Duncan, "Nonlinear Finite Element Analysis of Stresses and Movements in Oroville Dam"

Inspection of Table 4 shows good agreement between measured and computed vertical stresses. Inclined stresses and compression toward the downstream toe also show good agreement. The operable cells measuring stresses toward the upstream toe yield more erratic results when compared to the calculated values. The disagreement between the calculated and measured values for the inclined cells is understandable considering the difficulty of their placement and compaction of the adjacent embankment material.

Subsequent to the study of Oroville Dam by Kulhawy and Duncan, other investigators have been able to verify the incremental construction method and the hyperbolic stress-strain characterization.

Chang (1976) reported field data and computed stresses and deformations in three highway embankments. It was found that the layered incremental construction method and use of the hyperbolic stress-strain parameters predicted soil stresses and deformations that were in good agreement with the measured stresses and deformations. Figures 8 through 10 compare computed and observed vertical settlements for each of the three highway embankments. Like the study on Oroville Dam, the characterization of the hyperbolic stress-strain was derived from triaxial test results on materials compacted to the same density and water content as the materials comprising the three embankments.

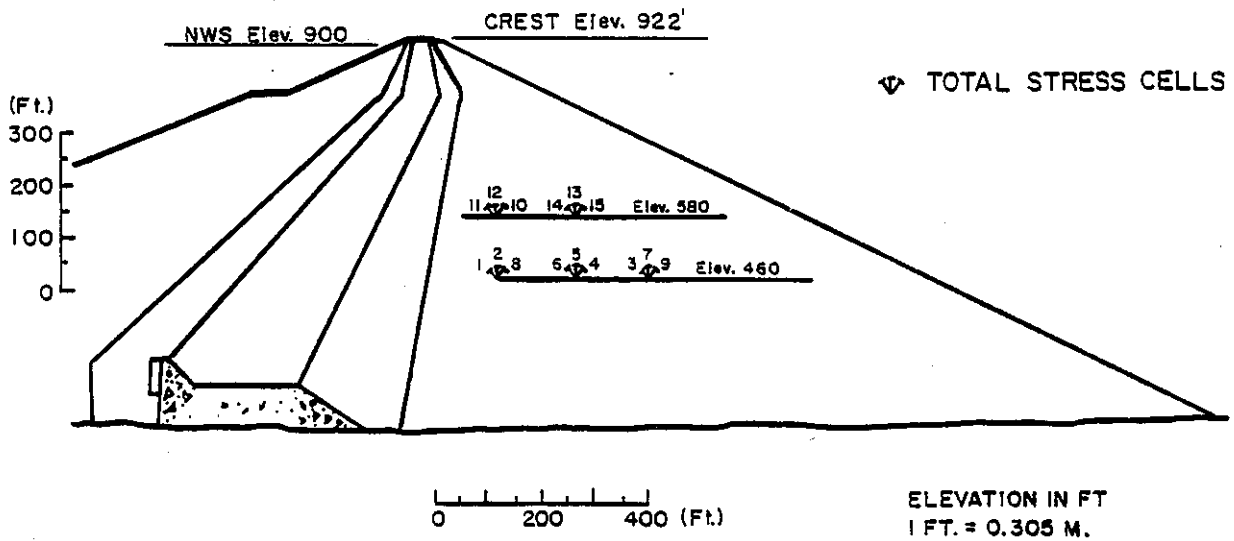
Since these methods used to compute stresses and movements have been verified, it is assumed, for the purpose of this report, that the estimation of stresses and deformations by the aforementioned techniques is appropriate for studying the effects of compaction on embankment performance.

Table 4. Static Stress Comparison

Cell No.	Stress Tsf		Direction of Stress
	Maihak Cell	FEM Analysis	
1	13.8	16.6	b
2	29.5	28.2	a
3	14.4	11.1	b
4	-	23.0	c
5	30.9	25.6	a
6	15.1	14.2	b
7	22.3	21.0	a
8	11.0	24.5	c
9	-	20.8	c
10	7.9	18.9	c
11	11.5	12.1	b
12	25.4	20.2	a
13	18.0	17.0	a
14	10.0	9.1	b
15		17.1	c

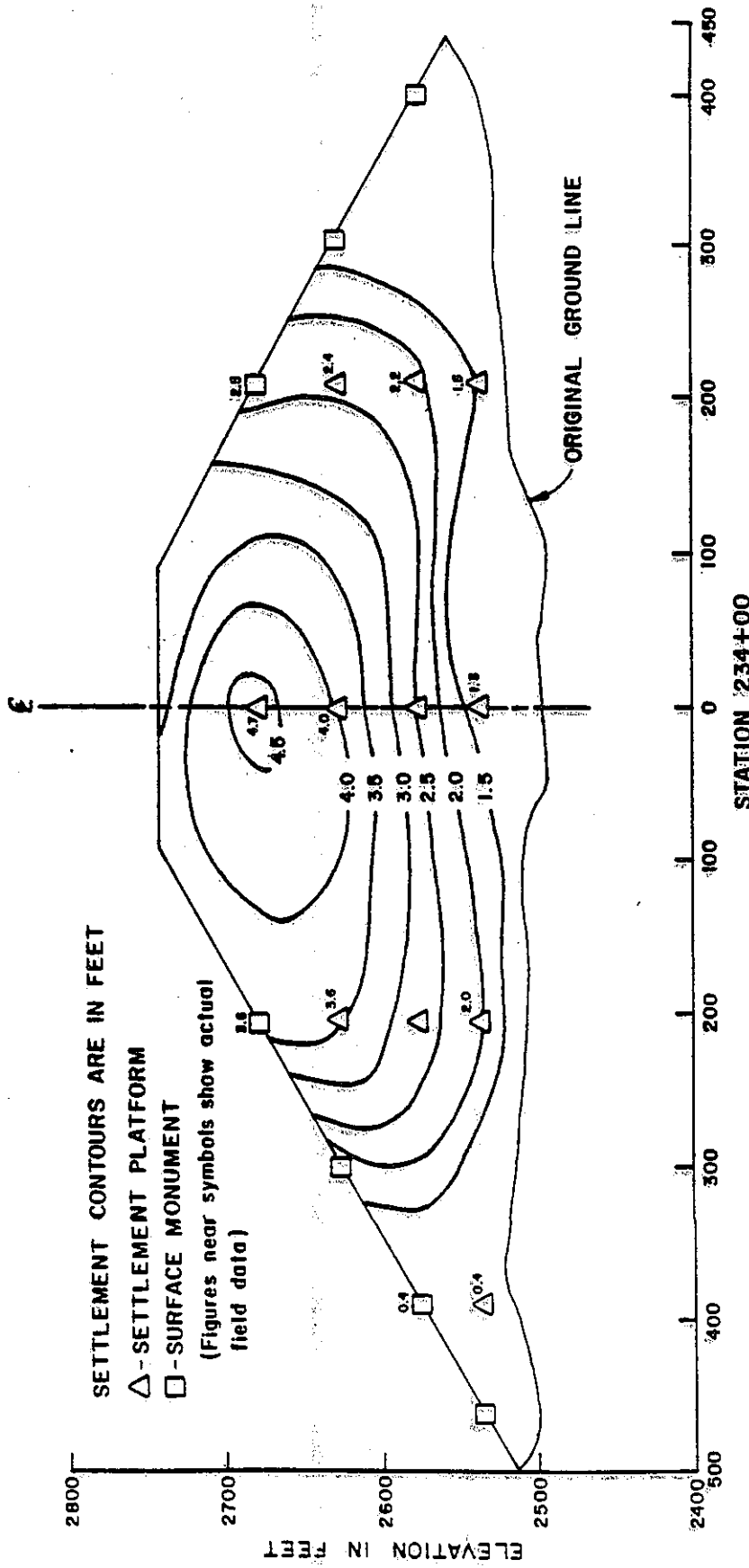
  

1 Tsf = 95.7 KPa



LOCATION OF STRESS CELLS

From Vrymoed, "Dynamic FEM Model of Oroville Dam"



CONTOURS OF SETTLEMENT (300 days after completion of fill)

Figure 8. OSITO CANYON ENBANKMENT

From Chang, "Stress Strain Relationships in Large Soil Masses"

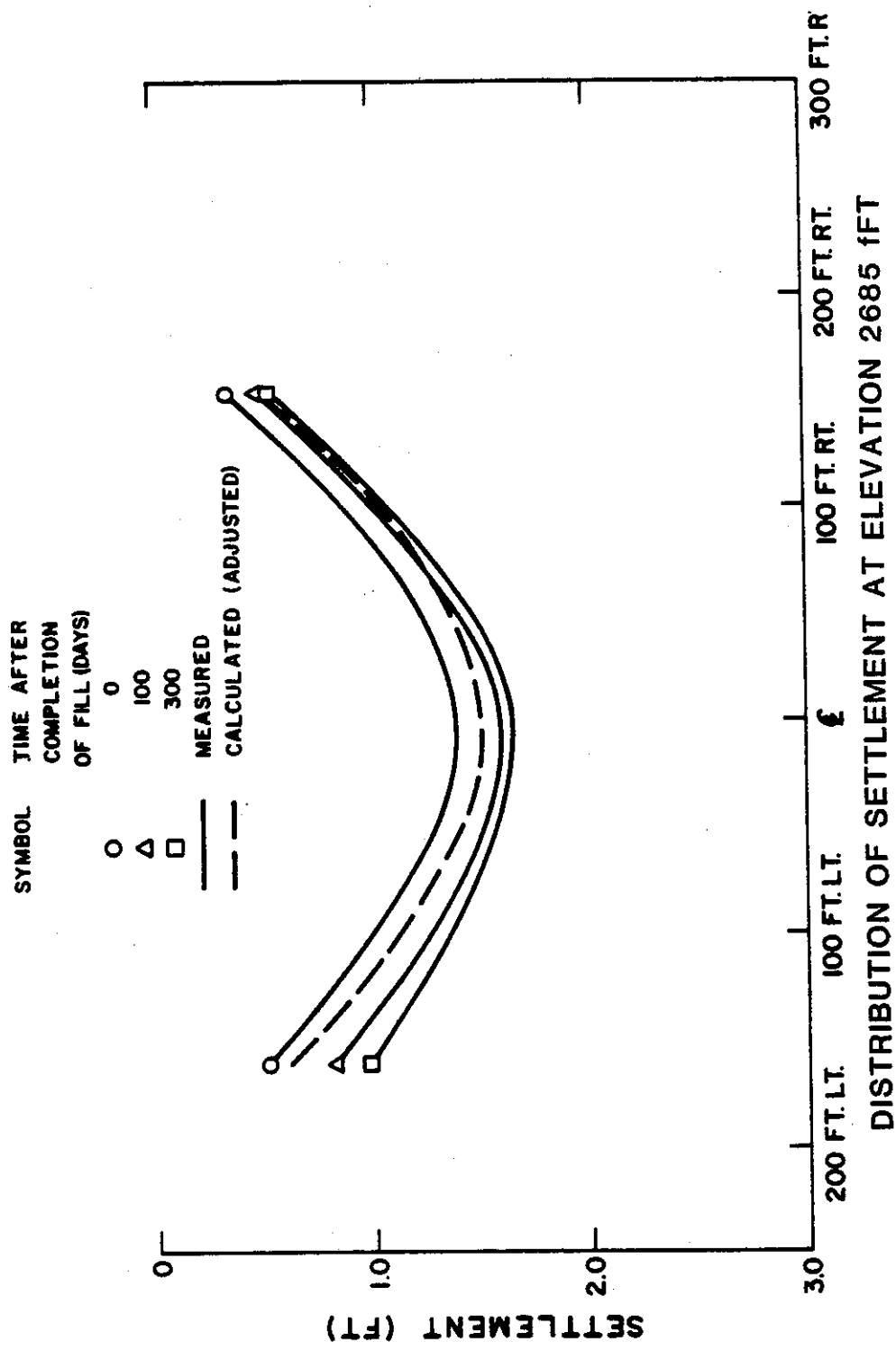


**Figure 9. NO NAME CANYON EMBANKMENT**

From Chang, "Stress Strain Relationships in Large Soil Masses"

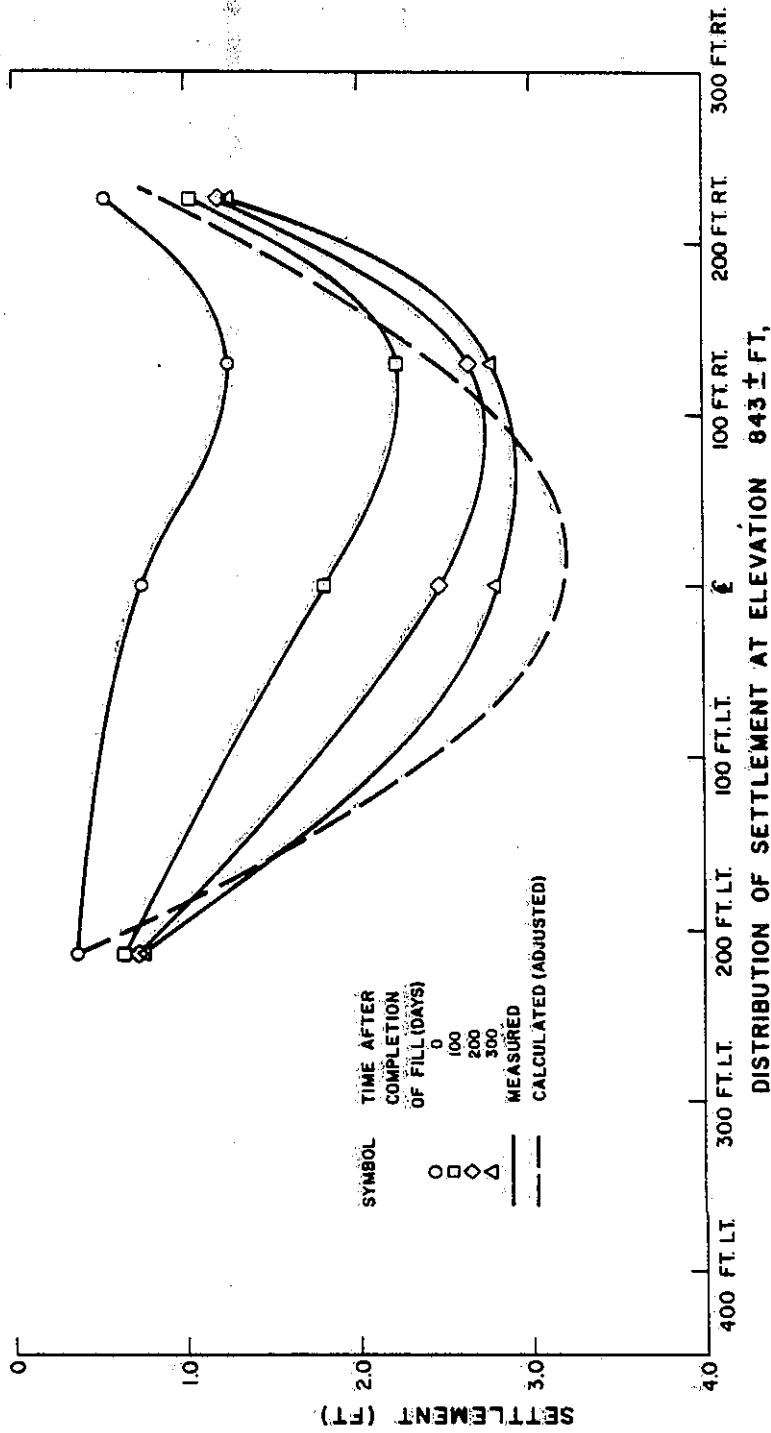


Figure 10. SAN LUIS RESERVOIR EMBANKMENT-STATION 80 ~

From Chang, "Stress Strain Relationships in Large Soil Masses"

## USAGE OF ELASTIC MODULI AT $10^{-4}$ PERCENT STRAIN

It is important to contrast the quantitative value of elastic moduli as determined by use of triaxial test procedures and hyperbolic stress-strain parameters and as determined by geophysical means. When the elastic moduli of a soil are determined by geophysical means, the level of strain is on the order of  $10^{-5}$  to  $10^{-4}$  percent. When the moduli values are determined by triaxial test procedures, the levels of strain are on the order of  $10^{-1}$  to 1 percent. The difference between the moduli values as determined by the two test procedures therefore ranges from a factor of 3 to 20 as shown in Figure 11.

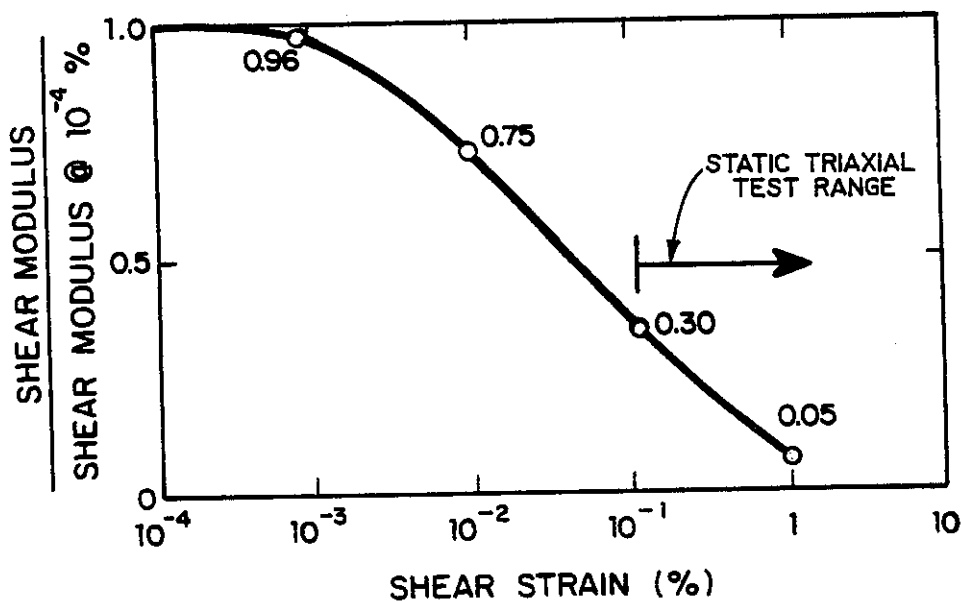


Figure 11. Behavior of Shear Modulus With Shear Strain

In addition to strain, the other two factors that greatly influence the elastic moduli are void ratio or density and confining pressure. Several researchers have developed relationships between elastic moduli and these two factors.

Hardin and Black (1968) developed the following relationship for angular grained materials based on many independent measurements of wave propagation velocities in clean dry cohesionless materials with seven different types of resonant column devices:

$$G = \frac{1230 (2.97 - e)^2 \sigma_0^{1/2}}{1 + e} \quad \text{Eq. 6}$$

Where  $G$  is the shear modulus at small strains ( $10^{-4}$ ) in pounds per square inch,  $e$  is the void ratio and  $\sigma_0$  is the effective confining pressure in pounds per square inch.

The following equation, developed by Seed and Idriss (1970) expressing shear modulus as a function of density and confining pressure, is very similar to Equation 6:

$$G = 1000K_2(\sigma'_m)^{1/2} \quad \text{Eq. 7}$$

Where  $G$  is the shear modulus in pounds per square foot,  $K_2$  is a dimensionless number varying with shear strain, soil type and relative density and  $\sigma'_m$  is the mean effective confining pressure in pounds per square foot.

Both Equations 6 and 7 are similar to the following equation used by Wong and Duncan (1974) in their development of the hyperbolic stress-strain parameters:

$$E_i = KP_a(\sigma_3/P_a)^n \quad \text{Eq. 8}$$

Where  $E_i$  is the initial elastic modulus,  $K$  and  $n$  are dimensionless numbers and are functions of material type and density and  $P_a$  is atmospheric pressure making conversion from one system of units to another more convenient, and  $\sigma_3$  is the minor principle stress.

The initial elastic modulus used in the hyperbolic stress-strain characterizations of soils is shown in Figure 12.

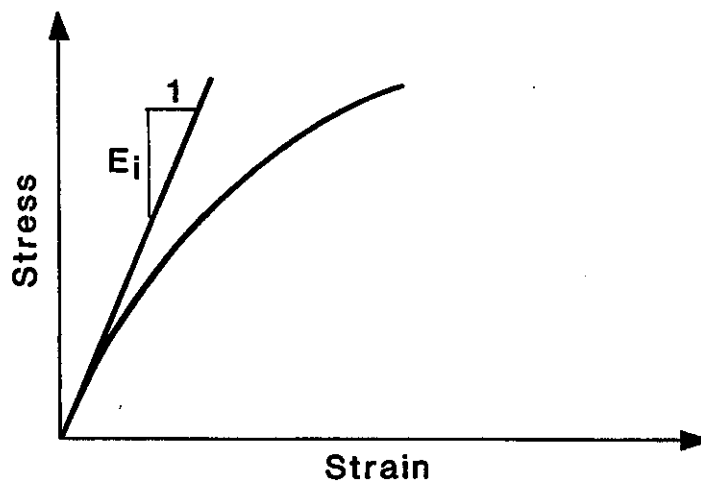


Figure 12. Initial Elastic Modulus

The value of initial elastic modulus would thus approach, quantitatively, the value of the elastic modulus determined at small strains. The initial elastic modulus is typically determined by conventional static triaxial testing methods which do not have the means of measuring strains at levels of  $10^{-4}$  percent.

Vrymoed (1981) determined and verified the  $K_2$  parameter as used in Equation 7 for the Oroville Dam gravels by noting the accelerations and displacements of the dam during seismic activity in the Oroville area in 1975. The seismic activity induced shear strains in the dam on the order of  $10^{-3}$  percent. It was determined that the  $K_2$  value at  $10^{-4}$  percent strain or  $K_{2max}$ , for the Oroville Dam shell material is 205.

Computing the shear modulus by Equation 7 and using a  $K_{2max}$  value of 205 can be compared to the initial elastic modulus as used in the hyperbolic stress-strain characterization of the Oroville Dam shell material. A comparison of elastic moduli is shown in Table 5 for a location in the downstream shell where the minor and major principal stresses are 5 and 10 TSF, respectively.

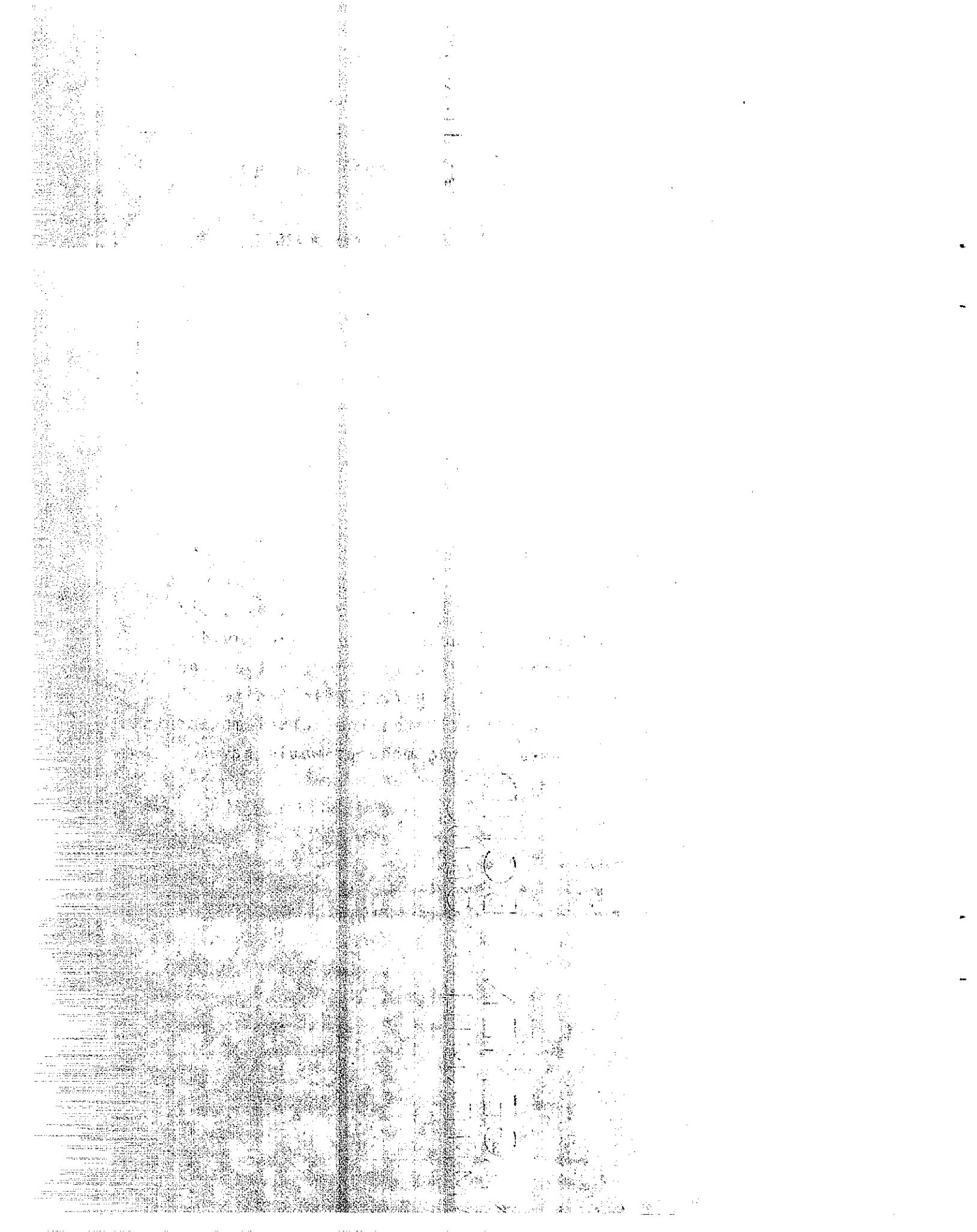
Table 5. Comparison of Elastic Moduli

$E_i = K P_a \left( \frac{\sigma_3}{P_a} \right)^n$	$G_{\max} = 1000 K_{2\max} (\sigma'_m)^{1/2}$
$K = 3780^*$	$K_{2\max} = 205$
$P_a = 1.058 \text{ TSF}$	$\sigma'_m = \frac{\sigma'_1 + \sigma'_3 + \sigma'_3}{3} = 6.7 \text{ TSF}$
$\sigma_3 = 5 \text{ TSF}$	$E^{**} = 2.9 \times 10^4 \text{ TSF}$
$n = 0.19^*$	
$E = 5.1 \times 10^3 \text{ TSF}$	

\*values taken from Table 1

\*\* $G = \frac{E}{2(1+\mu)}$  was used and  $\mu = 0.3$  at  $\sigma_3 = 5 \text{ TSF}$

The comparison shows the elastic modulus at  $10^{-4}$  percent strain to be greater than the initial elastic modulus by a factor of 6. Hence, if the greater elastic modulus would have been used by Kulhawy and Duncan (1970), they would have obtained movements smaller by a factor of 6 than the calculated movements shown in Figure 7. Their finite element solution already underestimated the actual movements and the use of an increased elastic modulus would have increased the underestimation.

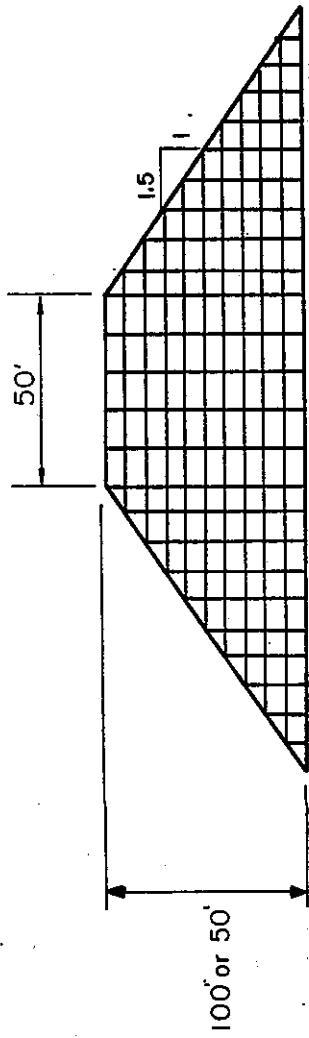


## EFFECTS OF VARIATION IN MOISTURE CONTENT AND COMPACTIVE EFFORT ON EMBANKMENT STRESSES AND MOVEMENTS

Finite element analyses of four hypothetical embankments were carried out to study the effect on embankment stresses and movements due to variations in moisture content and relative compaction of embankment fill. The four embankments were modeled as having heights of 50 and 100 feet and side slopes of 1.5:1 and 2:1. The finite element representation for each one of the four embankments is shown in Figure 13. A rigid foundation was assumed for each embankment.

Computer program REA, Herrmann (1978), was used in the analyses. The program simulates embankment construction by use of the incremental construction technique and uses the hyperbolic stress-strain characterization as developed by Wong and Duncan (1974).

Kulhawy, Duncan and Seed (1969) reported the effect of changes in compactive effort and moisture content on the hyperbolic stress-strain parameters for Pittsburg sandy clay. The report considered three different levels of compactive effort as shown in Figure 14. Specimens were compacted to the desired densities and moisture contents using a Harvard miniature kneading compaction apparatus. The maximum density obtained by the 50 lb tamp effort closely corresponds to the Modified AASHTO maximum density as shown in Figure 14. Assuming the maximum dry density obtained by the 50 lb tamp effort to represent 100 percent relative compaction, the maximum dry densities obtained by the 12.5 and 25 lb tamp efforts correspond to 92 and 96 percent relative compaction, respectively. The variation



No. OF ELEMENTS = 161

No. OF NODES = 170

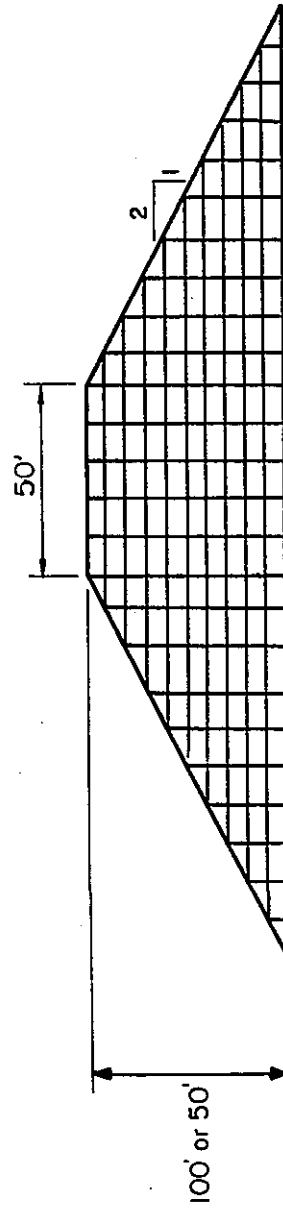
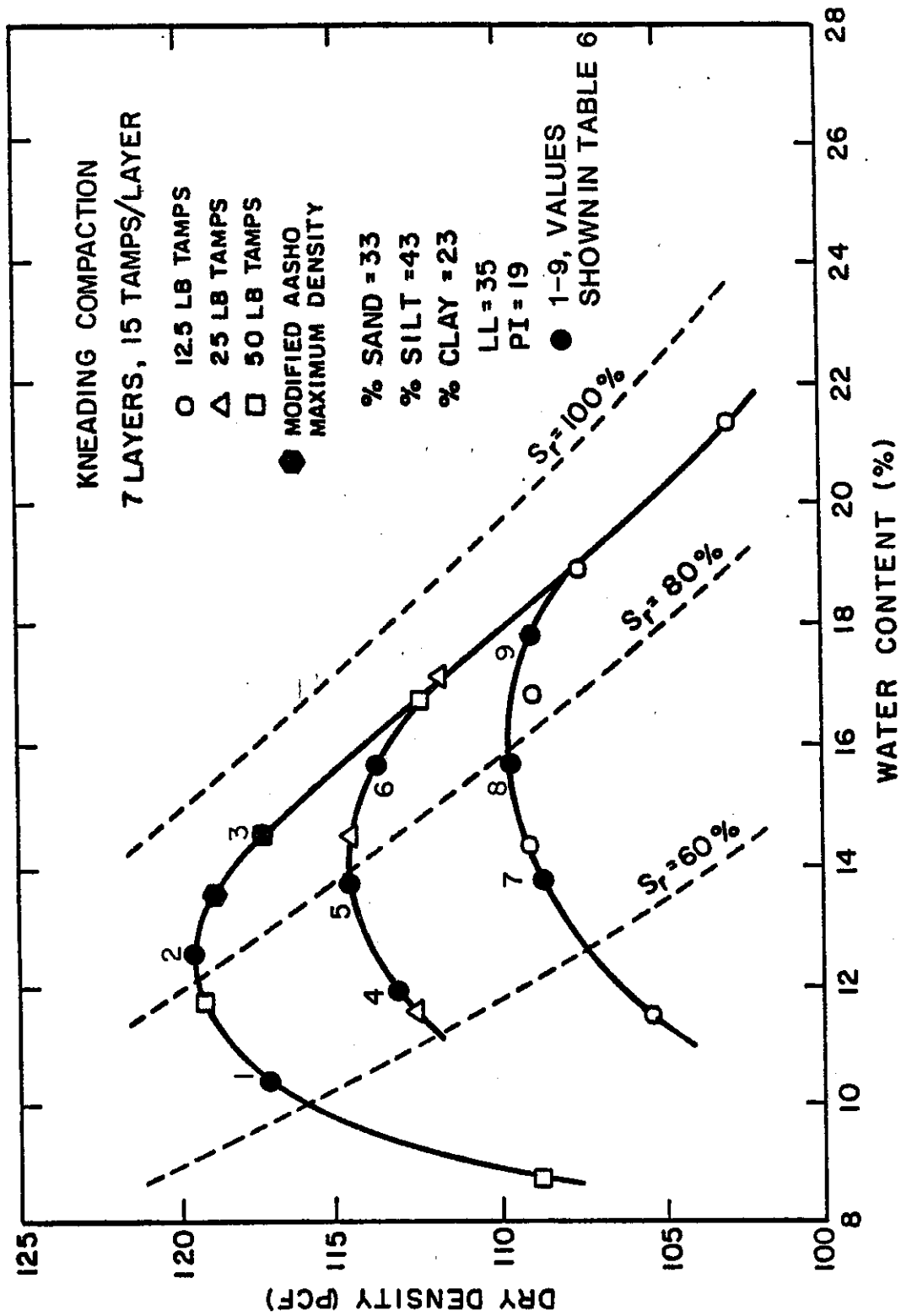


Figure 13. FEM MESH USED IN ANALYSES



**Figure 14. MOISTURE-DENSITY RELATIONSHIPS FOR COMPACTED PITTSBURGH SANDY CLAY**

From Wong & Duncan, "Hyperbolic Stress-Strain Parameters for Nonlinear Finite Element Analyses of Stresses and Movements in Soil Masses"

of hyperbolic stress-strain parameters with changes in relative compaction and moisture content, as determined by Kulhawy et al, is shown in Figures 15 through 17. The data shown in these figures represent a substantial amount of laboratory testing and are therefore utilized to examine the effects on embankment stresses and movements due to changes in compactive effort and moisture content.

For the purposes of this report, the hyperbolic stress-strain parameters corresponding to the maximum density for the three levels of compaction and moisture contents of plus and minus two percent of optimum were used as input to computer program REA, Herrmann (1978), for each of the four embankments. These parameters, reflecting the variations in moisture content and compactive effort for a total of nine different conditions, are summarized in Table 6.

The vertical, lateral and horizontal shear stresses shown in Figures 18, 19, and 20, respectively, were computed at midheight of the 100 foot embankment having side slopes of 1.5:1. Since the behavior shown in these figures is typical for the other embankments, the stresses for the other embankments are presented in Appendix C. The stresses shown are for one-half of the embankment since they are identical for the other half due to symmetry of each of the four embankments.

Results indicate that, generally for all embankments and for each level of compaction, the horizontal shear stresses were slightly greater for the dry of optimum case than the stresses computed for the wet of optimum case. The vertical stresses were greatest for the 100 percent relative compactive effort due to a greater unit weight than the

Table 6. Hyperbolic Stress-Strain Parameters

Material Properties	Symbol	Relative Comp. 100%		Relative Comp. 96%		Relative Comp. 92%	
		Moisture Content -2% opt. +2%	Moisture Content +2%	Moisture Content -2% opt. +2%	Moisture Content +2%	Moisture Content -2% opt. +2%	Moisture Content +2%
Unit Weight, pcf	$\gamma$	117	119	117	114	112	108
Cohesion, psf	C	6000	6200	4200	4000	3400	2000
Friction Angle, degree	$\phi$	22	16	9	21	15	9
Elastic	K	5200	4500	2500	2000	1700	900
Modulus	Ku	5200	4500	2500	2000	1700	900
Parameters	n	-.40	-.30	-.10	-.55	-.38	-.15
Failure Ratio	Rf	.98	.98	.98	.98	.98	.98
Poisson's	G	.28	.25	.27	.30	.30	.30
Ratio	F	.04	.05	.13	.15	.19	.09
Parameters	d	15	15	15	7	7	10
Reference Figs. 14-17		(1)	(2)	(3)	(4)	(5)	(6)
					(7)	(8)	(9)

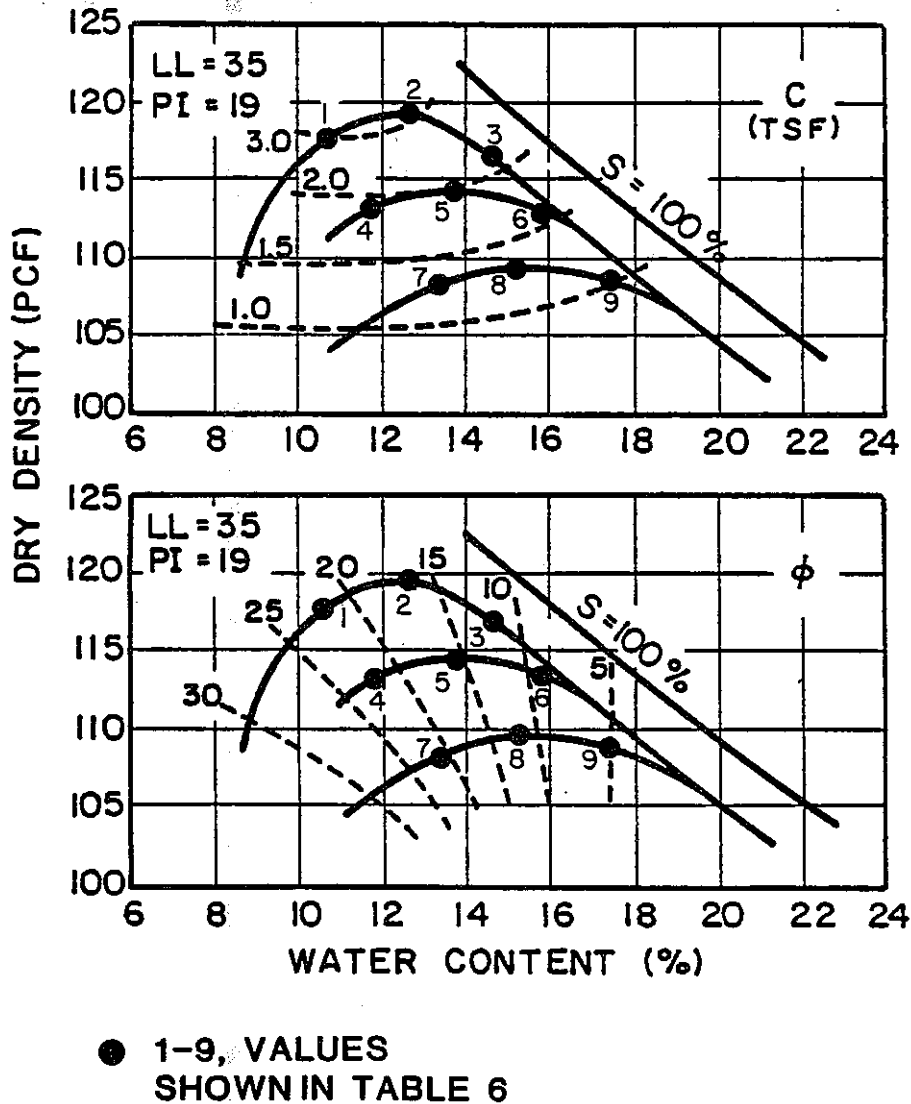
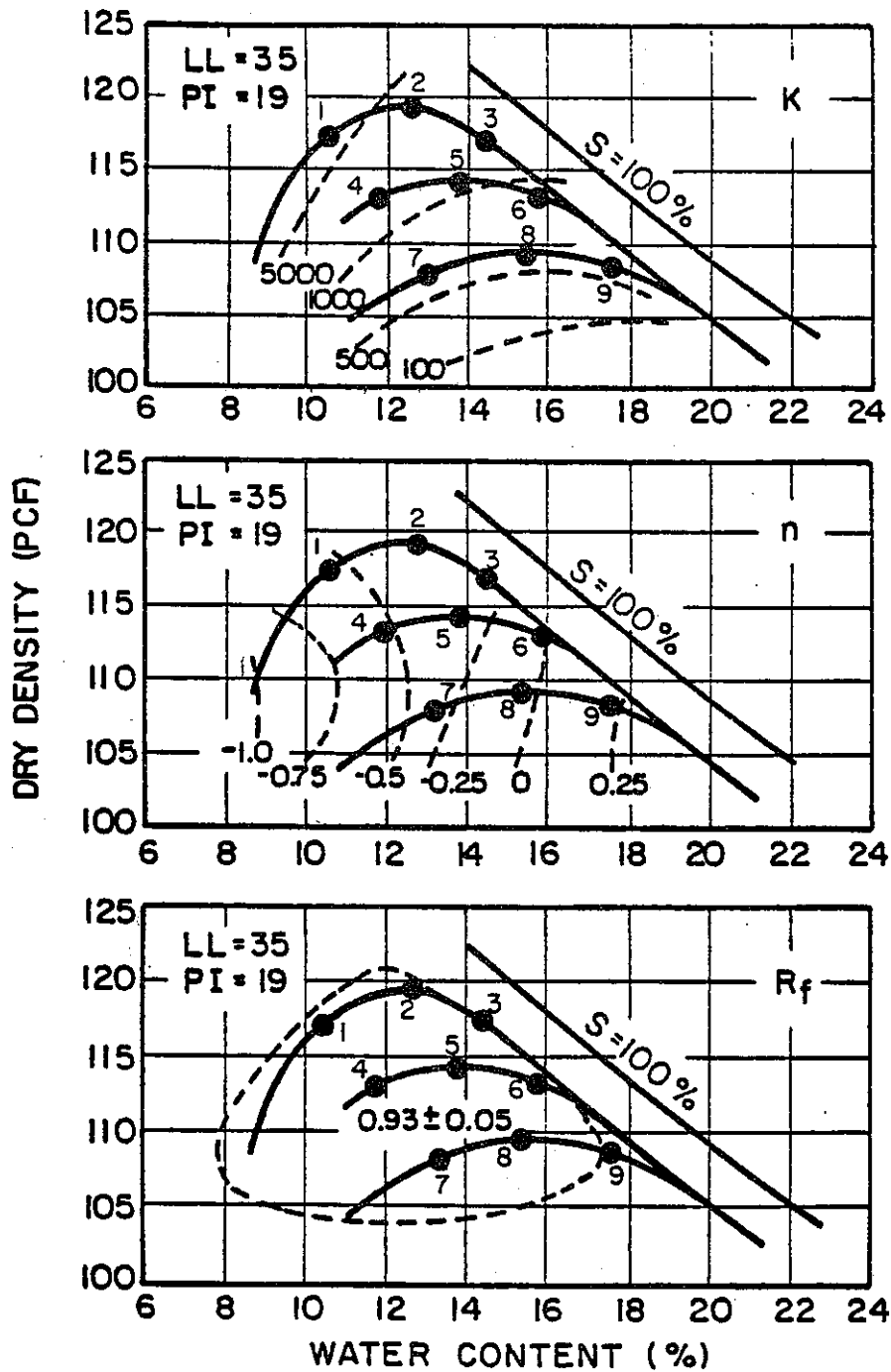


Figure 15. STRENGTH PARAMETERS FOR COMPACTED PITTSBURG SANDY CLAY TESTED UNDER UU TEST CONDITIONS

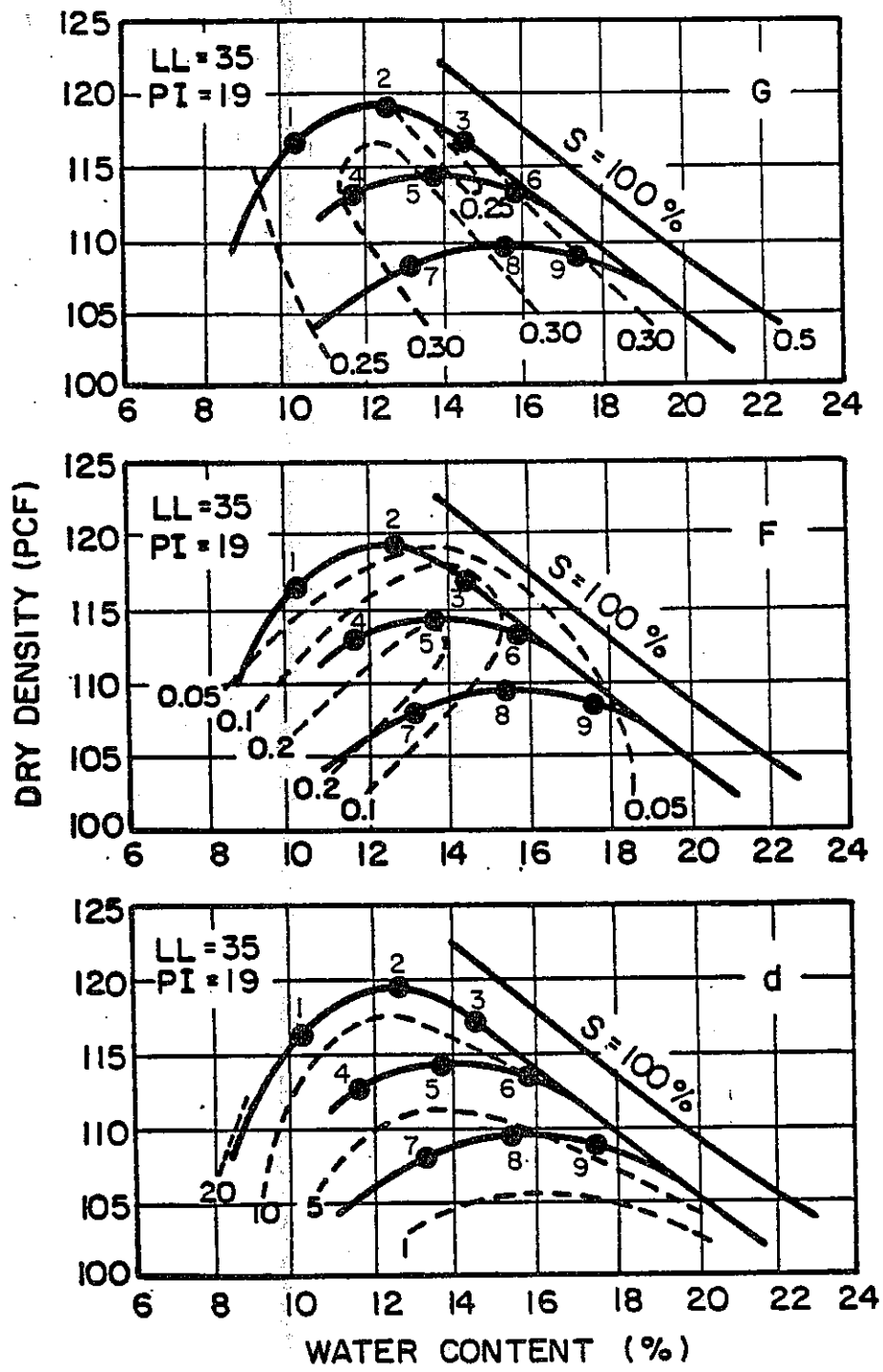
From Wong & Duncan, "Hyperbolic Stress-Strain Parameters for Nonlinear Finite Element Analyses of Stresses and Movements in Soil Masses"



● 1-9, VALUES SHOWN IN TABLE 6

**Figure 16. MODULUS PARAMETERS FOR COMPACTED PITTSBURG SANDY CLAY TESTED UNDER UU TEST CONDITIONS**

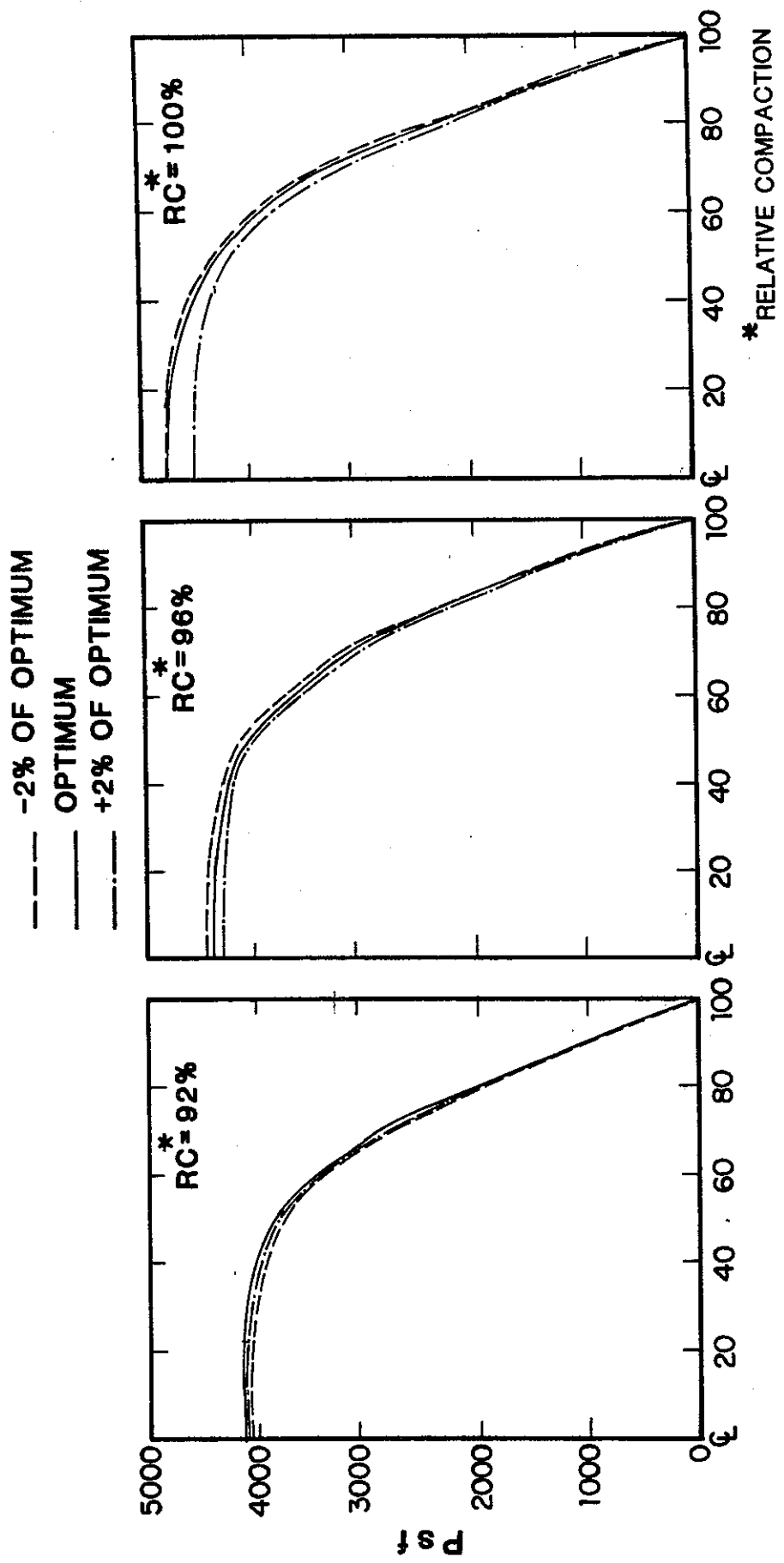
From Wong & Duncan, "Hyperbolic Stress-Strain Parameters for Nonlinear Finite Element Analyses of and Movements in Soil Masses"



● 1-9, VALUES SHOWN IN TABLE 6

Figure 17. POISSONS RATIO PARAMETERS FOR COMPACTED PITTSBURG SANDY CLAY TESTED UNDER UU TEST CONDITIONS (CL-5)

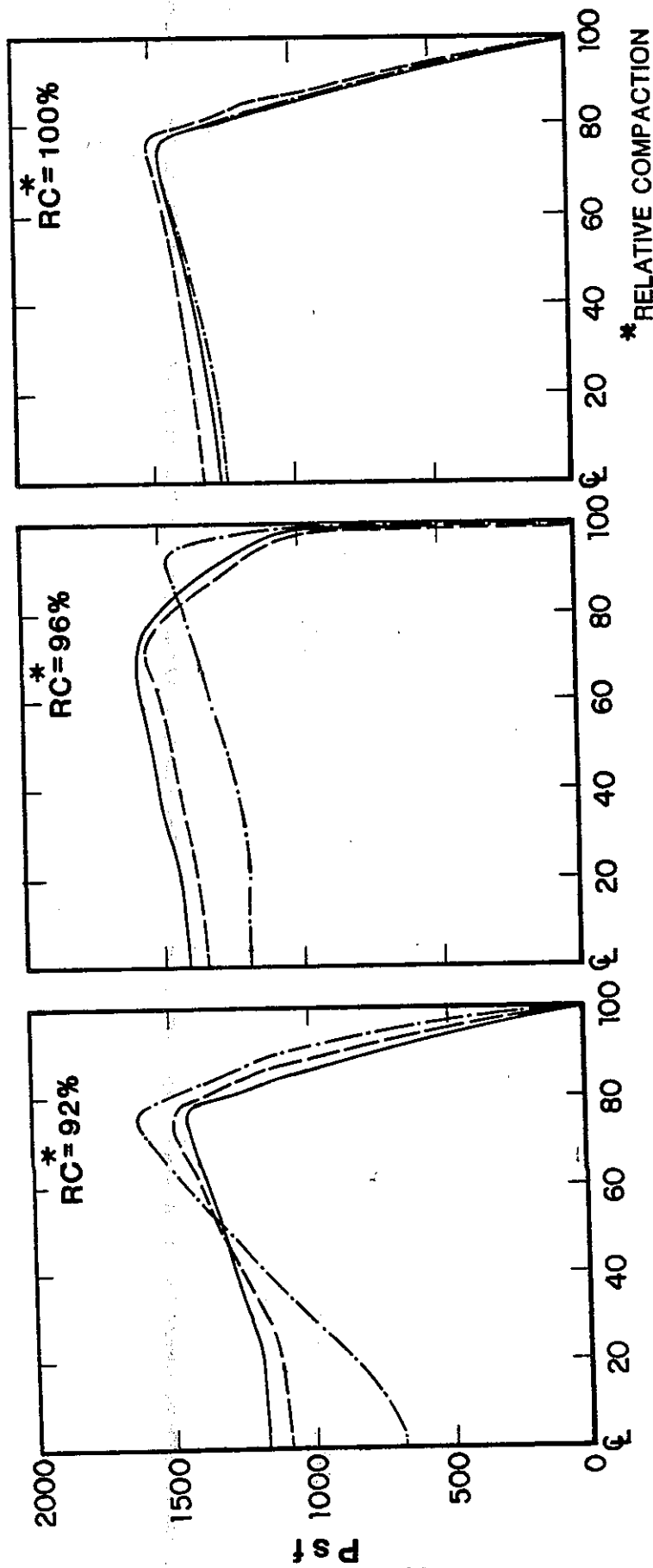
From Wong & Duncan, "Hyperbolic Stress-Strain Parameters for Nonlinear Finite Element Analyses of Stresses and Movements in Soil Masses"



Distance from Centerline (ft.)

Figure 18. VERTICAL STRESS @ MIDHEIGHT OF 100 FT. EMBANKMENT, 1.5 : 1 SLOPES

- - - -2% OF OPTIMUM  
 ——— OPTIMUM  
 - . - . +2% OF OPTIMUM



Distance from Centerline (ft.)

Figure 19. LATERAL STRESS @ MIDHEIGHT OF 100 FT.  
 EMBANKMENT, 1.5 : 1 SLOPES

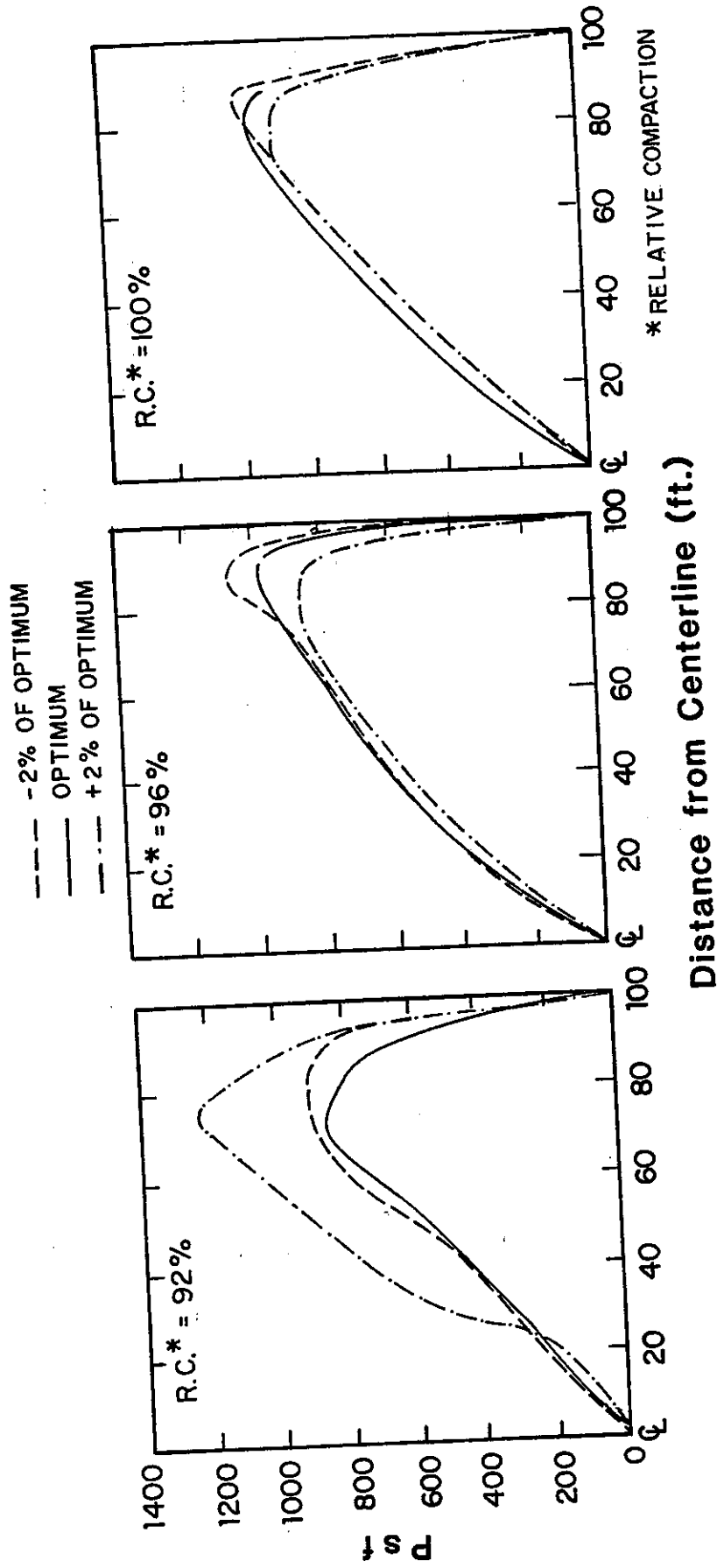


Figure 20. HORIZONTAL SHEAR STRESS @ MIDHEIGHT OF 100 FT. EMBANKMENT, 1.5:1 SLOPES

unit weights corresponding to the lower compactive efforts. Variations in lateral stresses were very minor for each embankment and for each of the compactive efforts and moisture contents considered.

For the material type and the cases considered in this study, the effect on stresses due to variations in compactive effort and moisture content can be summarized as being very minor and negligible in both qualitative and quantitative terms.

Variations of horizontal and vertical movements with depth of embankment are shown in Figures 21 and 22, respectively. The movements shown were computed for three locations for the 100 foot embankment having side slopes of 1.5:1. As in the case of embankment stresses, the behavior of computed movements were similar for the other embankments and are presented in Appendix D.

The following generally apply when considering movements computed due to simulation of embankment construction by the incremental construction technique.

1. Due to symmetry, the lateral movements at centerline are zero.
2. The vertical movement at centerline is greatest at midheight and zero at the top of the embankment.
3. Vertical and lateral movements at midslope are greatest midway between the slope and foundation and have some finite value at the top of the slope.

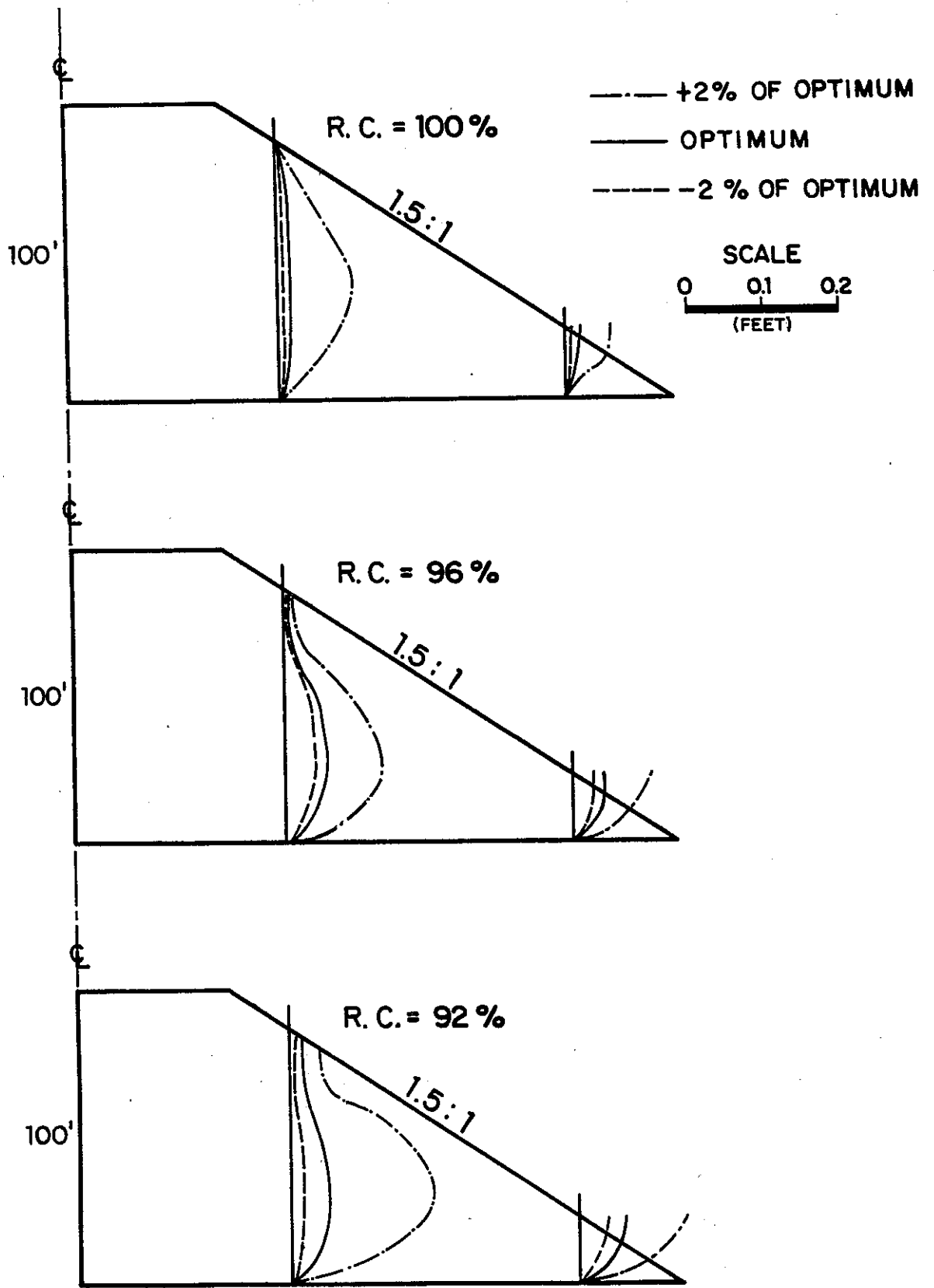


Figure 21. HORIZONTAL MOVEMENTS

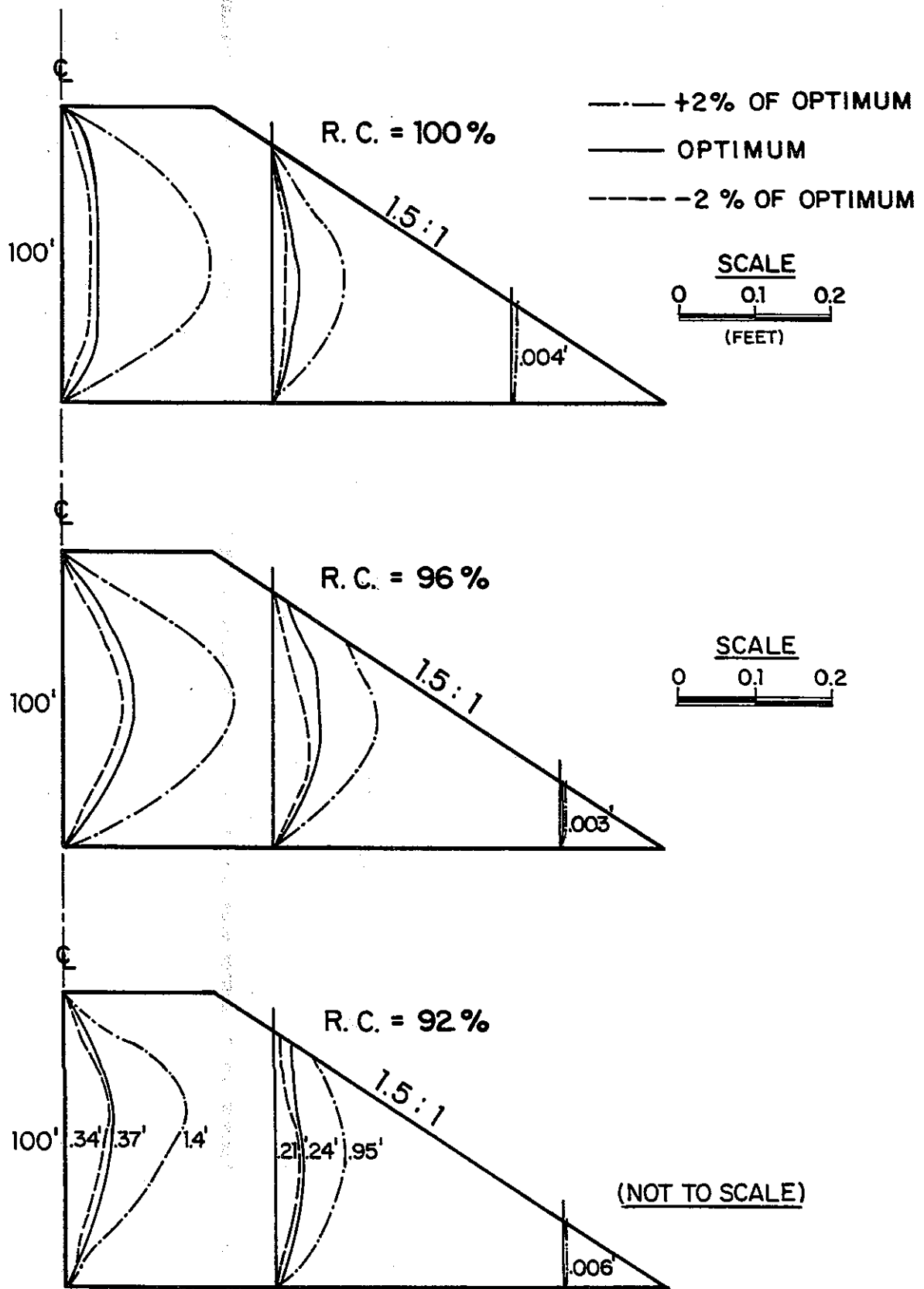


Figure 22. VERTICAL MOVEMENTS

4. Near the toe, the largest vertical and horizontal movements occur at the top of the slope.

The maximum vertical and horizontal movements for each embankment and for each variation in compactive effort and moisture content are shown in Tables 7 and 8, respectively. The data presented in these tables indicate very minor amounts of movement for all of the variables considered in this study. The movements do start to become appreciable, for the 92 percent relative compactive effort, wet of optimum, for both the 50 and 100 foot embankments.

Conventional slope stability analyses were carried out to assess the effect on factors of safety along a circular failure surface due to variations in compactive effort and moisture content. Analyses were carried out for each of the four embankments. The results of these analyses are summarized in Table 9.

Table 9. Minimum Factors of Safety

		100%			96%			92%		
		-2	0	+2	-2	0	+2	-2	0	+2
50'	1.5:1	9.4	7.4	5.9	5.9	6.8	5.8	4.0	4.7	3.2
	2:1	9.8	7.7	5.7	6.5	6.9	5.8	4.4	5.2	3.4
100'	1.5:1	5.9	4.2	3.5	4.1	4.1	3.3	2.6	3.3	2.0
	2:1	5.9	4.6	3.8	4.0	4.3	3.6	2.9	3.2	2.3

HEIGHT 50'	100 %												96 %												92 %											
	-2			0			+2			-2			0			+2			-2			0			+2											
	a	b	c	a	b	c	a	b	c	a	b	c	a	b	c	a	b	c	a	b	c	a	b	c	a	b	c									
1.5:1	.8	9	5	3	5	9	10	50	25	.0	7	11	.1	8.5	14	.6	24	33	1	22	45	2	25	50	3	55	90									
2:1	.1	3	5	.1	3	.07	.08	18	28	.1	7	12	.2	8.6	14	.1	20	33	.05	27	46	.1	34	54	1.54	87										
1.5:1	.7	19	28	1.7	20	62	4	130	200	.7	45	80	.9	60.	100	3	140	230	4	219	337	20	240	369	6	950	1400									
2:1	.4	21	31	.7	20	64	.8	119	186	.2	53	82	.3	60.	99	.7	142	224	.6	216	342	2	233	367	4	730	1359									

Movements in 10<sup>-3</sup> ft

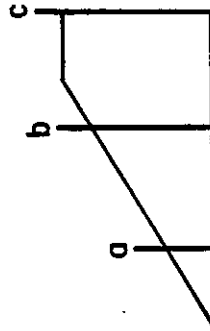


TABLE 7. Maximum Vertical Movements

HEIGHT 50'	HEIGHT 100'	100 %												96 %												92 %											
		-2			0			+2			-2			0			+2			-2			0			+2											
		a	b	c	a	b	c	a	b	c	a	b	c	a	b	c	a	b	c	a	b	c	a	b	c	a	b	c									
1.5:1	.1	.5	0	1.5	2.0	0	9	25	0	3	4	0	5	5.5	0	10	12	0	15	16	0	15	17	0	30	30	0										
2:1	.7	1.2	0	.5	2.0	0	6.4	27	0	2	4	0	.3	5.2	0	7	11	0	12	17	0	.13	19	0	20	30	0										
1.5:1	5	5	0	9	10	0	50	55	0	16	20	0	21	25.	0	40	60	0	.86	94	0	96	110	0	300	400	0										
2:1	3	5	0	6	5.0	0	31	47	0	12	18	0	16	24.	0	37	57	0	57	88	0	64	110	0	163	276	0										

Movements in 10<sup>-3</sup> ft

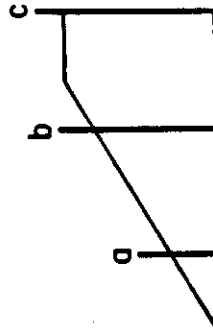


TABLE 8. Maximum Horizontal Movements

Examination of the results in Table 9 shows that the lowest factors of safety correspond to the 92 percent relative compactive effort and wet side of optimum condition. These results corroborate the findings regarding movements which were greatest for the same compactive effort and moisture content condition. The highest factors of safety correspond to the 100 percent relative compactive effort and dry side of optimum condition. This result again corroborates the findings regarding movements since the same compactive effort and moisture content condition resulted in the lowest computed movements.

## SUMMARY AND CONCLUSIONS

This report has attempted to place the concepts regarding embankment construction control, as stated in a 1972 research proposal, in context with the current state of the art in geotechnical engineering. The research proposal postulated the use of elastic parameters corresponding to strain levels of  $10^{-4}$  percent in finite element analyses to determine embankment movements and stresses. It is pointed out in this report, based upon previously published findings, that this usage is inappropriate. Instead, the use of elastic parameters determined at greater levels of strain has been demonstrated to accurately predict construction movements.

Attempts to determine shear modulus values in the field by the resonant footing technique as a part of the originally proposed research met with a limited amount of success. Problems encountered were primarily due to the large amount of sophisticated equipment and critical nature of footing contact with the ground surface. In view of these findings, it might be more advantageous to measure compressional wave velocity in the field and correlate this velocity to field density. It is not suggested that this be done to provide data for use in any type of analysis but instead to provide a means for a nondestructive and rapid test method as suggested by Moore (1973).

Traditional means of ensuring adequate embankment performance have centered around the specification of a minimum level of compaction and the implementation of field testing to determine if this minimum level is achieved during construction. The purpose of specifying a minimum level of

compaction has generally been done to limit settlement and increase the factor of safety against slope failure. Current embankment design methodology does not relate the level of compaction to allowable construction movements or embankment stresses. This report has studied the effect of different levels of compaction and moisture content on embankment stresses and movements for Pittsburg sandy clay.

Results of the studies showed the effect on stresses both in qualitative and quantitative terms to be minor and of no consequence. The computed movements for each embankment and compactive effort and moisture content conditions considered were all quantitatively small. The largest movements were computed for the lowest compactive effort and wet side of optimum condition. This condition also resulted in the lowest factor of safety as determined by conventional stability analyses. Based upon the result of these studies, it could be concluded that the 92 percent compactive effort on the dry or at optimum moisture content would result in tolerable movements and adequate factors of safety and therefore ensure satisfactory embankment performance. It should be noted that this conclusion is only valid for the conditions considered in the analyses, namely soil type, embankment configuration and foundation conditions. The level of compaction which will ensure satisfactory performance for other soil types or embankment conditions can be assessed in a manner similar to the one described in this report.

## RECOMMENDATIONS FOR FUTURE STUDY

- I. In conjunction with additional research concerning compaction control, adequate embankment performance standards or criteria should be formulated relating minimum performance to anticipated service loads.
  
- II. A proposed embankment could be designed with a specified minimum level of compaction so that predetermined embankment performance levels can be attained. Construction and post-construction movements could then be monitored and evaluated.
  
- III. Additional research could be undertaken to determine the practicality of using surface geophysical methods to monitor levels of compactive effort. It is recommended that compressional wave velocities of embankment fills be measured as described by Moore (1973). These measurements could be made in conjunction with nuclear density tests. The effect of time on the compressional wave velocity could, and should, be incorporated in any future study.

RECEIVED  
MAY 10 1964

RECEIVED  
MAY 10 1964

## REFERENCES

1. Afifi, S. S., Richart, F. E., "Stress History Effects on Shear Modulus of Soils," Soils and Foundations, Vol. 13, No. 1, March 1973, Japanese Society of Soil Mechanics and Foundation Engineering.
2. Afifi, S. S., Woods, R. D., "Long-Term Pressure Effects on the Shear Modulus of Soils," Journal of the Soil Mechanics and Foundations Division, ASCE, SM 10, October 1971.
3. Anderson, D. G., Stokoe, K. H., II, "Shear Modulus: A Time Dependent Material Property," Submitted to ASCE Geotechnical Division, March 1975.
4. Anderson, D. G., Woods, R. D., "Comparison of Field and Laboratory Shear Moduli," Proc. In Situ Measurement of Soil Properties, ASCE, Vol. I, Raleigh, N.C., 1975.
5. Chang, J. C., "Stress-Strain Relationships in Large Soil Masses," Report No. CA-DOT-TL-2509-10-76-12, California Department of Transportation, December 1976.
6. Floss, R., Gruber, N., Obermayer, J., "A Dynamical Test Method For Continuous Compaction Control," Proceeding of the Eighth European Conference on Soil Mechanics and Foundation Engineering, Helsinki, Vol. I, pp. 25-30, May 1983.
7. Hardin, B. O., "Suggested Method of Test for Shear Modulus and Damping of Soils by the Resonant Column," ASTM STP 479, p. 516, 1970.

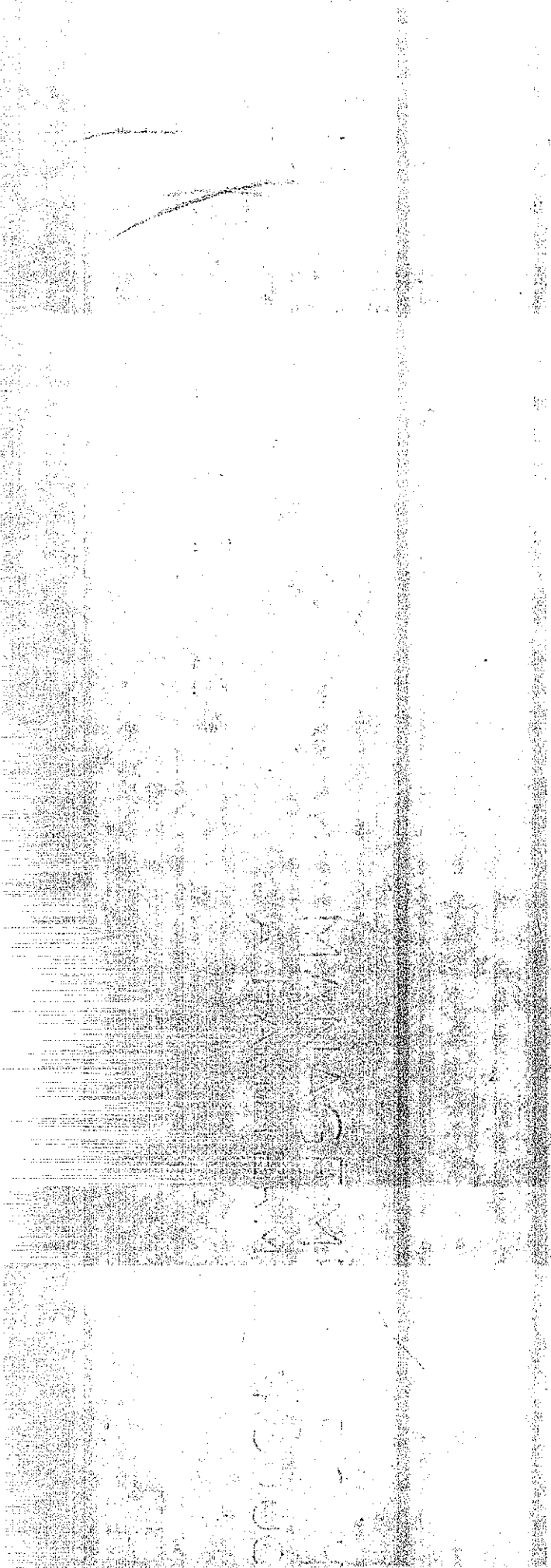
8. Hardin, B. O. and Black, W. L., "Vibration Modulus of Normally Consolidated Clay," Journal of the Soil Mechanics and Foundations Division, ASCE, Vol. 94, No. SM2, Proc. Paper 5833, March 1968, pp. 353-369.
9. Herrmann, L. R., "General Two Dimensional Soils and Reinforced Earth Analysis Program," University of California, Davis, January 1978.
10. Janbu, Nilmar (1963) "Soil Compressibility as Determined by Oedometer and Triaxial Tests," European Conference on Soil Mechanics and Foundation Engineering, Weisbaden, Germany, Vol. 1, p. 115.
11. Kulhawy, F. H., Duncan, J. M., "Nonlinear Finite Element Analysis of Stresses and Movements In Oroville Dam," Report No. TE 70-2, Department of Civil Engineering, Institute of Transportation and Traffic Engineering, 1970.
12. Kulhawy, F. H., Duncan, J. M. and Seed, H. B., "Finite Element Analysis of Stresses and Movements in Embankments During Construction," Report No. TE 69-4, Office of Research Services, University of California, Berkeley, California, 1969.
13. Marcuson, W. F., III, Wahls, H. E., "Time Effects on Dynamic Shear Modulus of Clays," Journal of the Soil Mechanics and Foundations Division, ASCE, Vol. 98, No. SM12, December 1972.
14. Moore, R. W., "Seismic Test For Compaction of Embankment, Base Course, and Pavement Layers," Report No. FHWA-RD-73-31, Federal Highway Administration, Offices of Research and Development, Washington, D.C., April 1973.

15. Schwab, E. F., Pregl, O., Kieres, W., "Compaction Control With the Compactometer," Proceedings of the Eighth European Conference on Soil Mechanics and Foundation Engineering, Helsinki, May 1983, Vol. I, pp. 73-82.
16. Seed, H. B., Idriss, I. M., "Soil Moduli and Damping Factors for Dynamic Response Analyses," Earthquake Engineering Research Center, Report No. EERC 70-10, University of California, Berkeley, December 1970.
17. Sowers, George, F. A., "There Were Giants on the Earth in Those Days," Journal of the Geotechnical Engineering Division, ASCE, Vol. 107, No. GT4, April 1981.
18. U.S. Army E.R.D.V. (1950), "An Investigation of the Compaction of Soils by Vibration," A research report sponsored by the Department of Army, Engineering Research and Development Laboratories, The Engineering Center, Fort Belvoir, Virginia, p. V-16, March 1950.
19. Stokoe, K. H., II, Abdel-razzak, K. G., "Shear Moduli of Two Compacted Fills," Proc. In Situ Measurement of Soil Properties, ASCE, Vol. I, Raleigh, N.C., pp. 66-92, 1975.
20. Vrymoed, J. L., "Dynamic FEM Model of Oroville Dam," Journal of the Geotechnical Engineering Division, ASCE, Vol. 107, No. GT8, August 1981.
21. Weiler, W. A., Kulhawy, F. H., "Factors Affecting Stress Cell Measurements in Soil," Journal of the Geotechnical Engineering Division, ASCE, Vol. 108, No. GT12, December 1982.

22. Wong, K. S., Duncan, J. M., "Hyperbolic Stress-Strain Parameters For Nonlinear Finite Element Analyses of Stresses and Movements in Soil Masses," Report No. TE-74-3, Department of Civil Engineering, University of California, Berkeley, July 1974.

## APPENDICES

	<u>Page</u>
A    Proposal For A New FHWA Financed Research Project, March 1972	A-1
B    Resonant Column Test Data	B-1
C    Plots of Embankment Stresses	C-1
D    Plots of Embankment Movements	D-1
E    Resonant Footing Test Procedure	E-1
F    Resonant Column Test Procedure	F-1



APPENDIX A

Proposal For A New FHWA-Finance Research Project

PROPOSAL FOR A NEW FHWA-FINANCE  
RESEARCH PROJECT

TITLE

Dynamic Approach to Embankment Construction Control  
(Formerly "Dynamic Approach to Compaction Control")

PROBLEM

Current practice in the design and construction of embankments requires the evaluation and control of stability and settlement. The problems associated with the traditional methods of embankment design analysis and construction control are as follows:

1. Laboratory shear strength measurements cannot be effectively employed for construction control purposes.
2. Relative compaction is an indirect means of assessing soils strength and controlling settlement.
3. Limit equilibrium methods of analysis do not permit the evaluation of stress-strain behavior of an embankment under either a static or dynamic loading condition.
4. Limit equilibrium analysis is essentially a pass-fail, look at an entire embankment-foundation system which does not permit evaluation of local variations in stress and strain.

BACKGROUND INFORMATION

Determination of the stability of an embankment foundation system usually involves analysis by a limit equilibrium method which assumes movement by a sliding mass along either a planar or circular failure surface. Data input includes embankment geometry, density and the shear strength parameters of the soil as determined by laboratory triaxial compression tests under conditions, hopefully, representative of the most severe loading conditions which will occur within the design life of the facility. These tests are conducted on undisturbed samples of foundation soil and remolded specimens of embankment material. The construction of the embankment must be controlled to insure that the average soil properties of the embankment materials are at least equal in quality to those assumed in the design. Since construction control by laboratory measurement of shear strength is not practical due to its time-consuming and expensive nature and field strength measurements, particularly on cohesionless soils, are not possible, basic construction control is exercised by compacting the soil to a minimum specified density which is comparable to that of the soil specimens on which laboratory shear strength measurements were made.

Past investigations, however, have indicated only a very general relationship between density and shear strength. Thus compaction to a fixed and in some respects arbitrary density may require the expenditure of more effort and time than is necessary to achieve the minimum required stability.

A point of diminishing return with respect to increased strength for a given embankment material may be achieved at say 87 percent of relative compaction rather than the required 90 percent. As stated in a report on the measurement of embankment density by the seismic method by Weaver and Rebull (1967)<sup>36</sup>:

"Improvements in density measuring techniques will not improve efforts for effective quality control of embankment compaction, because soil density is not capable of indicating an acceptable quality level of compaction. At best, density has only an incidental relationship to the soil condition brought about by "adequate" compaction, which produces "adequate" performance."

Similarly, a specified minimum relative compaction is also utilized to assure a minimum compressive settlement within the embankment. Densification, also, is an indirect control since settlement is also a function of the geometrical configuration of the embankment and foundation system.

The use of conventional limit equilibrium methods of analysis do not offer an insight into the stress-strain-time behavior of all parts of the embankment under either static or dynamic loading conditions. A realistic dynamic loading design requires analysis of the time dependent response of the embankment which includes the damping effect of the embankment material.

Recent advances in technology have resulted in an increased use of the finite-element method for analyzing the stress-strain-time characteristics of soil masses and soil-structure systems. This method enables prediction of the stress-strain characteristics of embankments comparing reasonably well with field measurements in the static state or under dynamic loading conditions. The finite-element method is an analytical approach based on theory of elasticity. The essential soil parameters required are density, the modulus of elasticity, the Poisson's ratio, and the damping coefficient. These parameters can be measured in the laboratory by the resonant-column apparatus and by various seismic tests in the field.

In order to extensively utilize the finite-element analysis to solve soil-structure problems, research is currently needed to:

- 1) Improve accuracy in the determination of elastic parameters of soils both by laboratory and field methods.
- 2) Verify the results of predicted stress-strain-time behavior of embankments by comparing the data with those obtained from field instrumentation.
- 3) Obtain relationship between the method and effect of compaction and the elastic moduli of soil.

The evaluation of elastic moduli and Poisson's ratio using non-linear stress-strain curves obtained from triaxial compression tests of soil samples was recently reported by Chang and Duncan (1970) (6). Using a modified approach, the Materials and Research Department of the California Division of Highways developed an empirical expression for calculating tangent modulus (M&R Report 632509-4, "Stress Deformation in Jail Gulch Embankment"). This empirical equation is expressed in terms of ultimate shear strength parameters and overburden loads as

$$E_t = [(A+B) (1-\sin\phi) \gamma H] \left[ 1 - \frac{\gamma H (1-\sin\phi) \sin\phi}{2C \cos\phi + \sin\phi \left( \frac{\gamma H}{N_\phi} - \frac{2C}{\sqrt{N_\phi}} \right)} \right]^2 \quad (1)$$

Where:  $E_t$  = tangent modulus of elasticity in pounds per square foot;

$C$  = ultimate cohesion parameter in pounds per square foot;

$\phi$  = ultimate internal friction angle in degrees;

$\gamma$  = density of soil in pounds per cubic foot;

$H$  = depth of overburden load in feet;

$N_\phi$  = Rankine's earth pressure coefficient =  $\tan^2(45^\circ - \frac{\phi}{2})$ ;

$A, B$  = Dimensionless constants obtained from plots of initial moduli and confining pressure.

Using the elastic moduli calculated from this equation, the stress-deformation behavior of the Jail Gulch embankment was analyzed using the finite-element method. The calculated results agree reasonably well with those obtained in the field.

A more direct laboratory testing technique to determine the elastic constants of soil using the resonant-column apparatus has been available for a number of years. With this method a cylindrical column of the material is set into resonance by a variable frequency exciter. The wave velocities and the corresponding elastic properties are then computed from the dynamic response of the sample. The equations for computing the elastic constants from the resonant-column tests were given by Pickett (1945)<sup>(31)</sup>. A resonant-column apparatus for measuring elastic constants of soils was described by Hardin and Music (1965)<sup>(18)</sup>, Drenevich (1967)<sup>(10)</sup>, and Richart, Hall, and Woods (1970)<sup>(34)</sup>. A testing procedure using this resonant-column apparatus has been recommended by Hardin (1970)<sup>(15)</sup> in an ASTM publication.

By laboratory testing of cohesionless soils in resonant-column apparatus, Hardin and Richart (1963)<sup>(19)</sup> were able to establish empirical expressions relating shear modulus to void ratio and confining pressure. For round-grained sands ( $0.3 \leq e \leq 0.8$ ), it was suggested that,

$$G = \frac{2,630 (2.17-e)^2}{1+e} (\sigma_o)^{\frac{1}{2}} \quad (2)$$

and for angular-grained sands ( $0.66 \leq e \leq 1.3$ ), the empirical equation was found to be,

$$G = \frac{1,230 (2.973-e)^2}{1+e} (\sigma_o)^{\frac{1}{2}} \quad (3)$$

Where:  $G$  = shear modulus of elasticity in pounds per square inch;  
 $\sigma_o$  = confining pressure in pounds per square inch;  
 $e$  = void ratio.

Hardin and Black (1968)<sup>(17)</sup> suggested that Equation (3) can also be used to obtain a reasonable approximation of the shear modulus of a normally consolidated clay with low surface activity. Richart, Hall and Woods (1970)<sup>(34)</sup> reported that Poisson's ratio generally varies from 0.25 to 0.35 for cohesionless soils and from 0.35 to 0.45 for cohesive soils. They suggested that, for ordinary design purpose, no significant error is introduced if Poisson's ratio is assumed as 1/3 for cohesionless soils and as 0.4 for cohesive soils. Once the shear modulus of elasticity and Poisson's ratio are determined, Young's modulus of elasticity can be computed by equation(4) derived from theory of elasticity,

$$E = 2 (1 + \mu) G. \quad (4)$$

Where: E = Young's modulus of elasticity;

$\mu$  = Poisson's ratio.

The in situ measurement of elastic properties of soils can be accomplished by the wave propagation approach. In an infinite elastic body a disturbance may be propagated by wave of volume change, designated as the compression wave (or P-wave), and by wave or distortion at constant volume designated as the shear wave (or S-wave). In a semi-infinite, elastic, half space, a third type of wave also develops at and near the surface. This surface wave has been designated as the Rayleigh wave or R-wave (Rayleigh, 1885)<sup>(33)</sup>. The velocities of the P-wave and S-wave have been given (Knopoff, 1952)<sup>(25)</sup> as a function of elastic constants,  $\mu$  and G, as follows:

$$V_s = \sqrt{\frac{G g}{\gamma}} = \sqrt{\frac{G}{\rho}}, \quad (5)$$

$$V_p = V_s \sqrt{\frac{2(1-\mu)}{1-2\mu}}, \quad (6)$$

in which  $V_s$  = S-wave velocity,  $V_p$  = P-wave velocity,  $V_R$  = R-Wave velocity, G is the shear modulus of elasticity,  $\gamma$  is the unit weight, g is the gravitational acceleration, and  $\rho$  is the mass density of the elastic material. Table 1 (Knopoff, 1952)<sup>(25)</sup> gives the theoretical value of the ratio of the velocities of P-wave and R-wave to S-wave velocity as a function of the Poisson's ratio.

TABLE 1

Poisson's Ratio $\mu$	$\frac{V_R}{V_s}$	$\frac{V_p}{V_s}$
0	0.875	1.418
0.1	0.893	1.493
0.2	0.911	1.626
0.3	0.927	1.869
0.4	0.942	2.439
0.5	0.955	0

Waves in non-isotropic or layered material are described by Leet (1950)<sup>(27)</sup> and by Ewing, Jardetzky, and Press (1957)<sup>(12)</sup>.

Using the wave-propagation approach the following methods are usually employed to measure the in-place modulus of elasticity of soils:

- (1) Seismic tests to determine the compression wave velocities through the soil mass.
- (2) Vibration tests to determine the shear and surface wave velocities through the soil mass.
- (3) A combination of the above tests to determine the natural frequency of soils and attenuation characteristics.

When sustained vibrations are induced into a soil mass, concentric waves are propagated outward from the source. The waves require a time to travel a distance through the soils. According to Jones (1958) <sup>(22)</sup>, if the waves are propagated at a known frequency  $f$ , then

$$V = \lambda f. \quad (7)$$

Where:  $V$  = wave velocity;

$\lambda$  = wave length;

$f$  = frequency of the vibrator in cycles.

This wave velocity depends upon the type of wave and ratio of the elasticity of the medium to its mass density  $\rho$ . The relation of shear modulus of elasticity,  $G$ , to shear-wave velocity,  $V_s$ , is given by Equation 5. As shown by Table 1, the Poisson's ratio is a function of the ratio of the compression wave velocity and shear wave velocity. According to Heiland (1963) <sup>(20)</sup> the relation between the Poisson's ratio and ratio of compression wave velocity and shear wave velocity is

$$\mu = \frac{V_r - 2}{2(V_r^2 - 1)}. \quad (8)$$

Where:  $V_r = \frac{V_c}{V_s} = \frac{\text{compression wave velocity}}{\text{shear wave velocity}};$

$\mu$  = Poisson's ratio.

With the in situ shear modulus of elasticity,  $G$ , and the Poisson's

ratio,  $\mu$ , known, the in-place Young's modulus of elasticity,  $E$ , can be computed by Equation 4.

In summary, theories and experimental techniques and procedures for determining both laboratory and in situ elastic properties of soils are available. Because soil masses are usually not homogeneous and isotropic in the field, and soil properties vary significantly, long-range research is needed to establish standardized procedures and to determine the elastic constants for each group or any combination of soils at different compaction efforts. The important factors which affect the determination of elastic constants of soils require extensive laboratory and field tests.

PERTINENT LITERATURE

1. Abbott, P. A., (1967), Simmons, K. B., Reiff, C. M., and Mitchell, S., "Recent Soil Stress Gage Research," Proceedings, International Symposium on Wave Propagation and Dynamic Properties of Earth Materials, University of New Mexico, pp. 221-238.
2. Afifi, S. S. and Woods, R. D., (1971), "Long-Term Pressure Effects on Shear Modulus of Soils," Journal of Soil Mechanics and Foundation Division, Proceedings of ASCE, Vol. 97, No. SM 10.
3. Bamert, E., Schmitter, S., and Weber, M., (1967), "A Field Method of Determining Soil Properties by Impact Loading," Proceedings, International Symposium on Wave Propagation and Dynamic Properties of Earth Materials, University of New Mexico, pp. 265-274.
4. Barkan, D. D., (1962), Dynamics of Bases and Foundations, McGraw-Hill Book Co., Inc., New York.
5. Biot, M. A., (1956), "Theory of Propagation of Elastic Waves in a Fluid Saturated Porous Solid," Journal, Acoustical Society of America, Volume 28.
6. Chang, C. Y. and Duncan, J. M., (1970), "Nonlinear Analysis of Stress and Strain in Soils," Journal of the Soil Mechanics and Foundation Division, Proceedings of ASCE, Vol. 96, SM5, Sept. 1970.
7. Chang, J. C. and Okasaki, D. K., (1971), "Stress and Deformations in Jail Gulch Embankment," Materials and Research Department, California Division of Highways, Report No. 632509-4.
8. Casagrande, D. R., (1967), "Dynamic Soils Investigation for Ground Radius Effects Study, Redstone Arsenal, Alabama," U. S. Army Engineer Waterways Experiment Station, Report No. 4-910.
9. DeRoock, B. and Cooper, A. W., (1967), "Relation Between Propagation Velocity of Mechanical Waves Through Soil and Soil Strength," Proceedings, Symposium on Wave Propagation and Dynamic Properties of Earth Materials, University of New Mexico, pp. 905-912.

10. Drenevich, V. P., (1967), "Effect of Strain History on the Dynamic Properties of Sand," Ph.d. Dissertation, University of Michigan.
11. Drenevich, V. P., Hall, J. R., and Richart, F. E., (1967), "Effect of Amplitude on Vibration of the Shear Modulus of Sand," Proceedings, Symposium on Wave Propagation and Dynamic Properties of Earth Materials, University of New Mexico, pp. 189-200.
12. Ewing, W., Jardetzky, W. S., and Press, F., (1957), "Elastic Waves in Layered Media," McGraw-Hill Book Co., 380 pp.
13. Hadala, P. F., (1967), "The Effect of Placement Method on The Response of Soil Stress Gages," Proceedings, Symposium on Wave Propagation and Dynamic Properties of Earth Materials, University of New Mexico, pp. 255-264.
14. Hardin, B. O., (1965), "The Nature of Damping in Sands," Journal, Soil Mechanics and Foundations Division, ASCE, Volume 91.
15. Hardin, B. O., (1970), "Suggested Methods of Test for Shear Modulus and Damping of Soils by the Resonant Column," ASTM, Special Technical Publication No. 479.
16. Hardin, B. O. and Black, W. L., (1966), "Sand Stiffness Under Various Triaxial Stresses," Journal, Soil Mechanics and Foundations Division, ASCE, Volume 92.
17. Hardin, B. O. and Black, W. L., (1968), "Vibration Modulus of Normally Consolidated Clay," Journal, Soil Mechanics and Foundations Division, ASCE, Volume 94.
18. Hardin, B. O. and Music, J., (1965), "Apparatus for Vibration of Soil Specimens During Triaxial Test," Symposium on Instruments and Apparatus for Soils and Rocks, STP-392, ASTM, pp. 55-74.
19. Hardin, B. O. and Richart, F. E., (1963), "Elastic Wave Velocities in Granular Soils," Journal, Soil Mechanics and Foundation Division, ASCE, Volume 89, SM1, pp. 33-65.
20. Heiland, C. A., (1963), "Geophysical Exploration," Hafner Publishing Company, New York, N.Y.

21. Heller, L. W. and Weiss, R. A., (1967), "Ground Motion Transmission from Surface Sources," Proceedings, Symposium on Wave Propagation and Dynamic Properties of Earth Materials, University of New Mexico, pp. 71-84.
22. Jones, R., (1958), "In-situ Measurement of Dynamic Properties of Soil by Vibration Methods," Geotechnique, Vol. 8, 1-21.
23. Jones, R., (1962), "Surface Wave Technique for Measuring Elastic Properties and Thickness of Roads, Theoretical Development," British Journal Applied Physics, V 13 (1), pp. 21-29.
24. Jones, R., Thrower, E. N., and Garfield, E. N., (1967), "Surface Wave Method," Proc. Second Internat. Symp. on the Structural Design of Asphalt Pavements, pp. 404-421.
25. Knopoff, L., (1952), "On Rayleigh Wave Velocities," Seismological Society of America, Bulletin V. 42, pp. 207-308.
26. Ladd, C. C., (1964), "Stress-Strain Modulus of Clay from Undrained Triaxial Tests," MIT, Department of Civil Engineering. Paper also appears in "ASCE Technical Conference on Design of Foundations for Control of Settlements," Northwestern University.
27. Leet, L. Don, (1950), "Earth Waves," Harvard U. Press and J. Wiley, p. 122.
28. Kennedy, T. E. and Hendron, A. J., Jr., (1966), "The Dynamic Stress-Strain Relation for a Sand as Deduced by Studying Its Shock-Wave Propagation Characteristics in a Laboratory Device," Report No. 1-831, U. S. Army Engineers Waterways Experiment Station.
29. Maxwell, A. A., and Fry, Z. B., (1967), "A Procedure for Determining Elastic Moduli of In Situ Soils by Dynamic Techniques," Proceedings, Symposium on Wave Propagation and Dynamic Properties of Earth Materials, University of New Mexico, pp. 913-920.
30. Olson, R. E. and Parola, J. R., (1970), "Dynamic Shearing Properties of Compacted Clay," Proceedings, Symposium on Wave Propagation and Dynamic Properties of Earth Materials, University of New Mexico, p. 170.
31. Pickett, G., (1945), "Equations for Computing Elastic Constants from Flexural and Torsional Resonant Frequencies of Vibration of Prisms and Cylinders," Proceedings, ASTM, V. 45, pp. 846-865.

32. Rao, H. A. B., (1966), "Wave Velocities Through Partially Saturated Sand-Clay Mixtures," Research Report R66-13, Soils Publication No. 194, Department of Civil Engineering, MIT.
33. Rayleigh, L., (1885), "On Wave Propagated Along the Plane Surface of an Elastic Solid," Proceedings of the London Mathematical Society, V. 17, pp. 4-11.
34. Richart, R. E., Jr., Hall, J. R., and Woods, R. E., (1970), Vibrations of Soils and Foundations, Prentice-Hall, Englewood Cliffs, N. J.
35. Timoshenko, S. P. and Goddier, J. N., (1951), Theory of Elasticity, McGraw-Hill Book Co., New York.
36. Weaver, Robert J. and Rebull, Peter M. (1967) "Determination of Embankment Density by the Seismic Method", Physical Research Report No. RR67-5, New York State Department of Public Works, 1967 pp. 62.
37. Wilson, S. D. and Dietrich, R. J., (1960), "Effect of Consolidation Pressure on Elastic and Strength Properties of Clay," Proceedings, ASCE Research Conference on Shear Strength of Cohesive Soils, Boulder, Colorado, pp. 419-435.

### OBJECTIVES

The primary objective of this research project is to develop a standard procedure to evaluate and directly control the quality of a compacted fill in terms of its elastic properties. This will enable the advance tool of finite-element method of analysis to be extensively utilized for design and analysis of embankments. To achieve this objective, the present research project is intended specifically:

- (1). To develop or improve the existing laboratory testing technique to evaluate the elastic properties of soil;
- (2). To establish field testing techniques to evaluate in situ elastic properties of soil for the purpose of construction control;
- (3). To evaluate the performance and behavior of compacted fill through measured elastic properties and by finite-element analysis, and;
- (4). To develop the capability of evaluating the dynamic response of embankment to earthquake shocks.

### IMPLEMENTATION

Implementation of the results of this study will involve initiation of changes in the present practice of embankment design and construction. Embankment designs will be developed for both static and dynamic loading conditions based upon the results of laboratory dynamic tests of elastic properties of soils, in addition to the presently employed triaxial shear tests.

Similarly, procedures will be initiated for specification and construction control of embankments in the field primarily by in situ seismic testing of elastic constants and the evaluation of response of embankment to the induced vibrations.

### BENEFITS ANTICIPATED

Improved techniques of laboratory and field testing to determine elastic moduli of soils and the means of controlling construction of the embankments to meet the required elastic properties established by this study will initiate a new approach to highway design and construction of highway embankments. By using the tested elastic moduli of soils in the finite-element analysis, the stress-deformation behavior of embankments and other structures that interact with the soil (retaining walls, bridge abutments, culverts, etc.) can be predicted under any static and dynamic loadings. Thus, safer and more economical highway soil-structure systems can be constructed.

## PROPOSED PROCEDURE (Work Plan)

### 1. Review of the Method of Analysis

Initially a comprehensive review of the technology concerning the dynamic approach in determining the elastic properties of soils will be made. This will include theoretical consideration of the problem and a review of current laboratory and field testing apparatus and procedures. Data pertaining to the elastic moduli of soils available in the literature and in the previous M&R projects will be compiled for possible correlation. Empirical equations available in the literature may be evaluated using these data.

### 2. Laboratory Determinations of Elastic Constants

It is proposed to conduct laboratory tests of elastic constants in a triaxial cell using resonant-column apparatus. Both longitudinal and torsional vibrations may be applied to evaluate the elastic moduli, the Poisson's ratio, and the damping constant of soil specimen. The resonant-column test is especially useful in the small elastic-strain range, where the finite-element-method of analysis is considered most applicable. Undisturbed samples and laboratory fabricated samples will be tested under various confining pressures to study the effect of depth and confining pressures on the elastic moduli of soil with different densities and moisture content.

### 3. Field Determinations of Elastic Constants

Evaluations of dynamic soil properties from field tests are required. Essentially this will involve two methods of vibratory measurements.

- a. Impact type vibration for measurement of P-wave velocity. This is the so-called seismic method commonly used in refraction surveys. Only a simple seismic timer and its accessories are required.
- b. Steady-state type vibration for measurement of S-wave and R-wave velocities. This requires a source of harmonic vibration at the surface of soil and the determination of wave length of the resulting surface waves at various distances from the vibrating source. Electromagnetic oscillator or rotating mass type oscillator may be used as the source of vibration. An oscilloscope and its accessories can be used to measure the vibration, or it can be recorded with a standard seismograph. It is possible, using a computer, to analyze the dispersed train of surface waves (Rayleigh and Love) which follows the faster compressional wave to determine shear wave distribution for simple two-layer systems. These surface waves will properly delineate shear wave velocities even if rigidity decreases downwards.

Using the measured wave velocities data the shear modulus of elasticity, Young's modulus of elasticity, and Poisson's ratio can be calculated. The attenuation characteristics of vibration may also be studied for evaluation of the damping constant of the soil.

#### 4. Correlation Study of Laboratory and Field Tests

The results of field dynamic tests and laboratory tests on undisturbed or remolded samples will be analyzed for correlation purposes. This study is expected to provide empirical equations that will enable calculation of the elastic properties of soils. In addition to resonant-column test results, conventional laboratory test data from unconfined compression tests, triaxial compression tests, consolidation tests, and compaction tests may be used for this correlation study.

#### 5. Study of the Relationship Between Compaction Effort and Elastic Moduli

The elastic moduli of soil may vary, depending on the compaction method and effort. The relationship between different compaction methods and the elastic moduli of soil will be investigated. An effort will be made to determine if a constant modulus of elasticity for each type of soil can be established by a specified method and effort of compaction.

#### 6. Field Instrumentation

Test embankments will be selected for instrumentation to measure the stress-strain-time characteristics within the soil mass. This may include pressure cells to measure stress, piezometers for measurements of pore water pressures, and strain device for measurements of vertical and horizontal strains. The data observed from field instrumentation will be used to compare with its predicted behavior.

#### 7. Finite-Element-Analysis

The stress-strain of the embankment will be analyzed by the finite-element method using the field and laboratory elastic constants of the soil mass. The calculated stress-strain data will be compared to that obtained in the field to assess the validity of the analysis. The behavior of embankments under both static and dynamic loading conditions will be studied.

The proposed research procedure as discussed above will be divided into three phases as follows:

PHASE I - LABORATORY TESTS (FISCAL YEAR 1972-73)

1. Complete a literature search;
2. Acquire resonant-column apparatus and electronic control system for laboratory tests;
3. Set-up and calibrate laboratory test facilities;
4. Collect typical samples of clay, sand, gravel, or crushed rock;
5. Conduct laboratory pilot tests on soil samples; and
6. Analyze laboratory test data to determine the elastic properties of each type of soil sample and evaluate the results.

PHASE II - FIELD TESTS (FISCAL YEAR 1973-74)

1. Continue laboratory tests;
2. Acquire field test equipment and electronic control systems;
3. Conduct field pilot tests to determine the in-place elastic properties of each type of soil (clay, sand, gravel and crushed rocks);
4. Analyze field test data to determine those variables which most affect the elastic constants;
5. Study elastic properties of soils in relation to compaction effort;
6. Correlate the laboratory and field test results; and
7. Prepare an interim report.

PHASE III - INSTRUMENTATION AND IN-PLACE TEST OF  
CONSTRUCTION PROJECT (FISCAL YEAR  
1974-75)

1. Select test embankment sections from District's construction projects;
2. Obtain soil samples of embankment material for laboratory correlation tests;
3. Acquisition and installation of field instrumentation to measure stress-strain behavior in the embankment;
4. Accumulate embankment stress-strain data during construction and after completion of construction;
5. Conduct field seismic and vibration tests to determine the in-place elastic properties of embankment material during and after completion of construction;
6. Finite-element-analysis using the elastic properties obtained from laboratory and field tests;
7. Correlate the study of the stress-strain data relative to the measured and predicted results;
8. Prepare a standard procedure of field tests for embankment construction control; and
9. Prepare the final report.

EQUIPMENT

The major apparatus needed in this research project are described as follows:

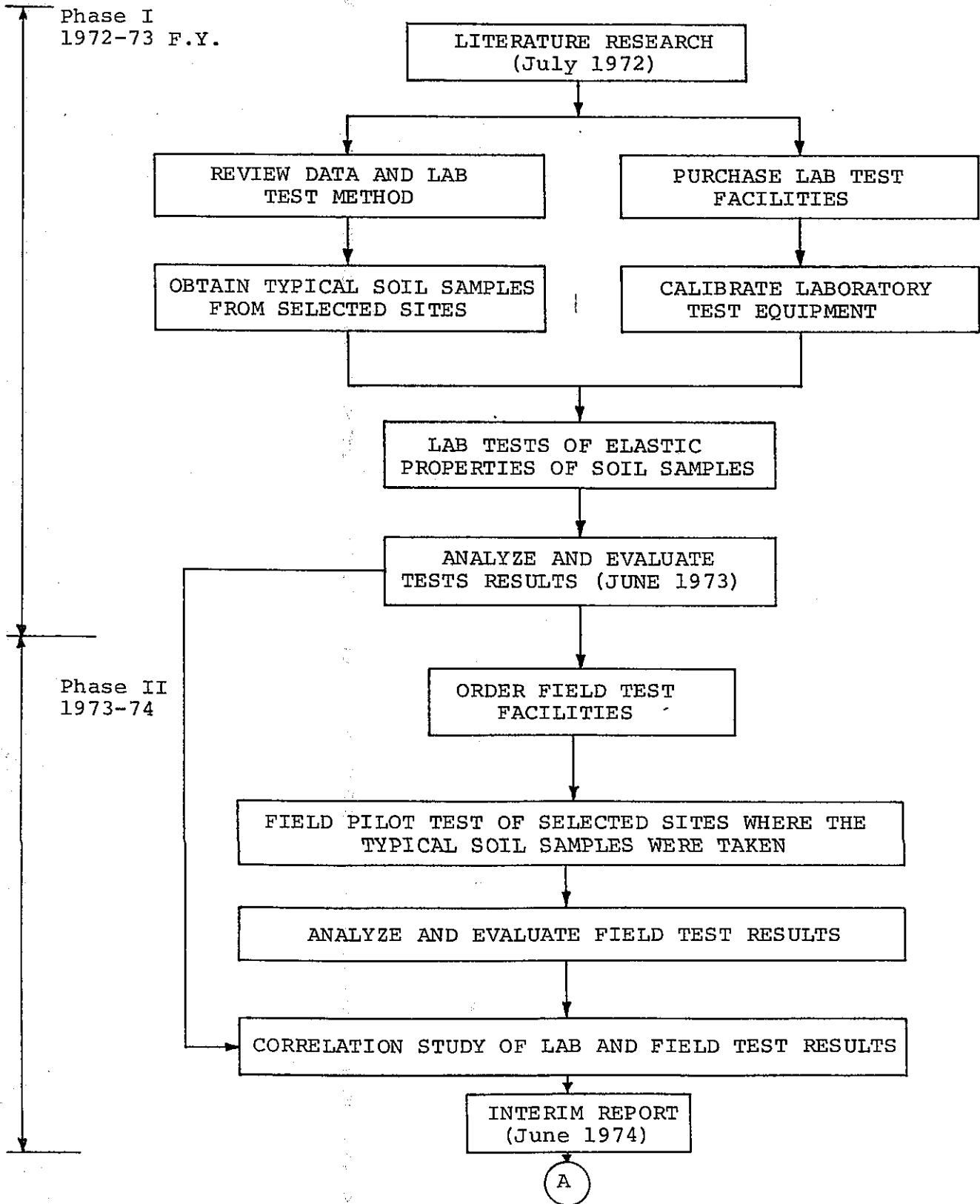
1. Resonant Column Basic Unit. This is a laboratory test apparatus for determining the elastic moduli, Piosson's ratio, and the damping constant of a cylindrical soil specimen (undisturbed or laboratory compacted) in a triaxial chamber. The basic unit consists of a triaxial chamber, an accelerometer, magnets, coils, a load cell, a specimen cap, a pneumatic apparatus support for test set-up, connecting wires, calibration charts, and computational aids for the test. The apparatus is manufactured under patent by Soil Dynamic Instruments, Inc., of Lexington, Kentucky.

2. Resonant Column Electronic Unit. This is an electronic readout device for the resonant-column test apparatus. It includes a bridge amplifier for the load cell, an AC meter with maximum sensitivity range of 1 mv RMS full scale with DC output, a digital DC voltmeter, and a Tektromix X-Y oscilloscope. This electronic unit provides for digital readout of all voltages, phase comparisons and observation of the wave form. This unit can be obtained from Soil Dynamic Instruments, Inc., of Lexington, Kentucky.
3. Seismograph and Accessories. This is a field-test device commonly used for refraction survey. The compression wave velocity and depth of layered soil deposits may be obtained. The apparatus includes an electronic seismic timer, a hammer, a vibration transducer, and wires. An oscilloscope may be used in place of the electronic timer to display the wave form.
4. Oscillator. This device is used for a field test to produce a steady-state ground vibration for evaluation of the dynamic moduli of soil from the measurements of the vibration-induced surface waves. This steady-state vibration can be produced by either an electromagnetic oscillator or a rotating-mass type mechanical oscillator. An electromagnetic oscillator is used to produce high-frequency (small wave length) vibrations while the rotating-mass type oscillator is used for producing low frequency vibrations. In order to analyze surface wave trains, it may be necessary to produce vibrations over a range of frequencies. It will, at least, be necessary to have equipment capable of producing steady state vibrations at low and at high frequencies.
5. Two-Channel Vibration Recorder. This device will be used in the field to measure the wave form of the ground vibration produced by the oscillators. The system should be able to record two simultaneous vibrations on a common time basis. A portable system is required for convenient transport in the field. The system consists of a dual-channel recorder with two velocity transducers. Some of the requirements in this system is the sensitivity and chart speed of the recorder, and the sensitivity and natural frequency of the velocity transducers.

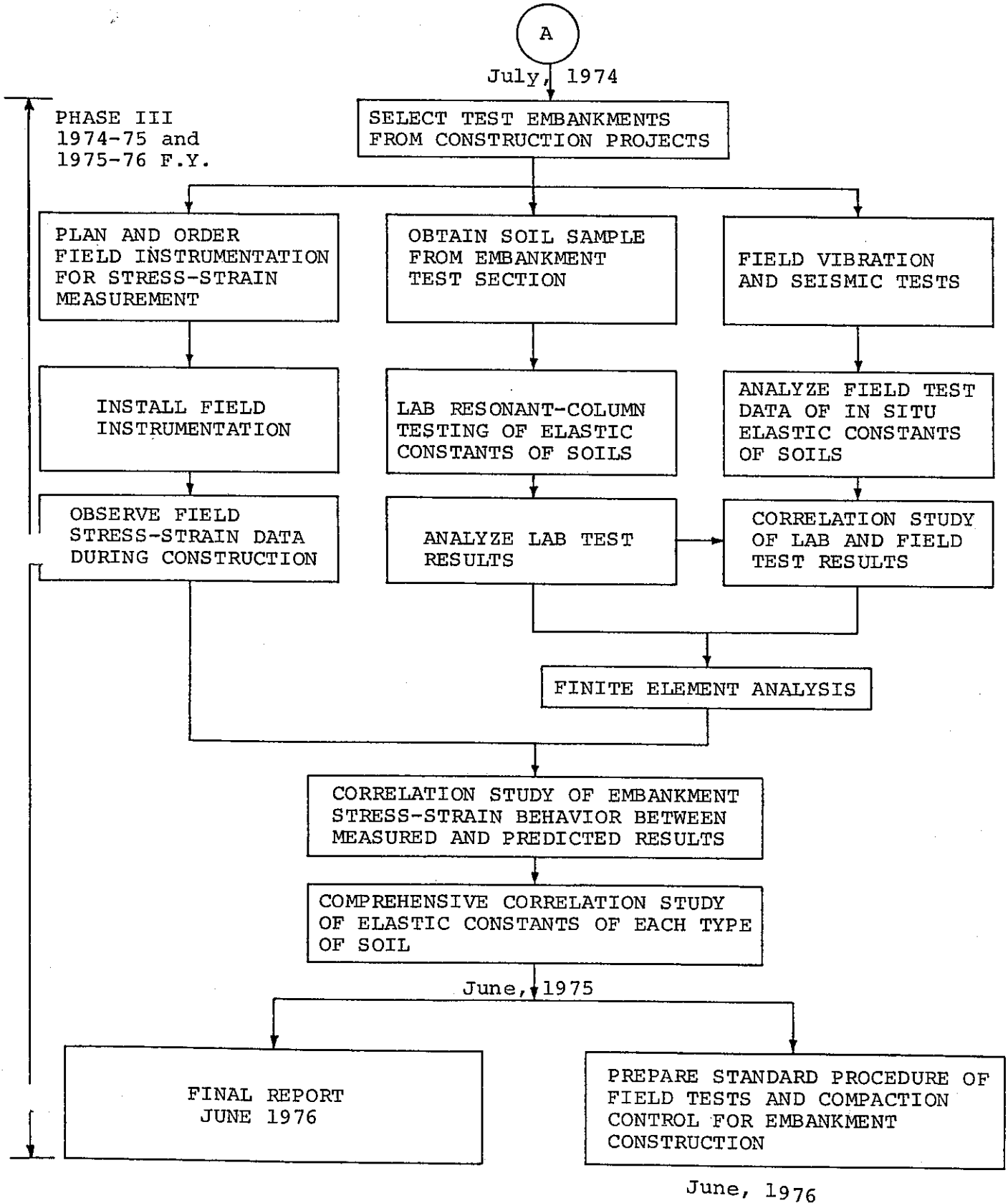
STAFF RESPONSIBILITY

This project will be performed in the Foundation Section under the general direction of Mr. Travis Smith, Assistant Materials and Research Engineer - Foundation. His co-investigators will be Mr. Raymond A. Forsyth, Senior Materials and Research Engineer, and Mr. Jerry C. Chang, Associate Materials and Research Engineer. Coordinator for the Construction Department will be Mr. John C. Obermuller, Supervising Highway Engineer. Dr. H. H. Su, Associate Professor of Civil Engineering, Sacramento State College will be contracted as a part-time consultant for this research project. Dr. H. H. Su's qualifications are attached.

PROJECTED WORK SCHEDULE



PROJECTED WORK SCHEDULE (CONTINUED)



COST ESTIMATE

PHASE I  
1972 - 1973

EQUIPMENT COST

<u>Item</u>	<u>Cost</u>
Resonant Column Basic Unit	\$ 6,000
Resonant Column Electronic Unit	<u>6,000</u>
Sub-Total	\$12,000

LABOR COST

<u>Item</u>	<u>Man-Hours</u>	<u>Cost</u>
Project Supervision	100	\$ 1,000
Literature Search	300	3,000
Laboratory test apparatus set-up and pilot tests	800	8,000
Analysis of test data	300	3,000
Consultant services	<u>800</u>	<u>8,000</u>
Sub-Total	2300	\$ 23,000
		TOTAL \$35,000

PHASE II  
1973 - 1974  
EQUIPMENT COST

<u>Item</u>	<u>Cost</u>
Electromagnetic Oscillator	\$ 2,000
Hydraulic Vibrator	4,000
Electric-power system	5,000
Seismic refraction equipment	<u>5,000</u>
Sub-Total	\$16,000

LABOR COST

<u>Item</u>	<u>Man-Hours</u>	<u>Cost</u>
Project Supervision	100	\$ 1,000
Continue laboratory tests	400	4,000
Field vibration tests	600	5,000
Data analysis (including computer time) and interim reporting	<u>400</u>	<u>4,000</u>
Sub-Total	1800	\$18,000
	TOTAL	\$34,000

PHASE III

1974 - 1975

FIELD INSTRUMENTATION

<u>Item</u>	<u>No</u>	<u>Unit Cost</u>	<u>Cost</u>
Pressure cells	40	250	\$10,000
Extensometer	30	200	6,000
Settlement Device	30	200	<u>6,000</u>
Sub-Total			\$22,000

PHASE III - LABOR COST

<u>Item</u>	<u>Man-Hours</u>	<u>Cost</u>
Project Supervision	150	\$ 1,500
Read field instrumentation	300	3,000
Travel expenses	- -	1,000
Laboratory tests	300	3,000
Expendable materials	- -	500
Field vibration tests	550	5,500
Data analysis (including computer time) and reporting	<u>350</u>	<u>3,500</u>
Sub-Total	1650	\$18,000
		TOTAL \$40,000

PHASE III  
1975 - 1976  
LABOR COST

<u>Item</u>	<u>Man-Hours</u>	<u>Cost</u>
Project Supervision	200	\$ 2,000
Read field instrumentation	400	4,000
Travel expenses	- -	1,000
Expendable materials	- -	500
Data analysis, computer services and reporting	<u>1750</u>	<u>17,500</u>
Sub-Total	<u>2350</u>	<u>\$25,000</u>
TOTAL	8,400	\$ 134,000

BUDGET ESTIMATE

<u>Fiscal Year</u>	<u>Man-Hours</u>	<u>Approved Funds</u>	<u>Non-Participating Overhead</u>	<u>This Request</u>
1971-72 (Proposal Preparation)	210	\$ 1,000	\$ 650	\$ 2,100*
1972-73 (Phase I)	2300	-0-	7,130	35,000
1973-74 (Phase II)	1800	-0-	5,580	34,000
1974-75 (Phase III)	1650	-0-	5,115	40,000
1975-76 (Phase III)	<u>2350</u>	<u>-0-</u>	<u>7,285</u>	<u>25,000</u>
TOTAL	8,310	\$1,000	\$25,760	\$136,100

\*Estimated Expenditures for 1971-72 F.Y.

<u>Fiscal Year</u>	<u>Salaries</u>	<u>Equipment</u>	<u>Materials</u>	<u>Travel</u>	<u>Totals</u>
1971-72	\$ 2,100	\$ -0-	\$ -0-	\$ -0-	\$ 2,100
1972-73	23,000	12,000	-0-	-0-	35,000
1973-74	18,000	16,000	-0-	-0-	34,000
1974-75	16,500	22,000	500	1,000	40,000
1975-76	<u>23,500</u>	<u>-0-</u>	<u>500</u>	<u>1,000</u>	<u>25,000</u>
TOTAL	\$83,100	\$50,000	\$ 1,000	\$ 2,000	\$136,100

APPENDIX B

Resonant Column Test Data

## Resonant Column Test Data

Resonant column tests were carried out for the following projects:

1. Soil Cement
2. I-15, San Diego
3. Dunsmuir, Reinforced Earthen Wall
4. Pasadena, 7-11 Interchange
5. I-5, 56th Avenue, Sacramento
6. State Capitol, Sacramento

Resonant column test data for the above projects are reported in the following figures showing the variation in shear modulus and damping with shear strain.

The following notation shown in the figures is used:

- Sp. G. - Specific Gravity
- $W_c$  - Water Content
- S - Degree of Saturation
- $\gamma_d$  - Dry Unit Weight
- $\gamma_w$  - Wet Unit Weight
- e - Void Ratio
- G - Shear Modulus
- Y - Shear Strain
- D - Damping Ratio
- $\sigma_o$  - Confining Pressure

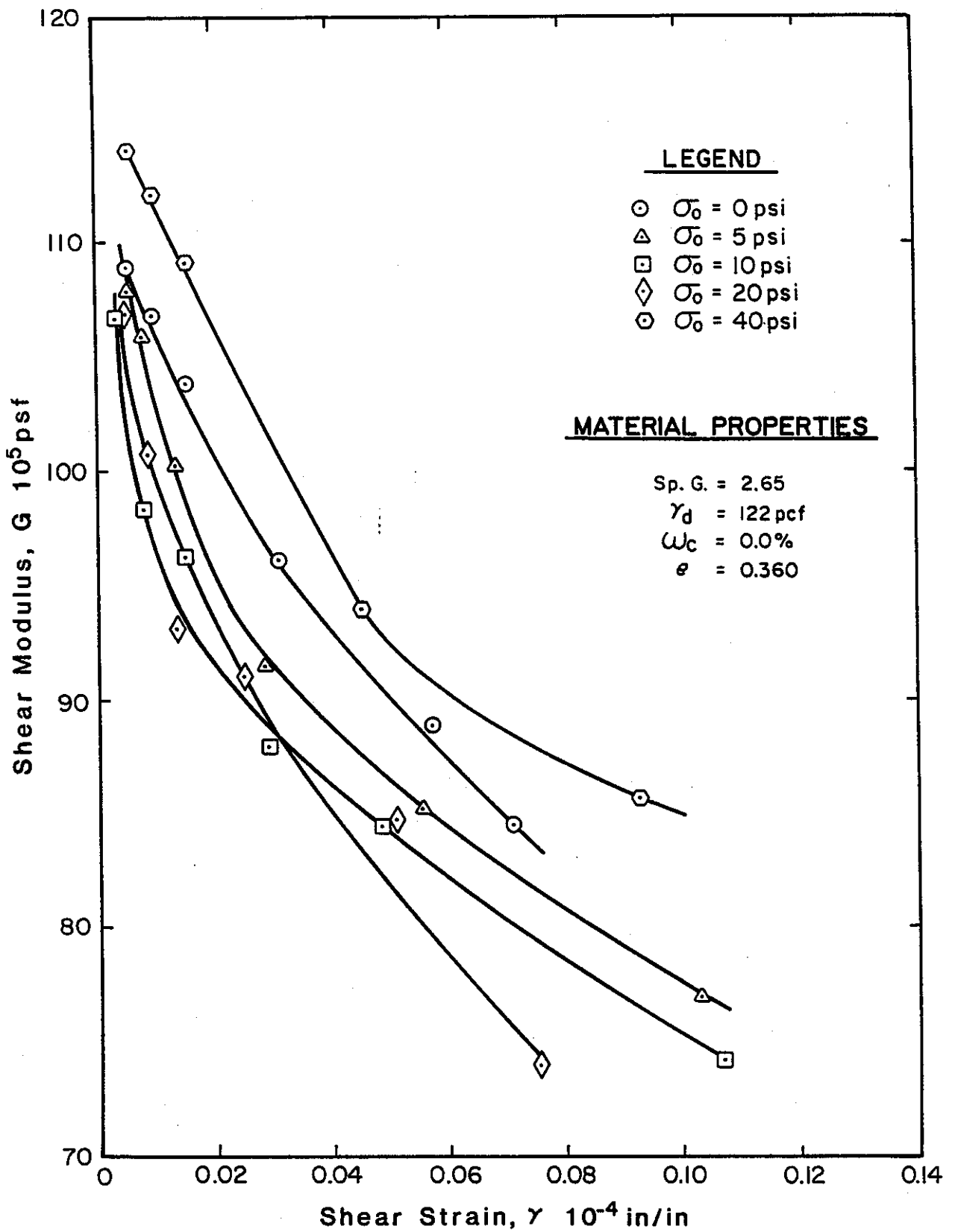


**Fig. B.1. SHEAR MODULUS, SOIL CEMENT**

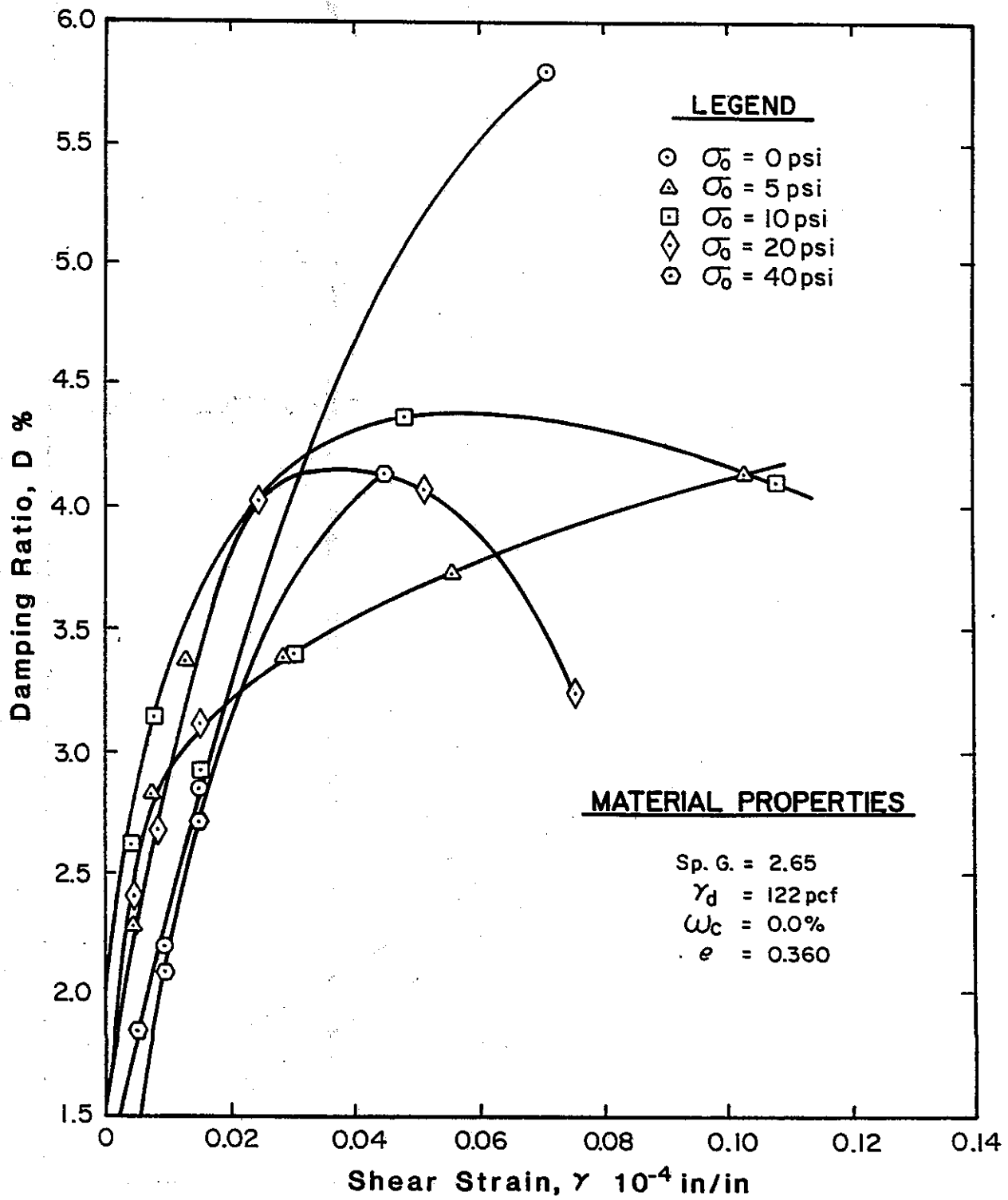
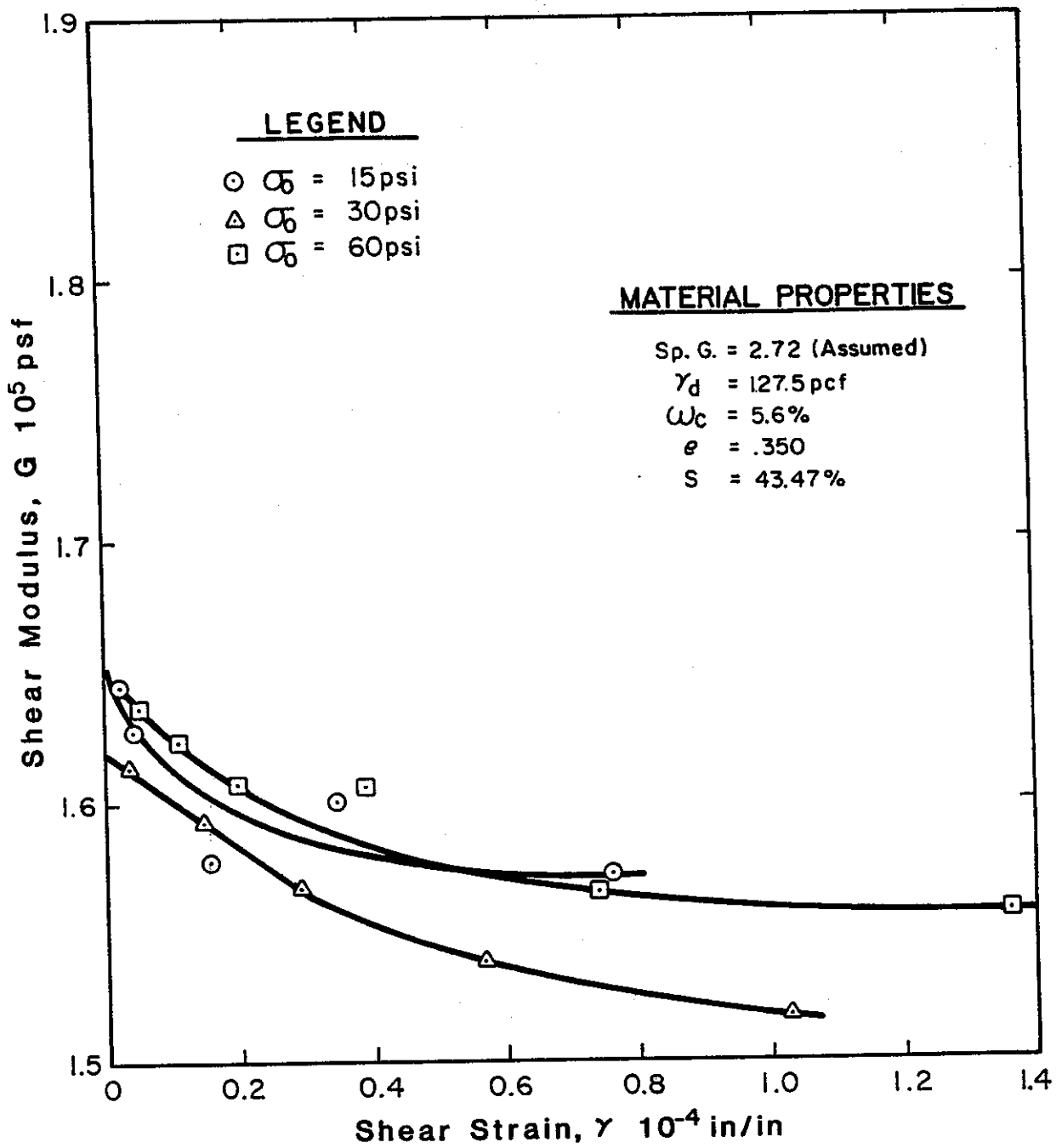


Fig. B.2. DAMPING RATIO, SOIL CEMENT



**Fig. B.3. SHEAR MODULUS, GRAY SAND I-15, SAN DIEGO**

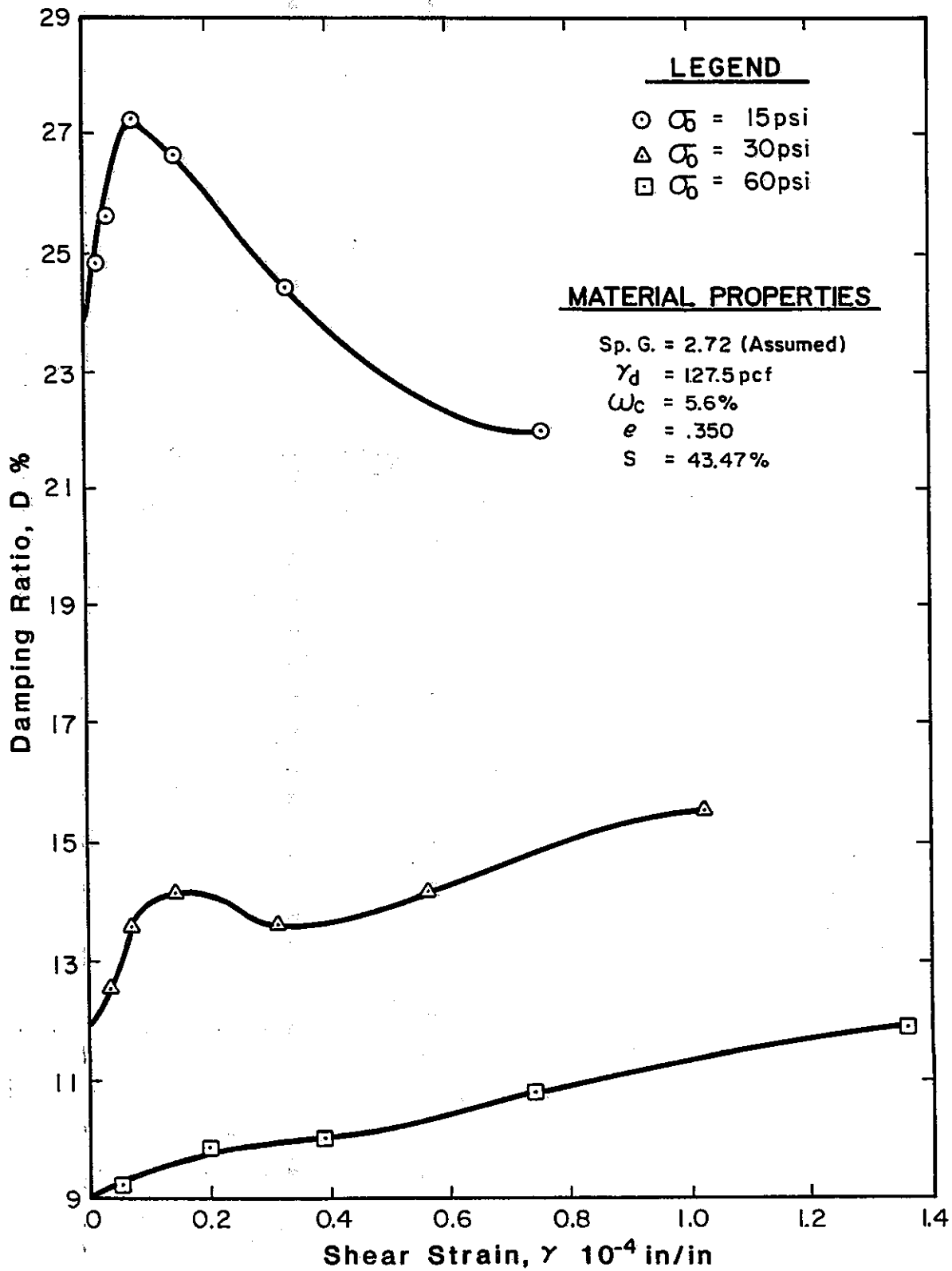


Fig. B.4. DAMPING RATIO, GRAY SAND; I-15, SAN DIEGO

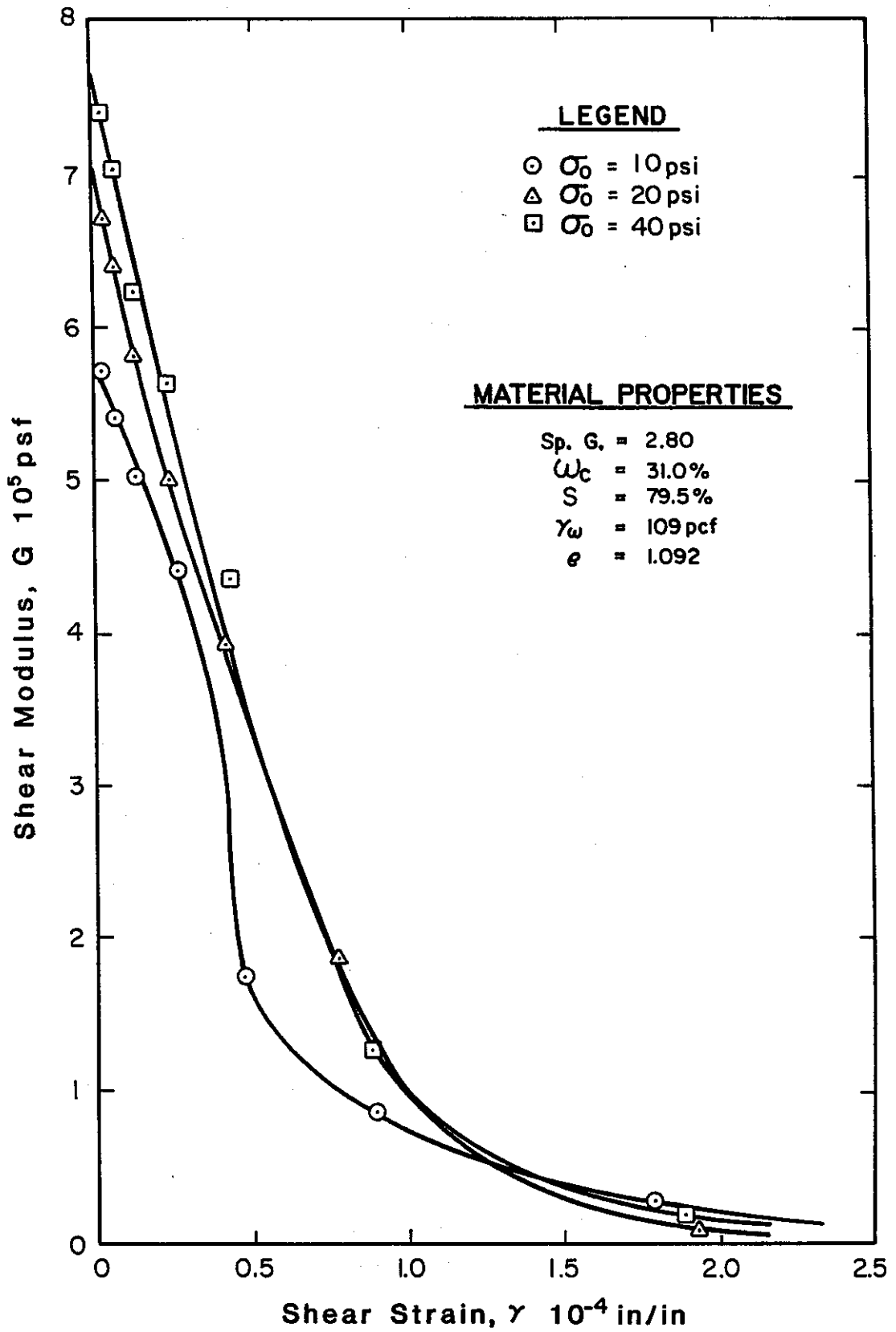


Fig. B.5. SHEAR MODULUS, DUNSMUIR, REINFORCED EARTHEN WALL

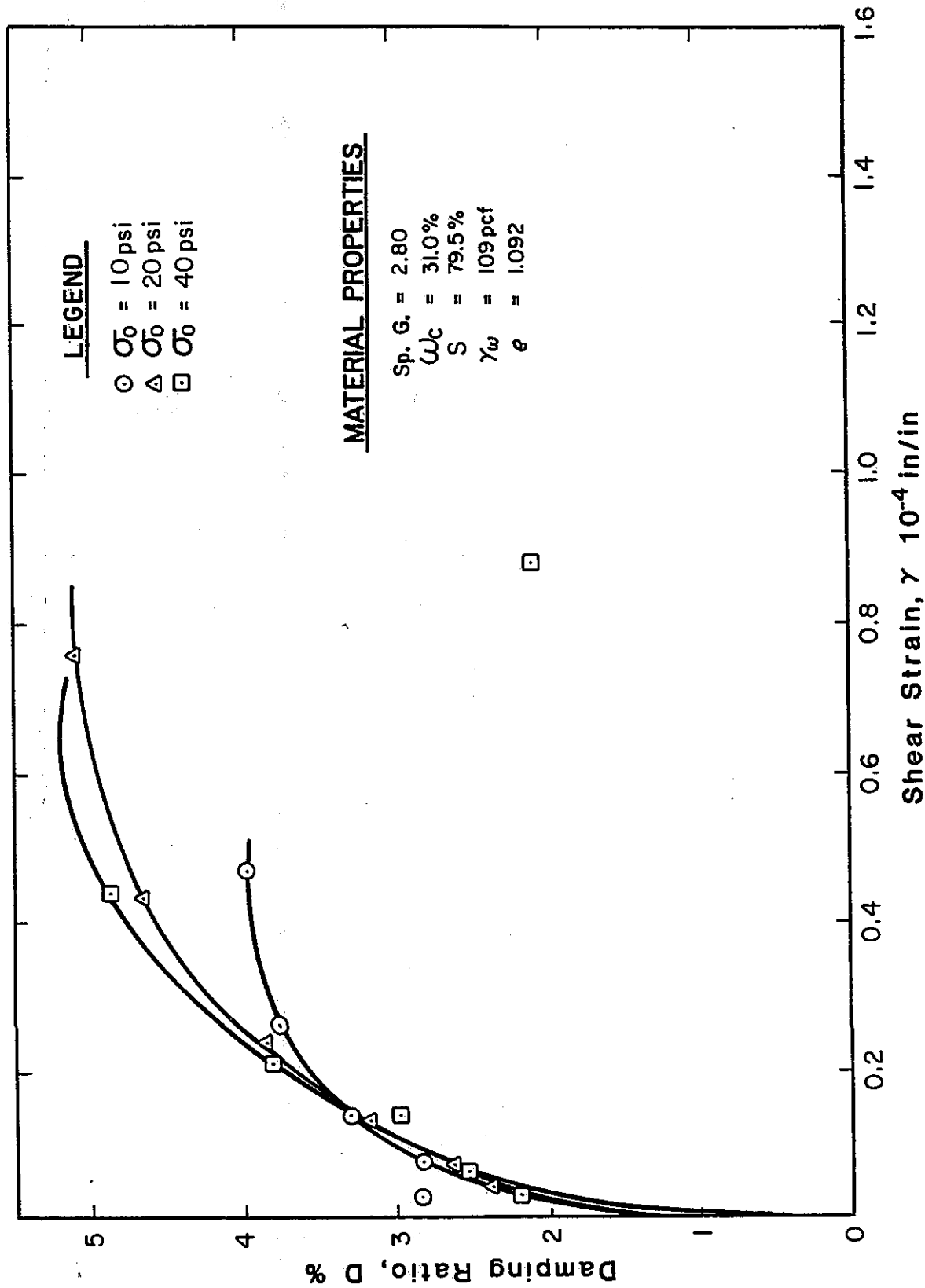


Fig. B.6. DAMPING RATIO, DUNSMUIR, REINFORCED EARTHEN WALL

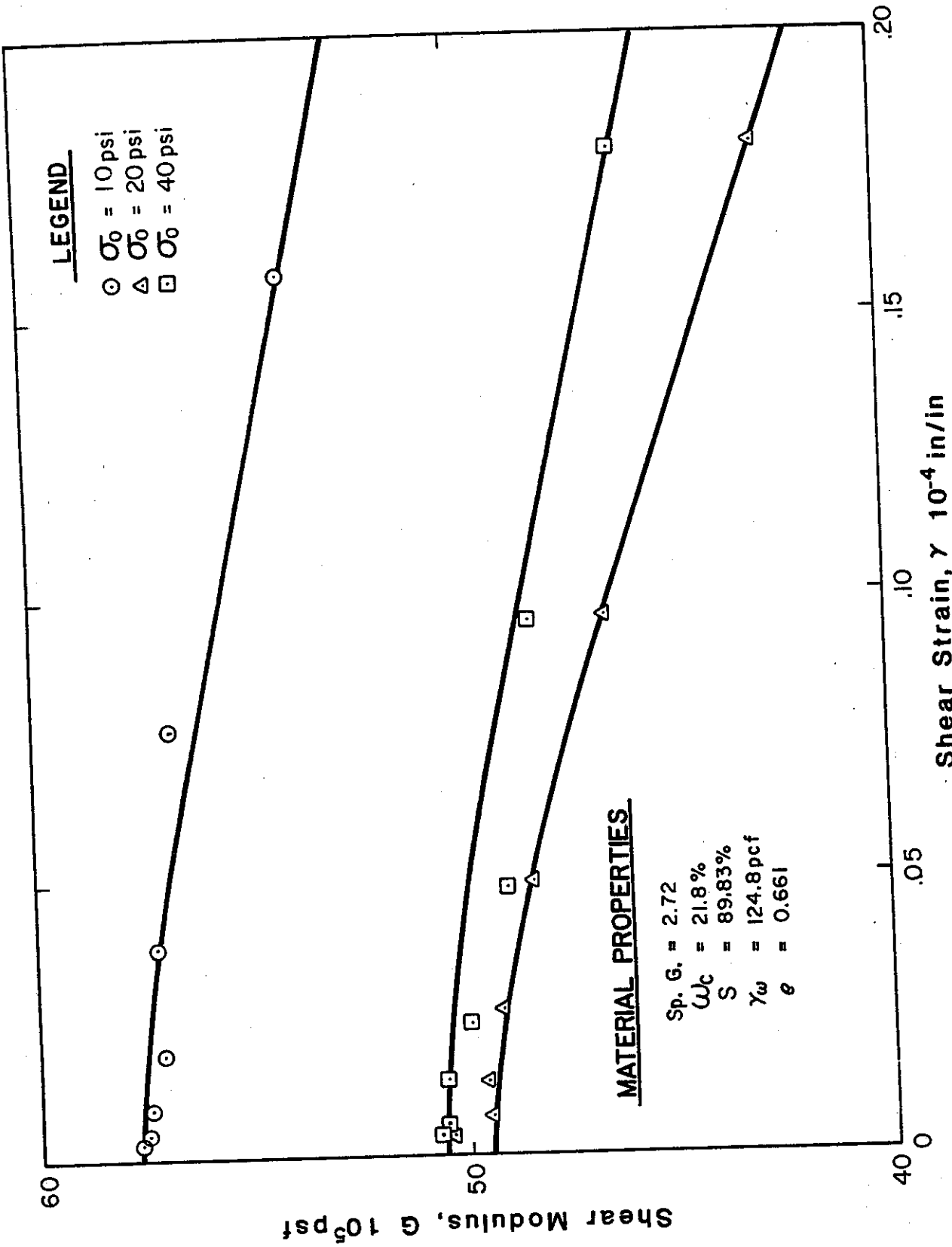


Fig. B.7. SHEAR MODULUS, SILTY SAND; 7-11 INTERCHANGE, PASADENA

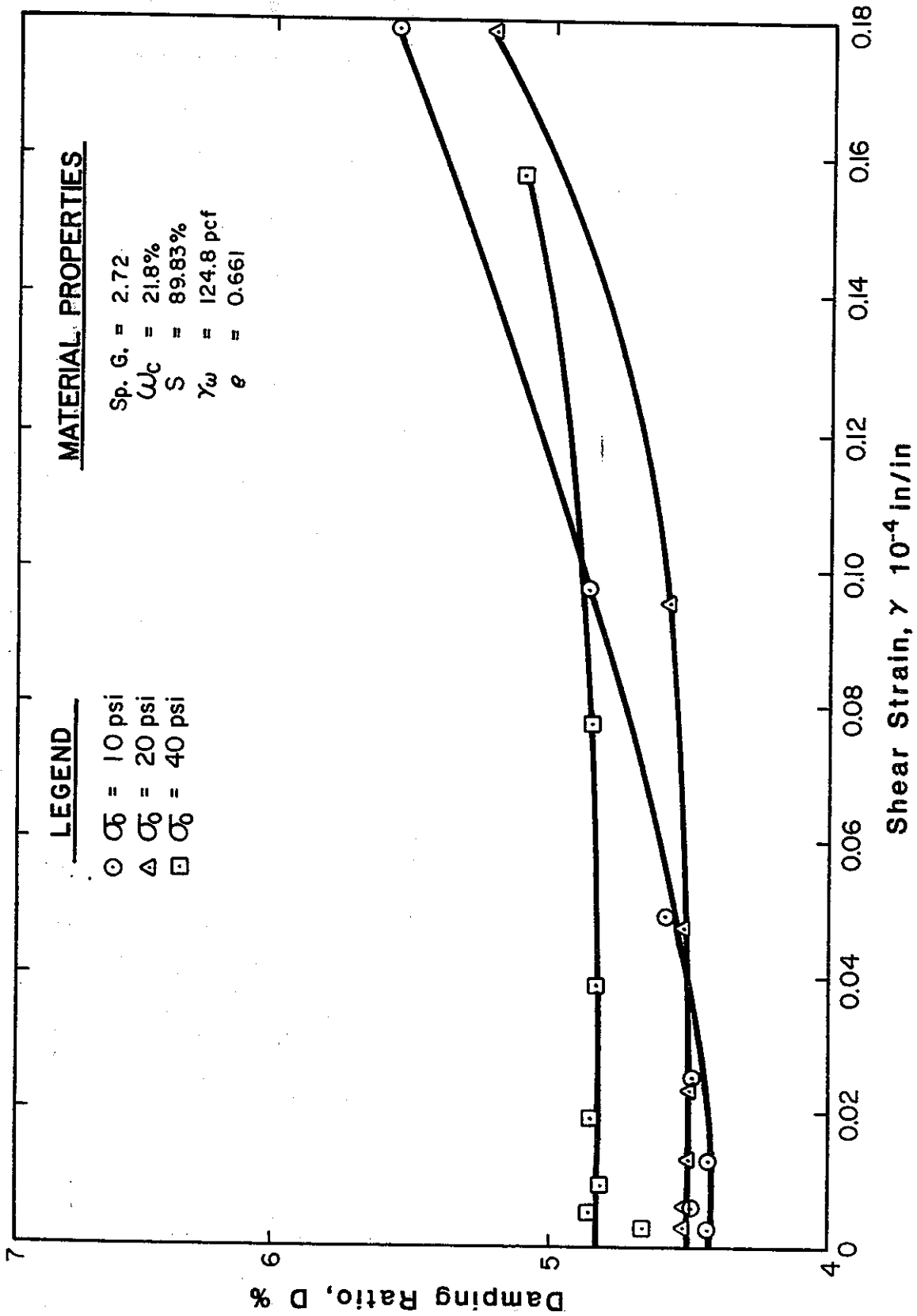


Fig. B.8. DAMPING RATIO, SILTY SAND; 7-11 INTERCHANGE, PASADENA

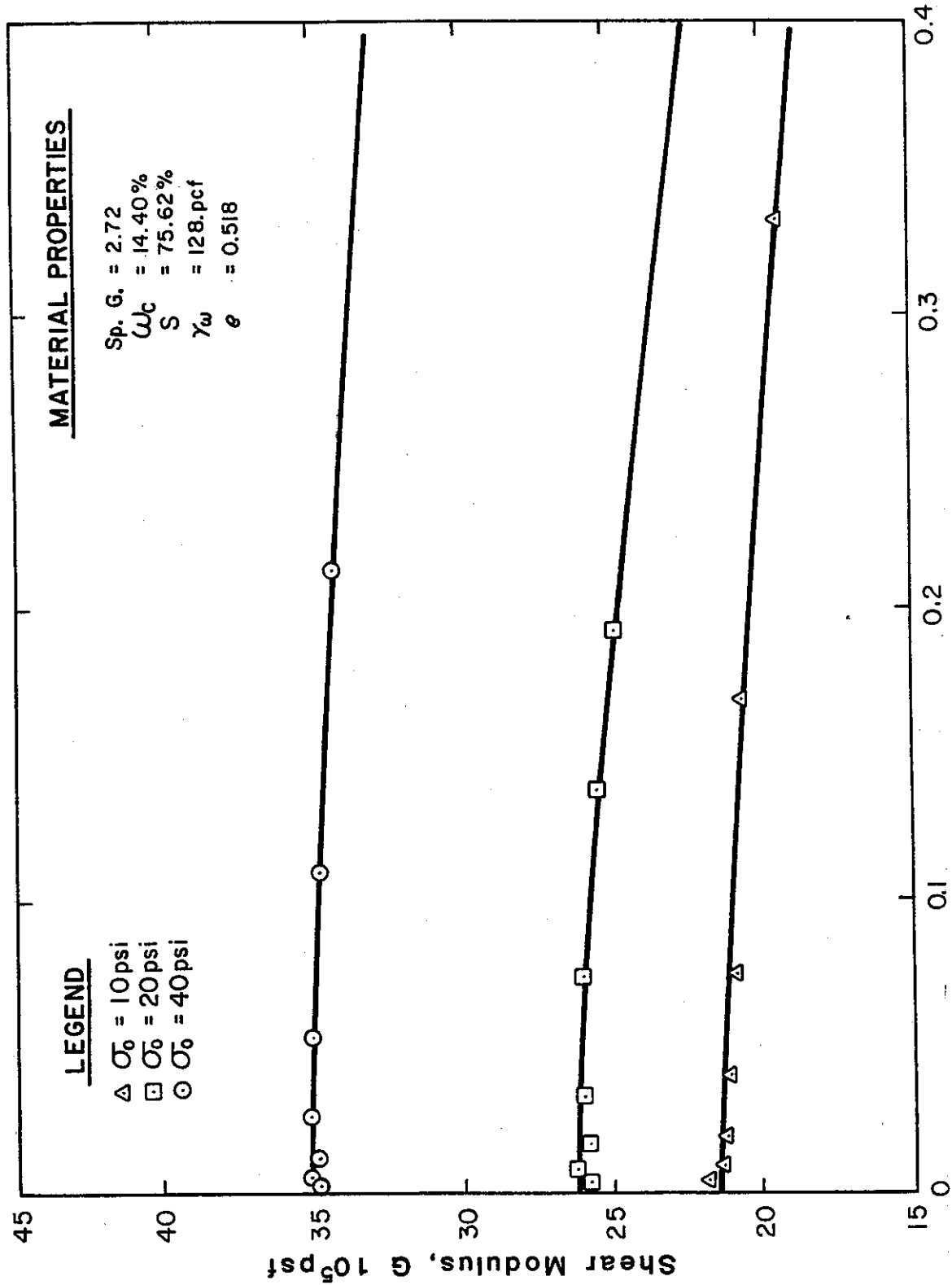


Fig. B.9. SHEAR MODULUS, SILTY SAND; 7-11 INTERCHANGE, PASADENA

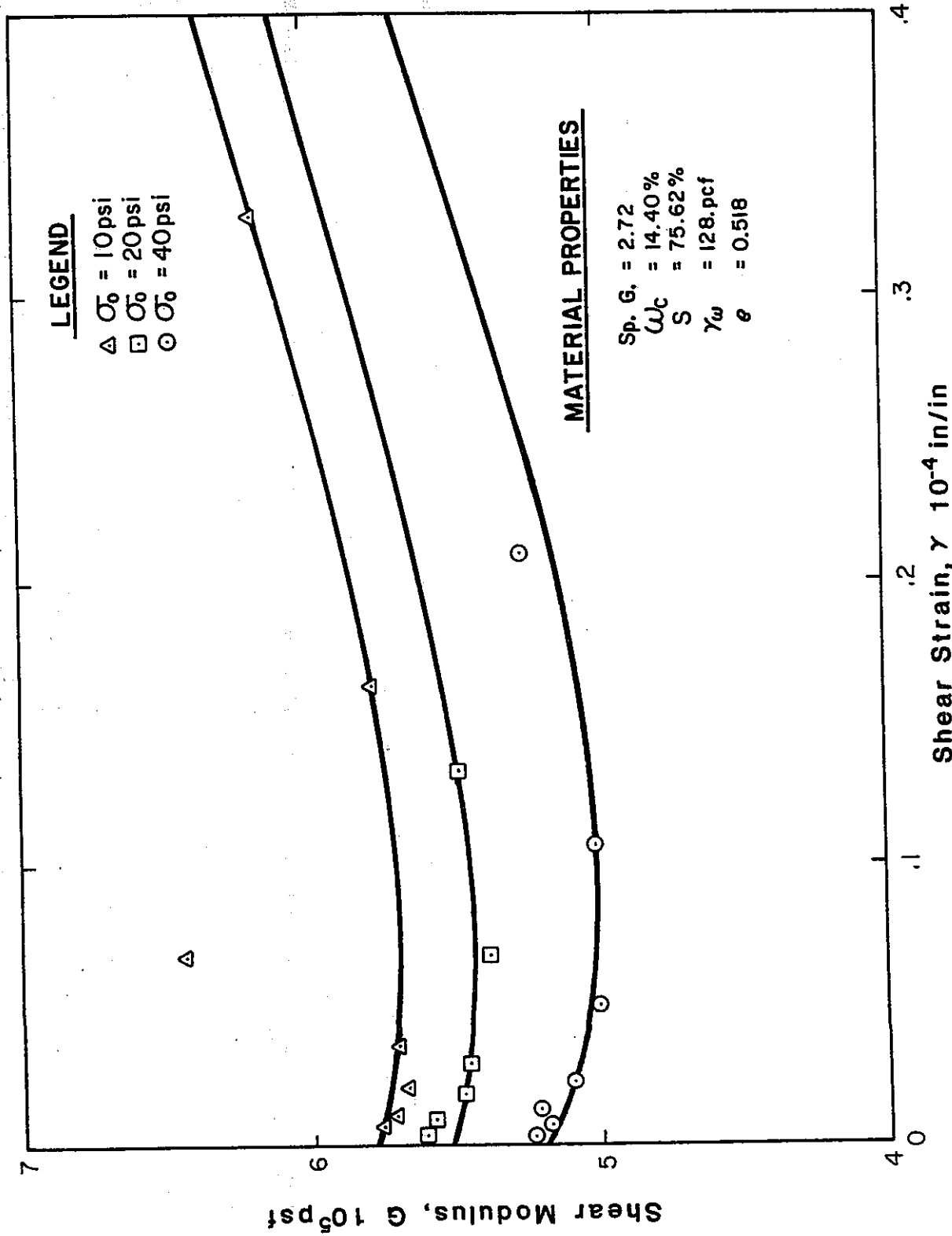


Fig. B.10. DAMPING RATIO, SILTY SAND; 7-11 INTERCHANGE, PASADENA

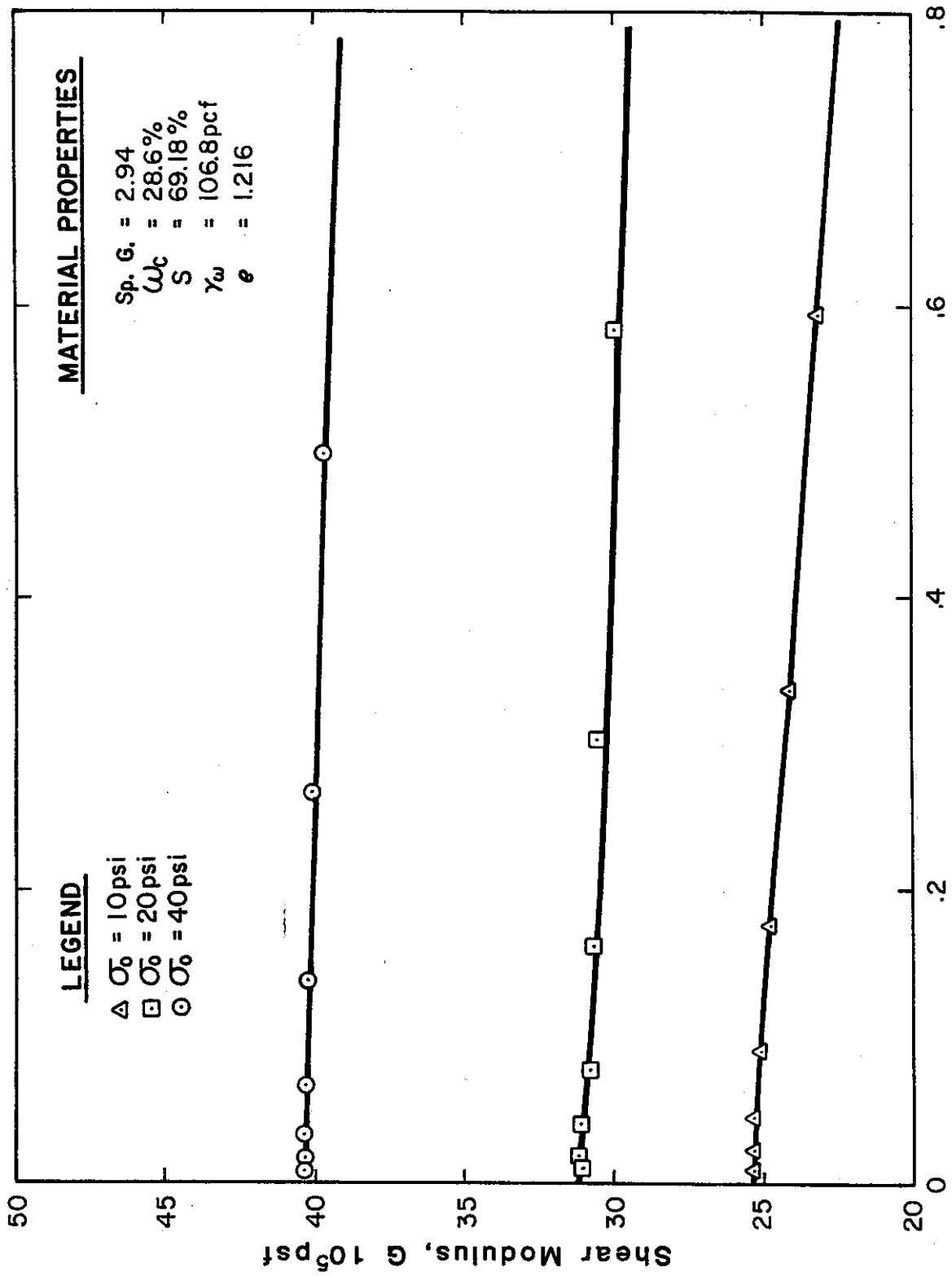


Fig. B.11. SHEAR MODULUS, FIRM SILTY SAND; I-5, SACRAMENTO

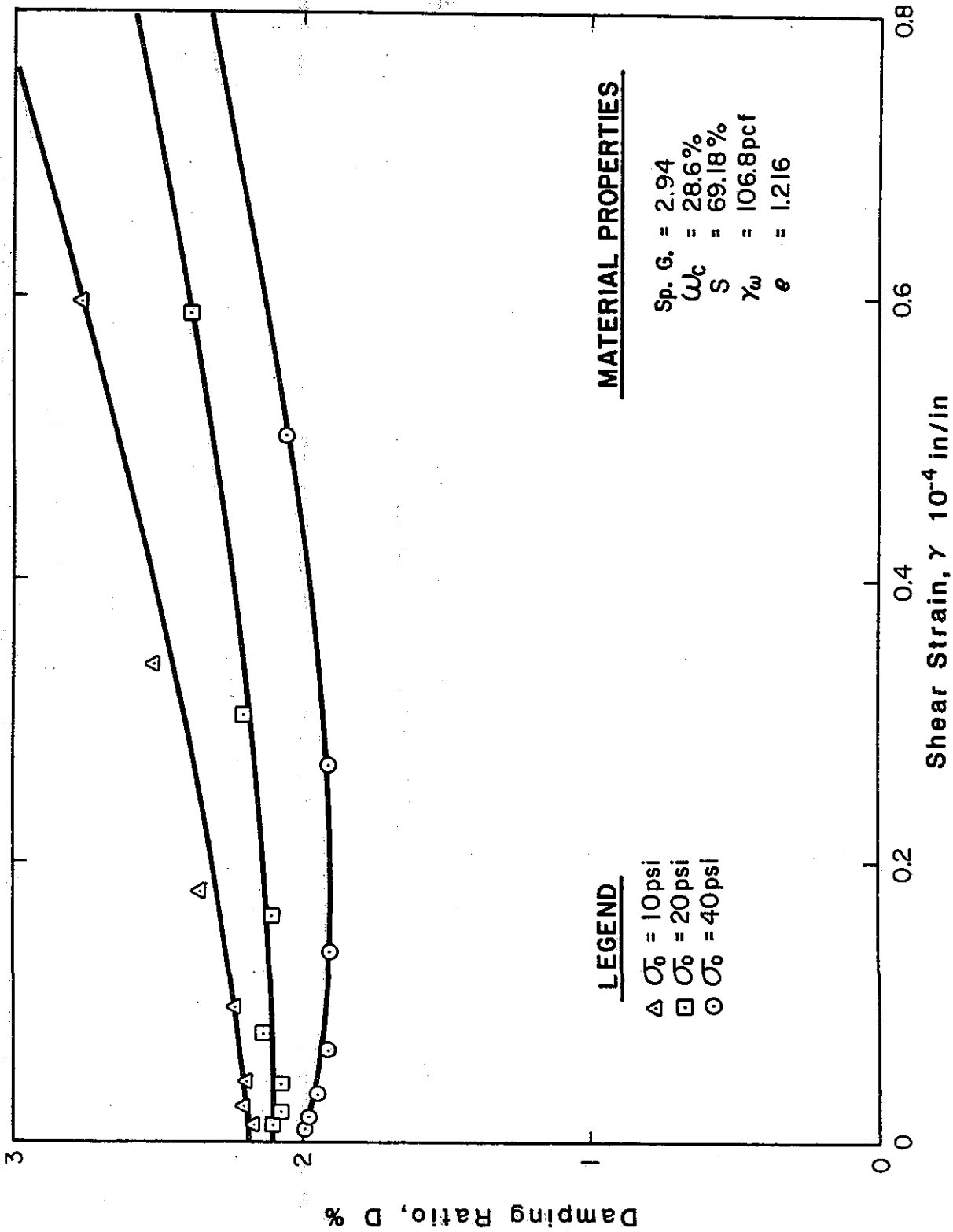
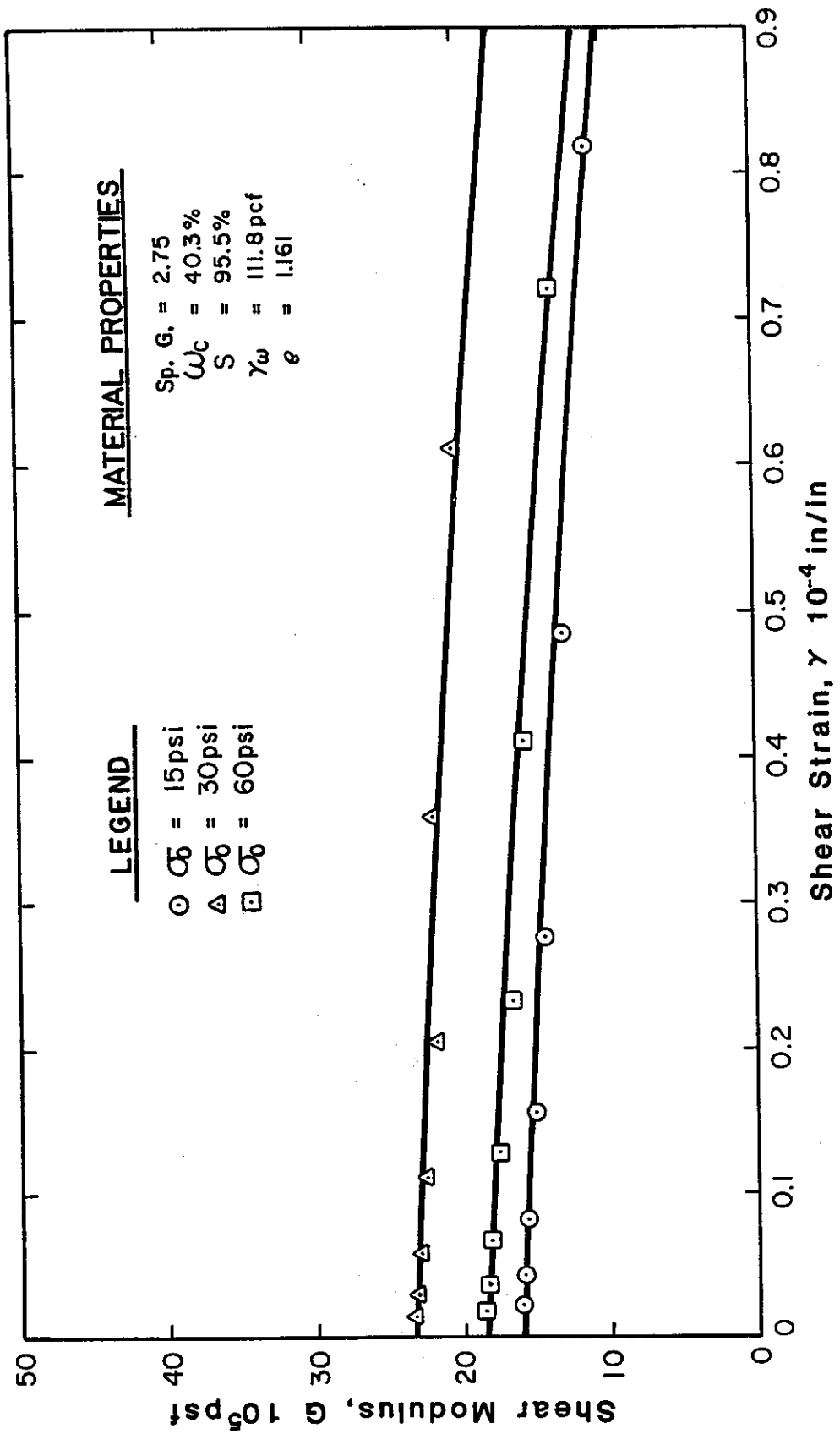


Fig. B.12. DAMPING RATIO, FIRM SILTY SAND; I-5 SACRAMENTO



**Fig. B.13. SHEAR MODULUS, STIFF SILTY CLAY, STATE CAPITOL, SACRAMENTO**

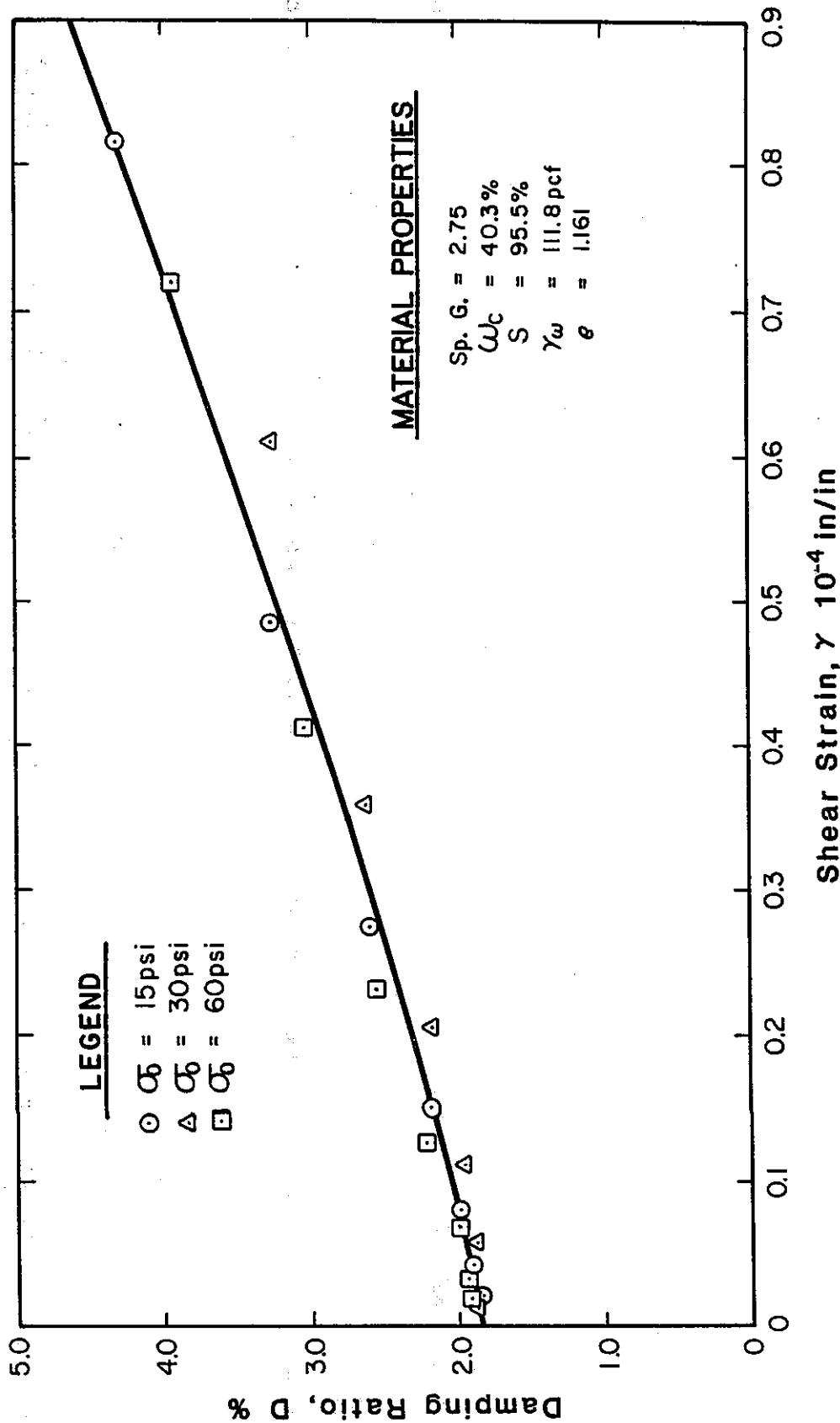
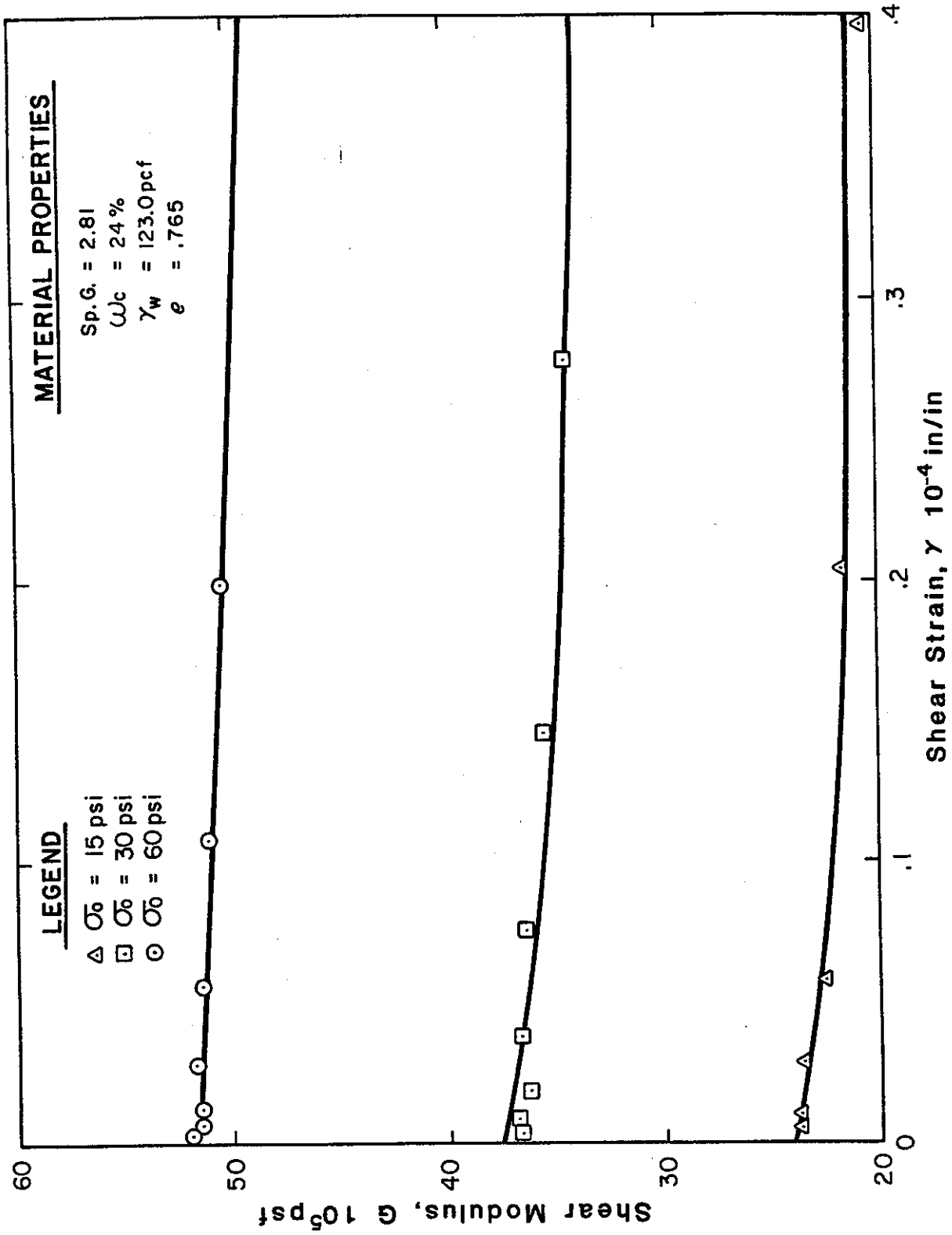


Fig. B.14. DAMPING RATIO, STIFF SILTY CLAY; STATE CAPITOL, SACRAMENTO



**Fig. B.15. SHEAR MODULUS, FIRM SILTY SAND; STATE CAPITOL, SACRAMENTO**

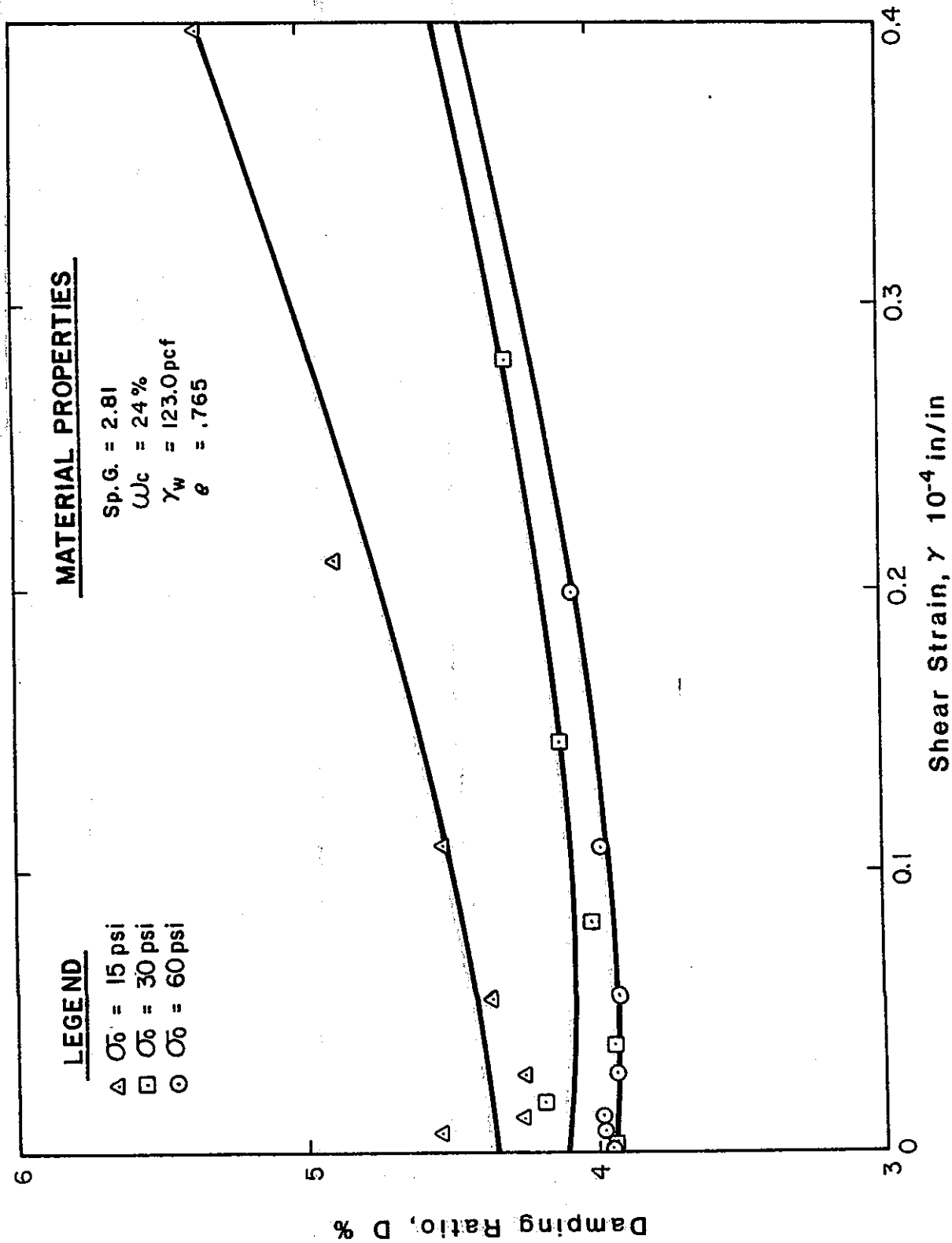


Fig. B.16. DAMPING RATIO, FIRM SILTY SAND; STATE CAPITOL SACRAMENTO

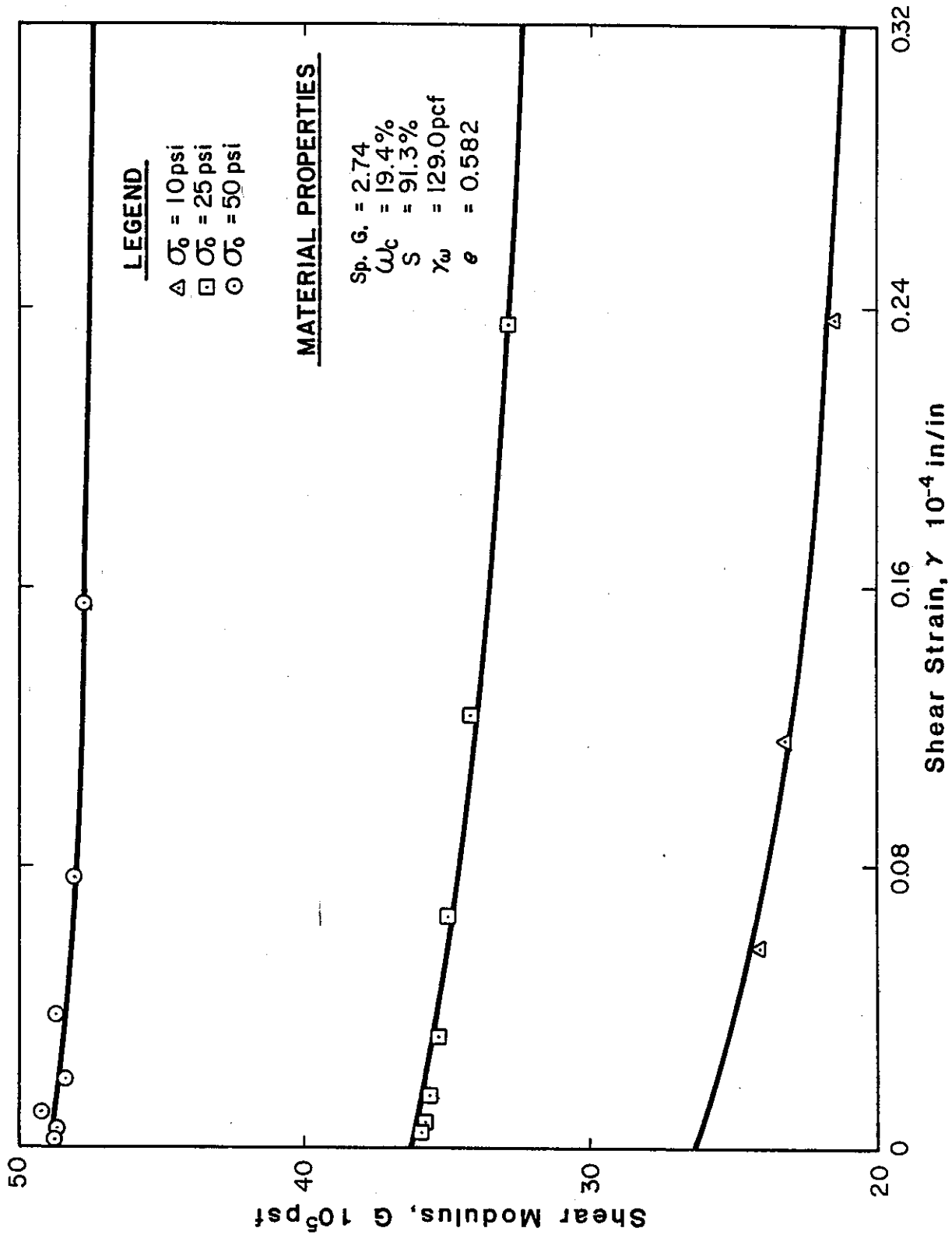


Fig. B.17. SHEAR MODULUS, STIFF SILTY CLAY, STATE CAPITOL, SACRAMENTO

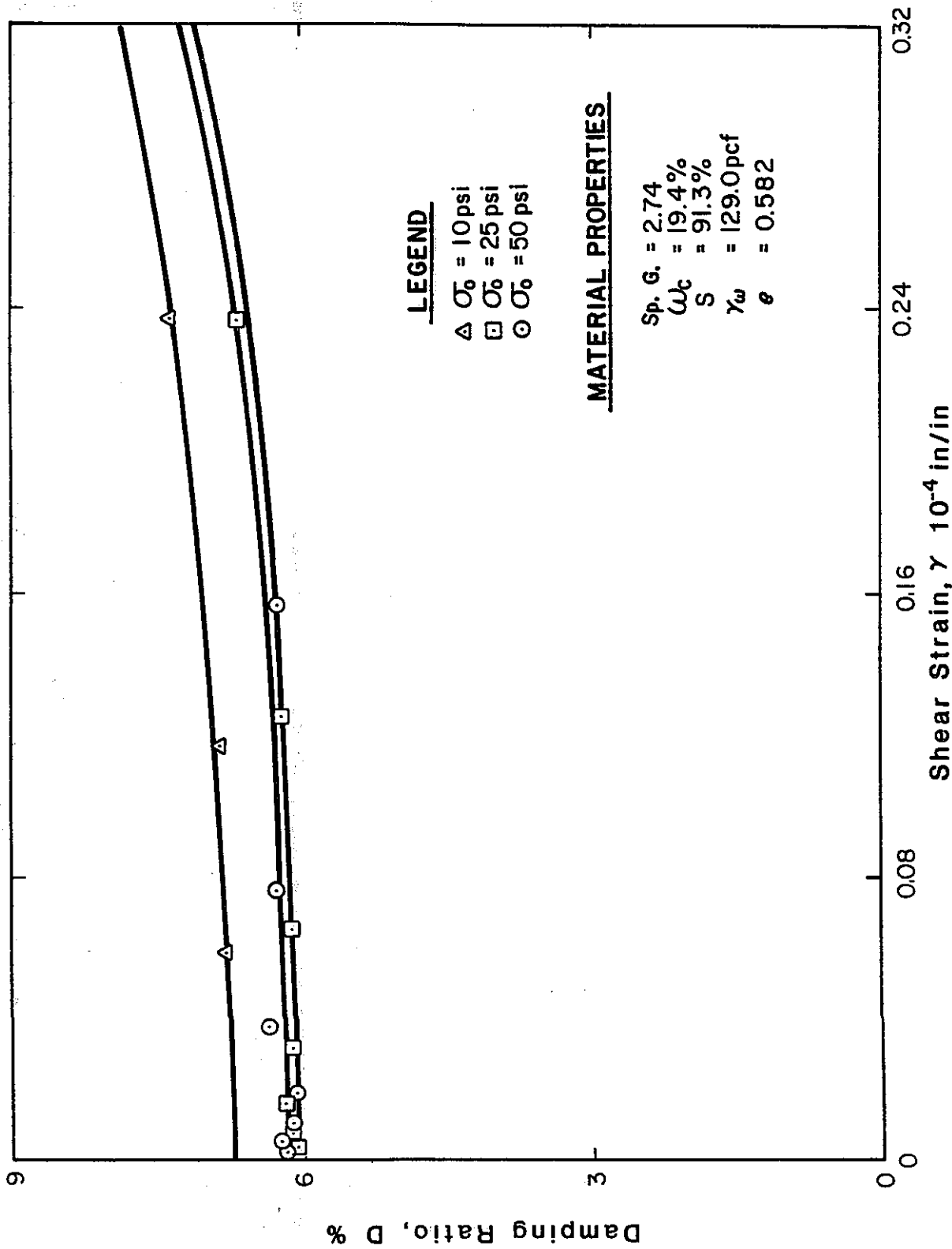


Fig. B.18. DAMPING RATIO, STIFF SILTY CLAY, STATE CAPITOL, SACRAMENTO

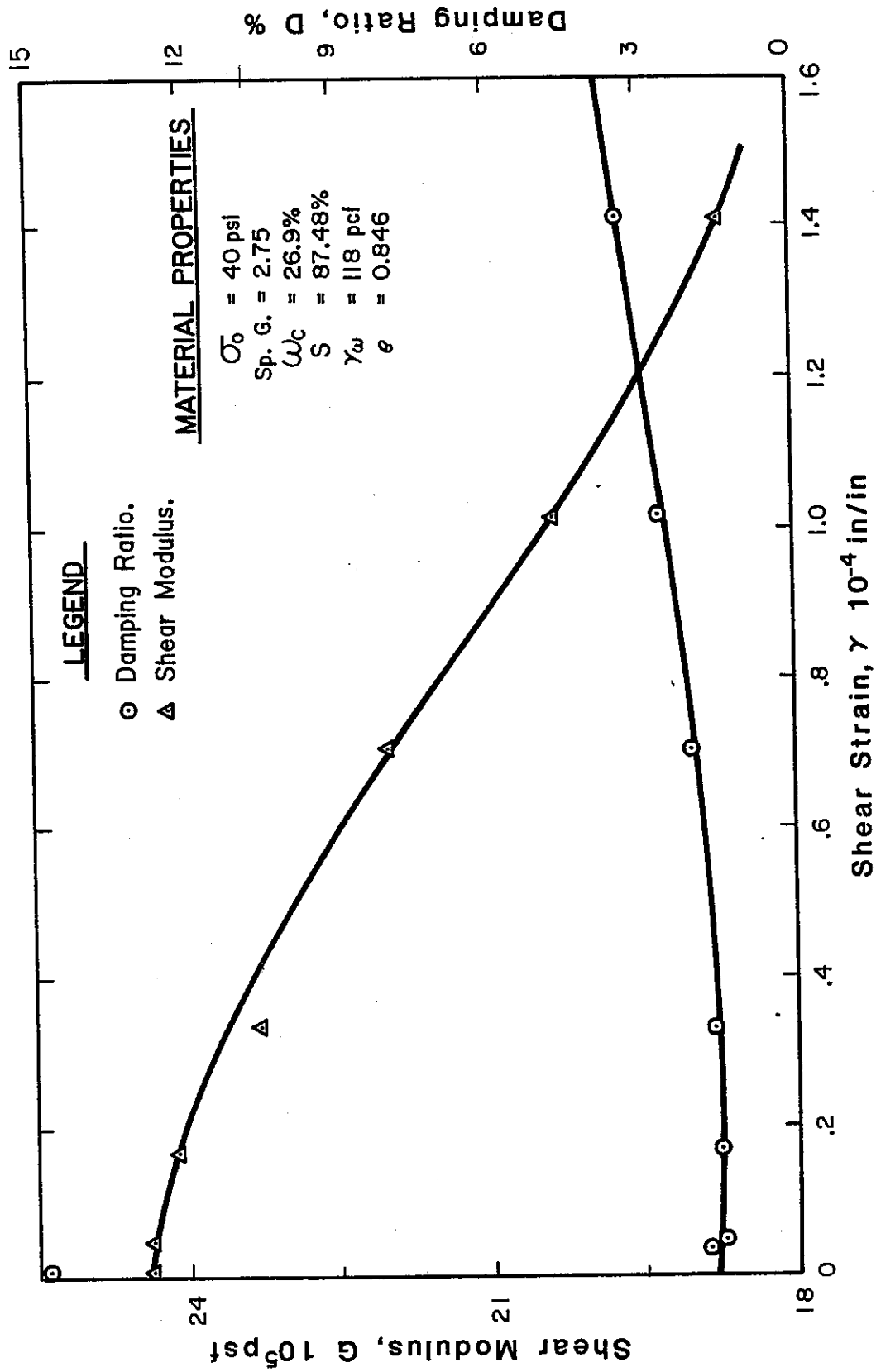


Fig. B.19. SHEAR MODULUS AND DAMPING, SILTY CLAY;  
STATE CAPITOL, SACRAMENTO

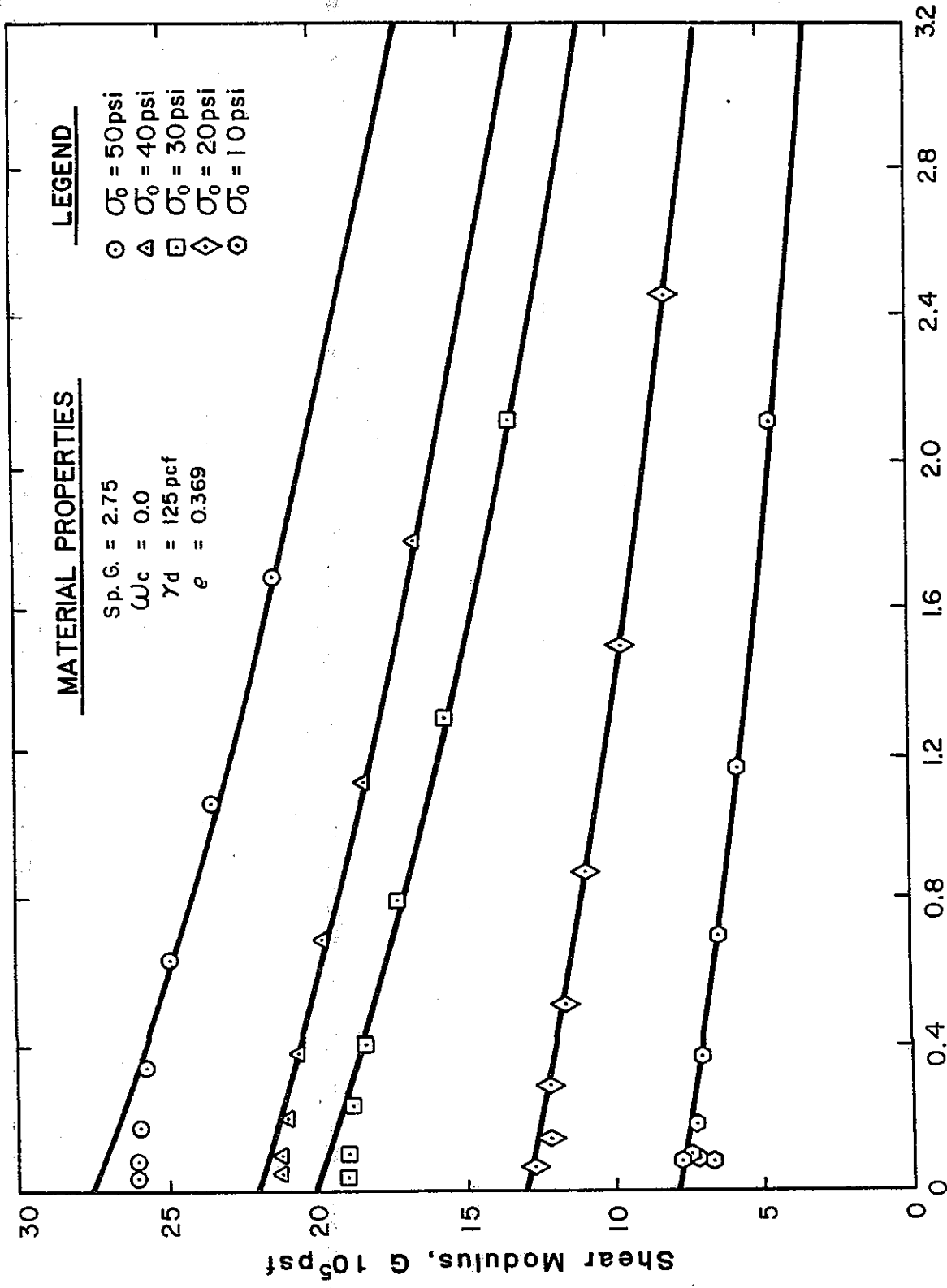


Fig. B.20. SHEAR MODULUS, SOFT, BROWN CLAYEY SILT;  
 STATE CAPITOL, SACRAMENTO

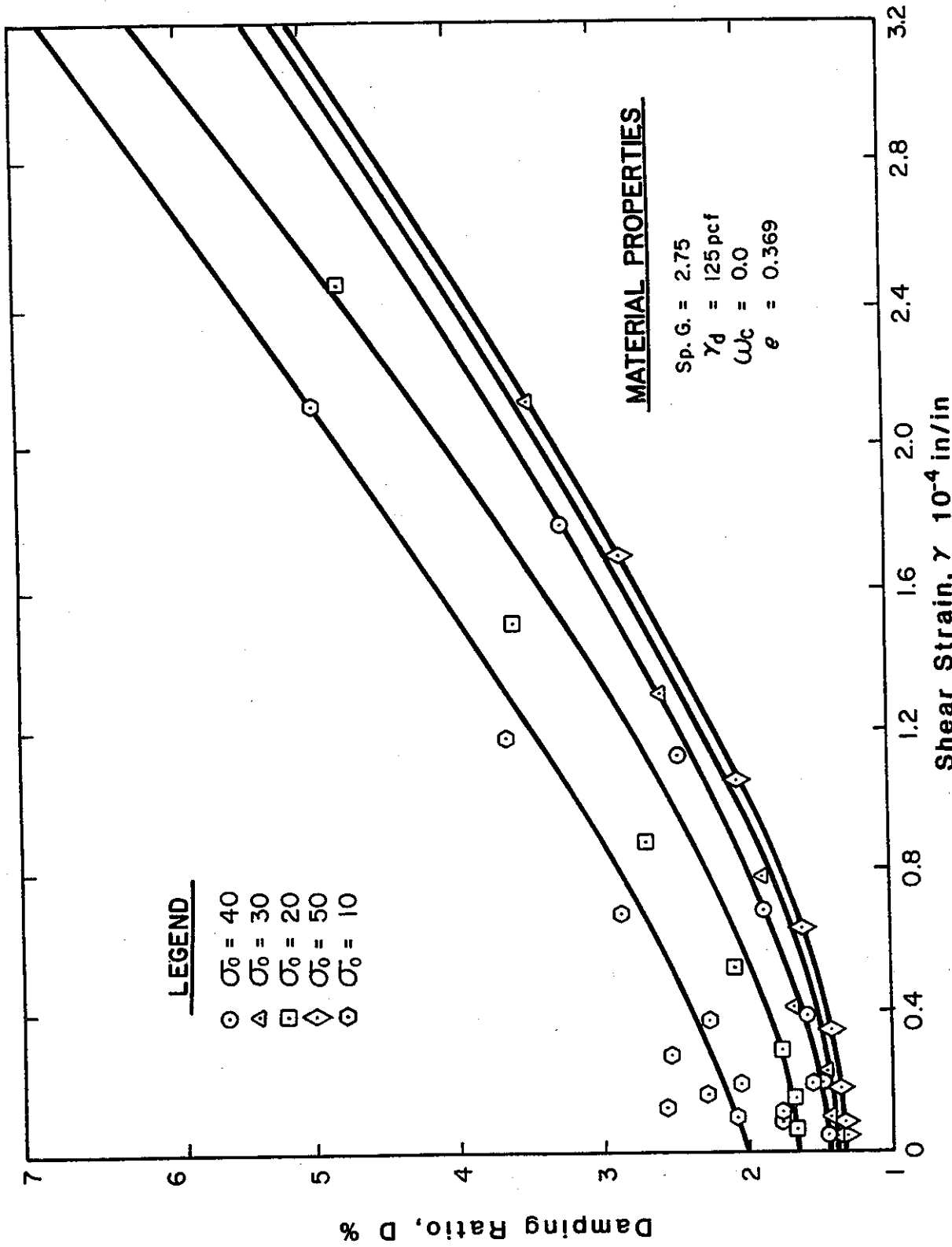


Fig. B.21. DAMPING RATIO, SOFT, BROWN CLAYEY SILT; STATE CAPITOL, SACRAMENTO

1957

1958

1959

1957

1958

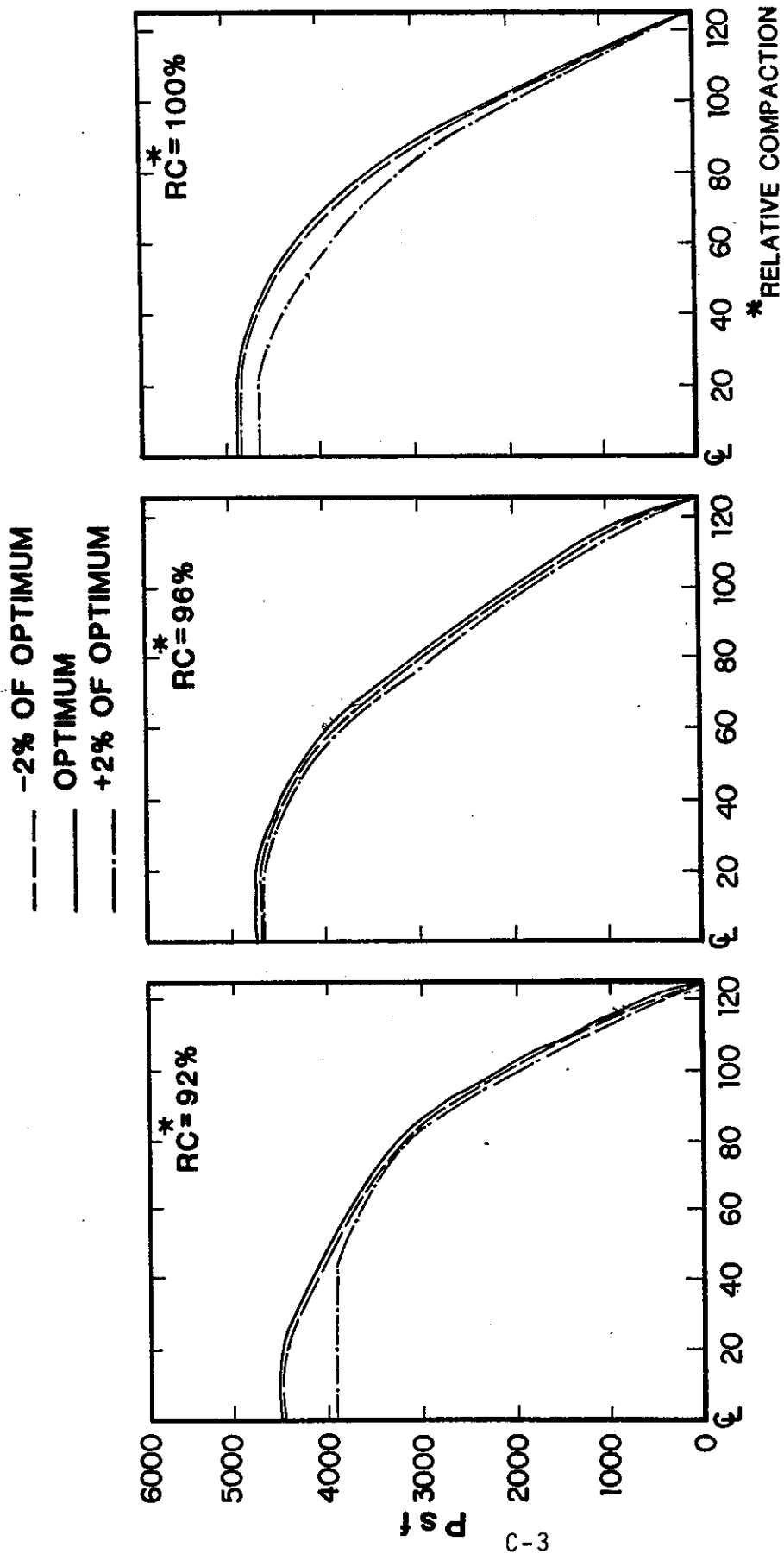
1959

APPENDIX C

Plots of Embankment Stresses

## LIST OF FIGURES

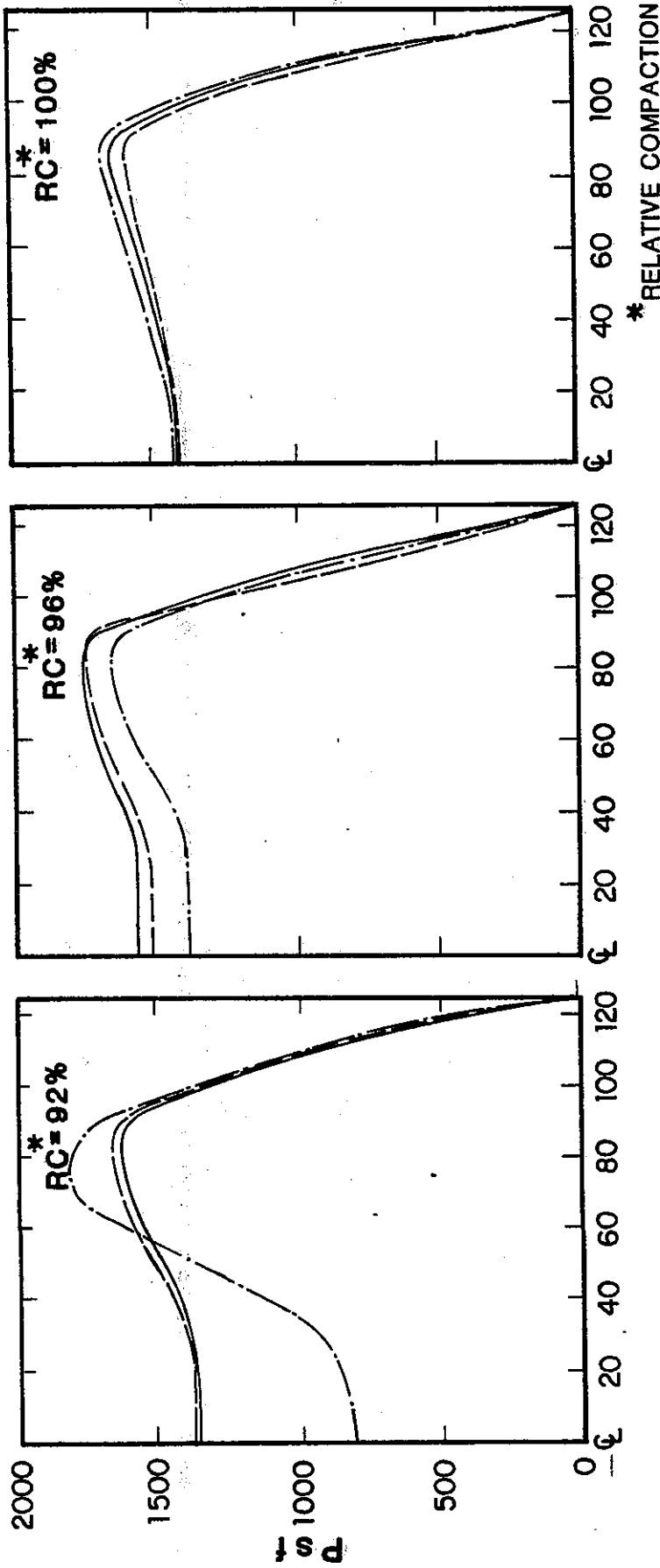
	<u>Page</u>
C1 Vertical Stress @ Midheight of 100 ft. Embankment, 2:1 Slopes	C-3
C2 Lateral Stress @ Midheight of 100 ft. Embankment, 2:1 Slopes	C-4
C3 Horizontal Shear Stress @ Midheight of 100 ft. Embankment, 2:1 Slopes	C-5
C4 Vertical Stress @ Midheight of 50 ft. Embankment, 1.5:1 Slopes	C-6
C5 Lateral Stress @ Midheight of 50 ft. Embankment, 1.5:1 Slopes	C-7
C6 Horizontal Shear Stress @ Midheight of 50 ft. Embankment, 1.5:1 Slopes	C-8
C7 Vertical Stress @ Midheight of 50 ft. Embankment, 2:1 Slopes	C-9
C8 Lateral Stress @ Midheight of 50 ft. Embankment, 2:1 Slopes	C-10
C9 Horizontal Shear Stress @ Midheight of 50 ft. Embankment, 2:1 Slopes	C-11



Distance from Centerline (ft.)

Figure C1. VERTICAL STRESS @ MIDHEIGHT OF 100 FT. EMBANKMENT, 2 : 1 SLOPES

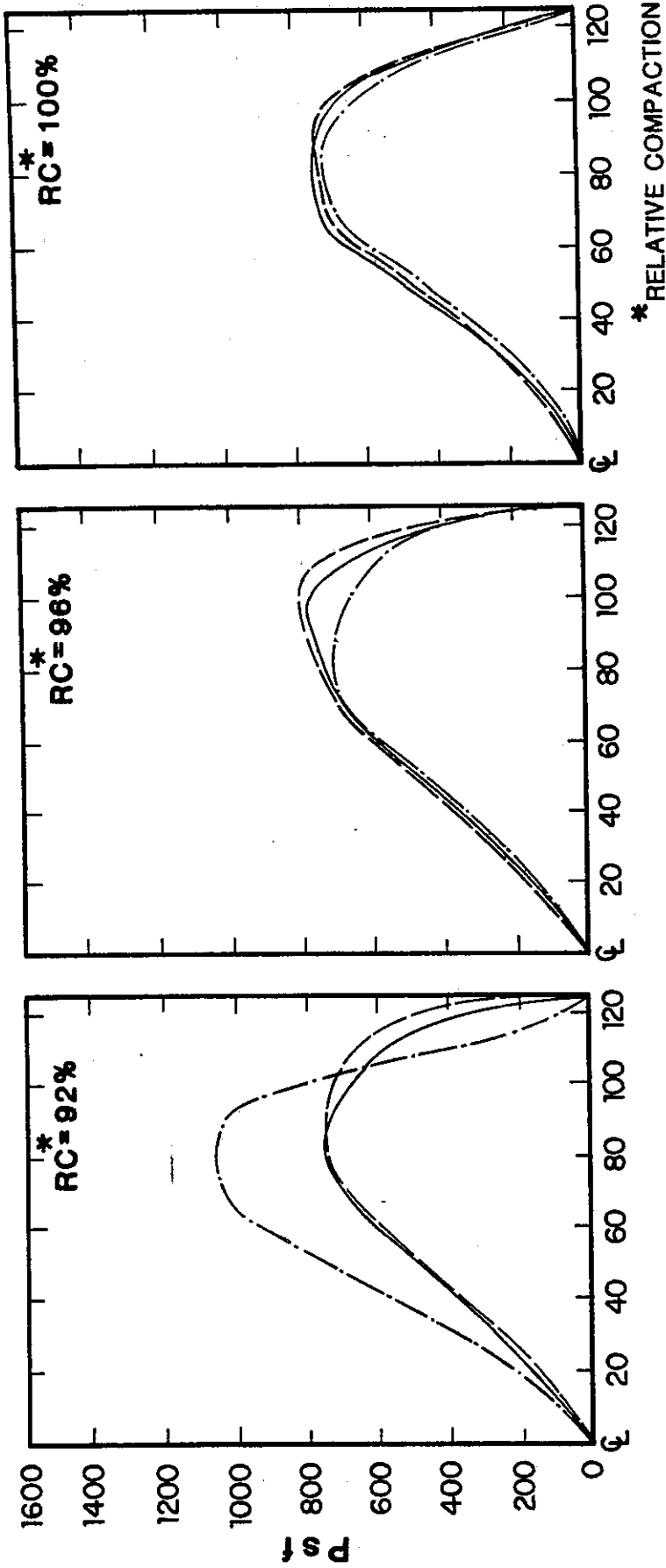
- - - -2% OF OPTIMUM  
 ——— OPTIMUM  
 - - - +2% OF OPTIMUM



Distance from Centerline (ft.)

Figure C2. LATERAL STRESS @ MIDHEIGHT OF 100 FT.  
 EMBANKMENT, 2 : 1 SLOPES

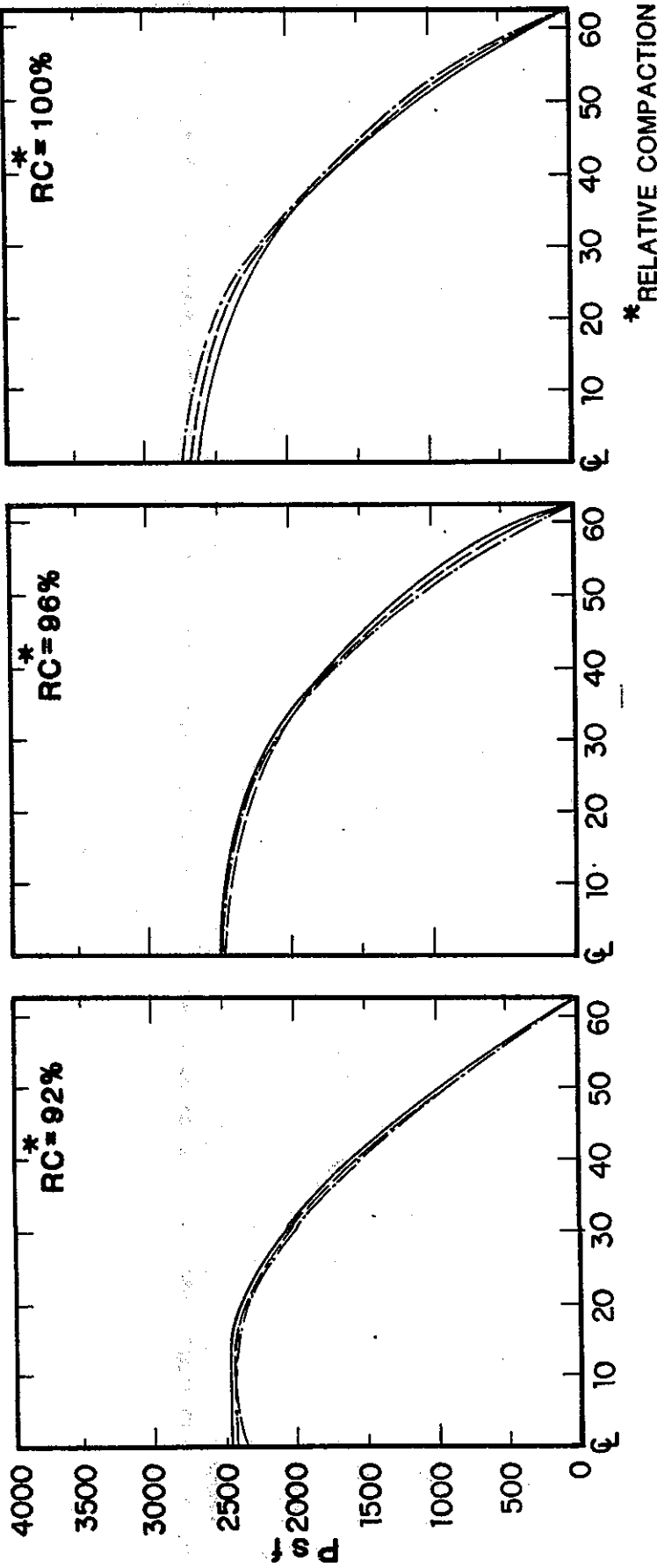
- - - -2% OF OPTIMUM  
 ——— OPTIMUM  
 - · - -2% OF OPTIMUM



Distance from Centerline (ft.)

Figure C3. HORIZONTAL SHEAR STRESS @ MIDHEIGHT OF 100 FT. EMBANKMENT, 2 : 1 SLOPES

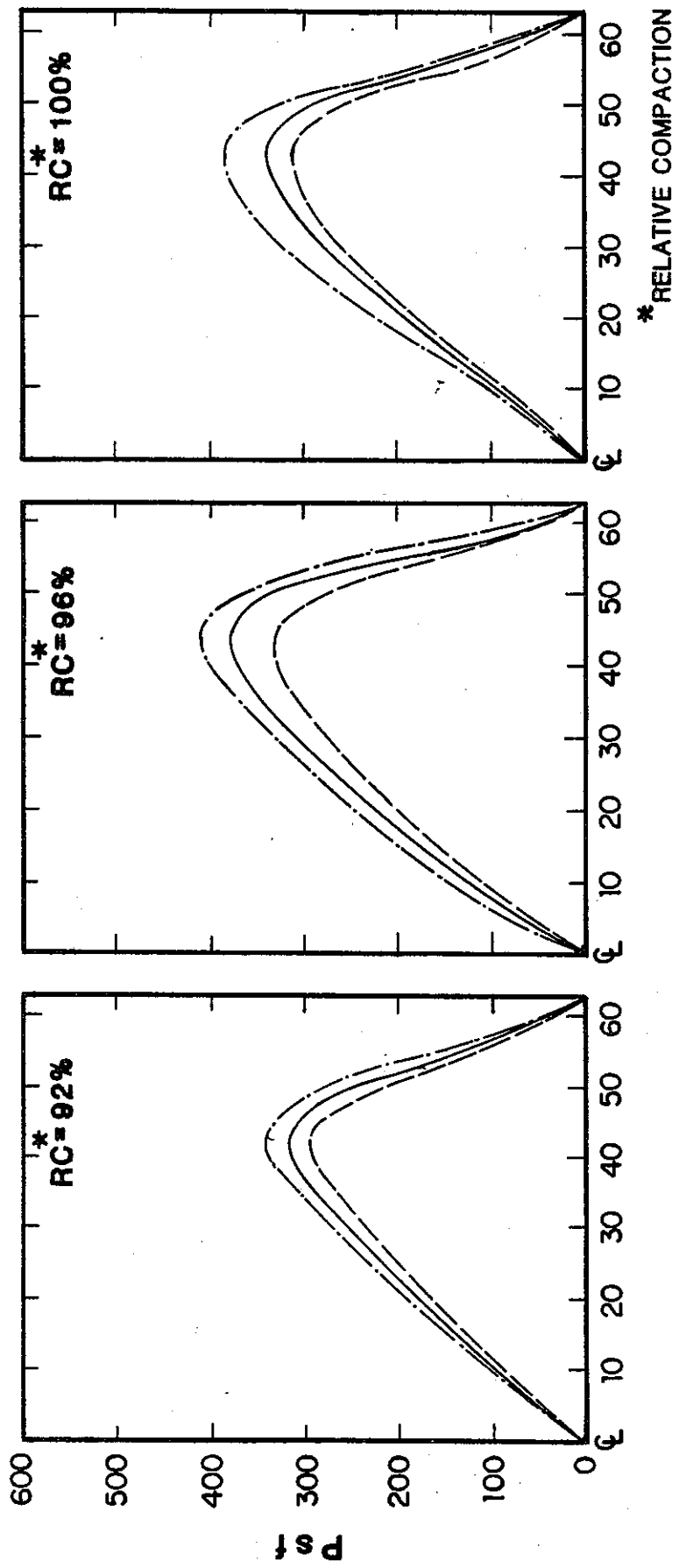
- - - -2% OF OPTIMUM  
 ——— OPTIMUM  
 - . - . +2% OF OPTIMUM



Distance from Centerline (ft.)

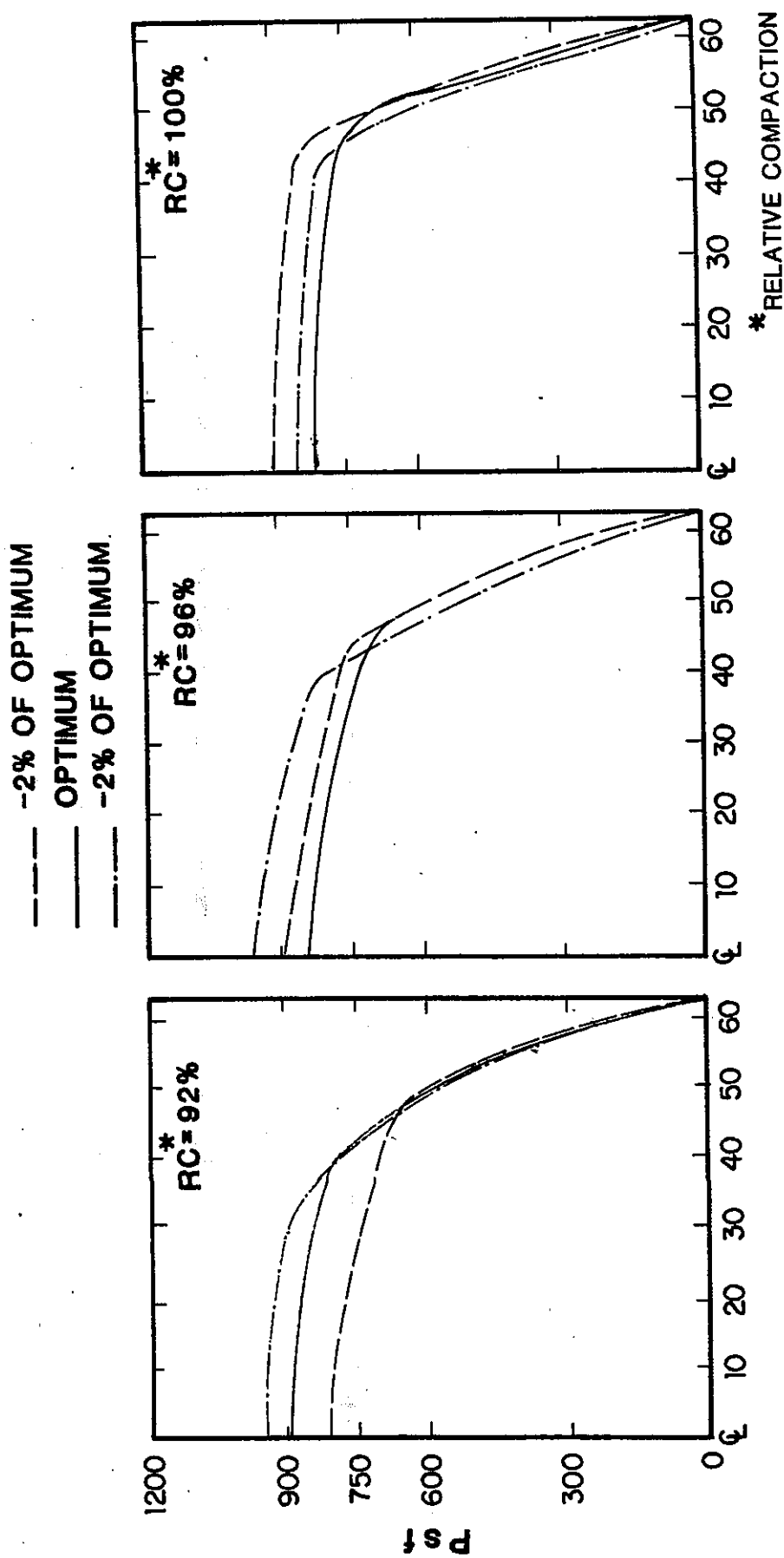
Figure C4. VERTICAL STRESS @ MIDHEIGHT OF 50 FT. EMBANKMENT, 1.5 : 1 SLOPES

- - - -2% OF OPTIMUM  
 ——— OPTIMUM  
 - - - +2% OF OPTIMUM



Distance from Centerline (ft.)

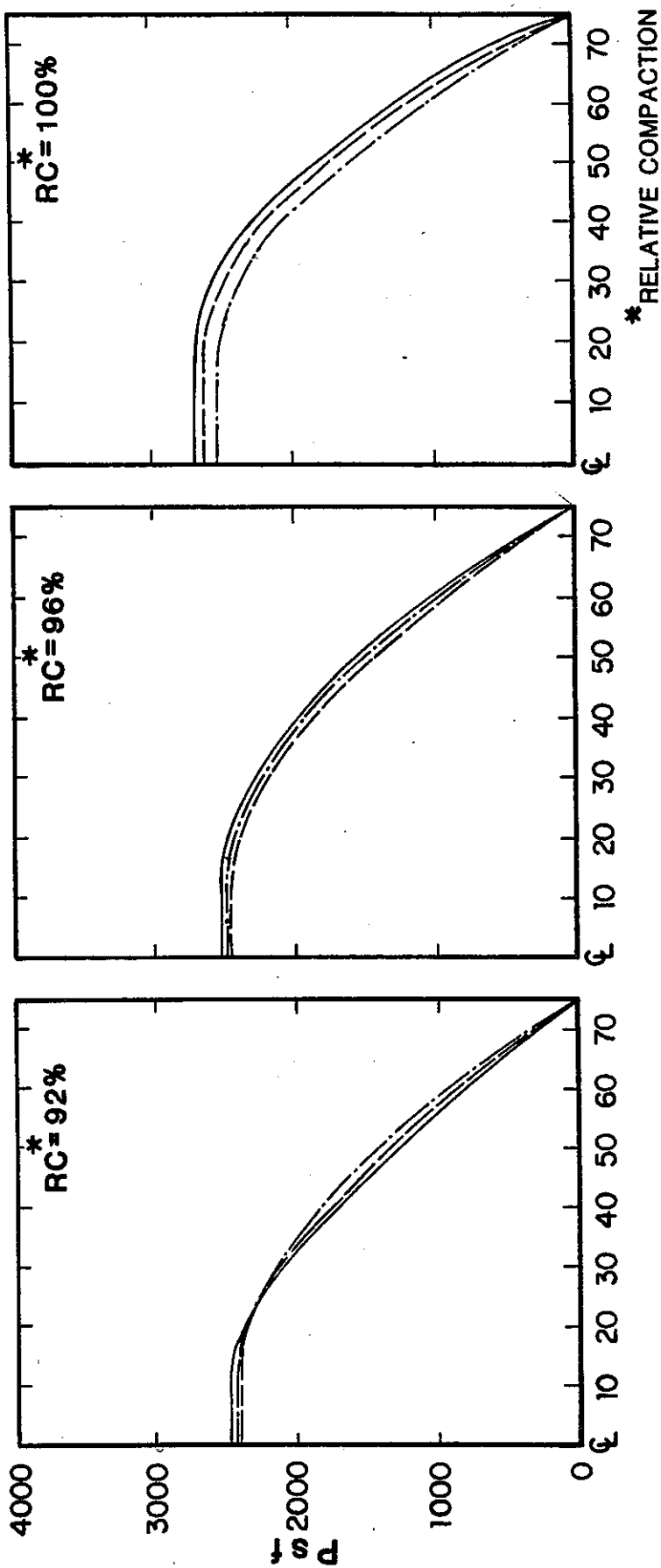
Figure C6. HORIZONTAL SHEAR STRESS @ MIDHEIGHT OF 50 FT.  
 EMBANKMENT, 1.5 : 1 SLOPES



Distance from Centerline (ft.)

Figure C5. LATERAL STRESS @ MIDHEIGHT OF 50 FT. EMBANKMENT, 1.5 : 1 SLOPES

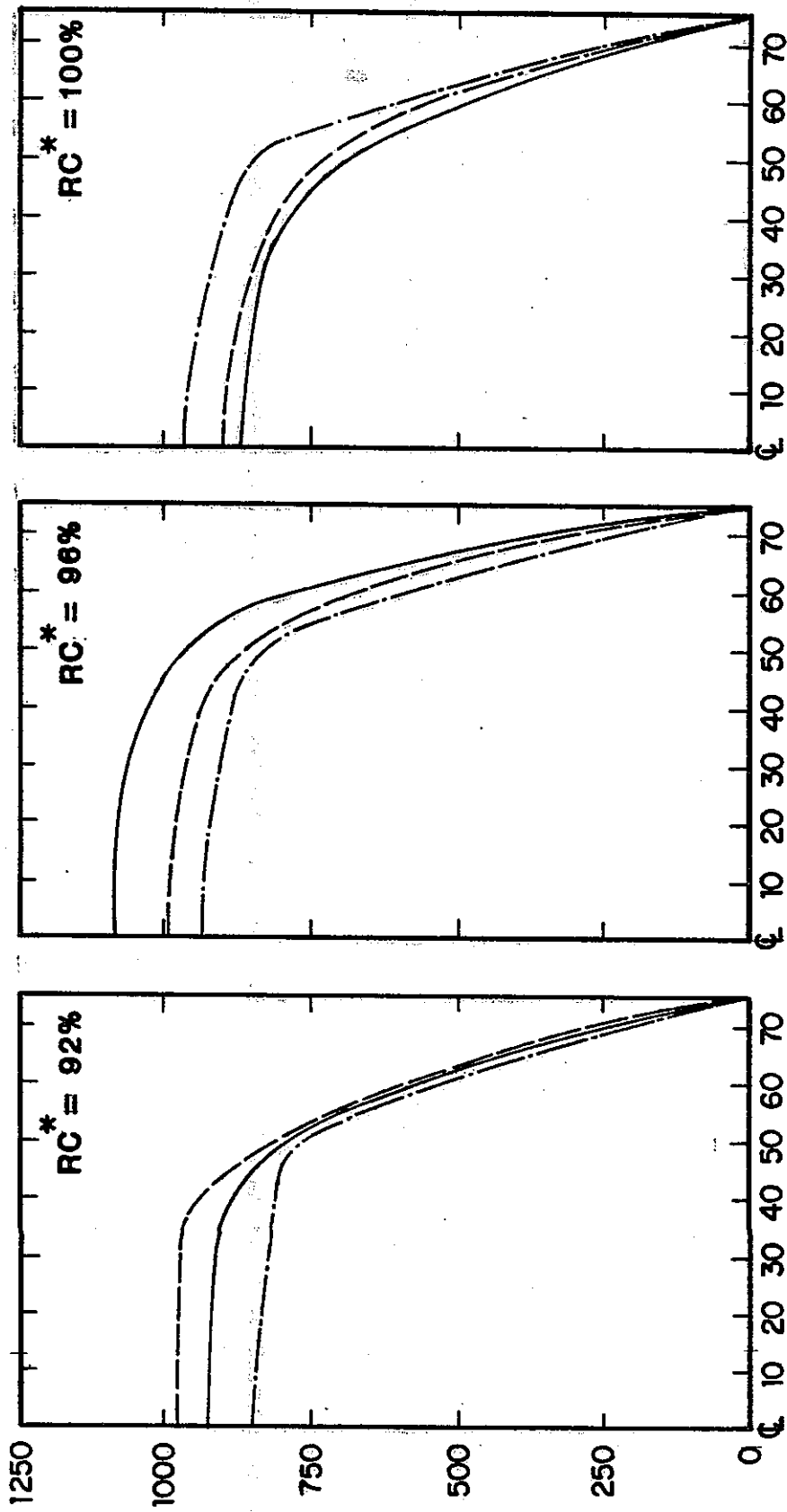
- - - -2% OF OPTIMUM  
 ——— OPTIMUM  
 - . - . +2% OF OPTIMUM



Distance from Centerline (ft.)

Figure C7. VERTICAL STRESS @ MIDHEIGHT OF 50 FT.  
 EMBANKMENT, 2 : 1 SLOPES

- - - -2% OF OPTIMUM  
 ——— OPTIMUM  
 - - - +2% OF OPTIMUM

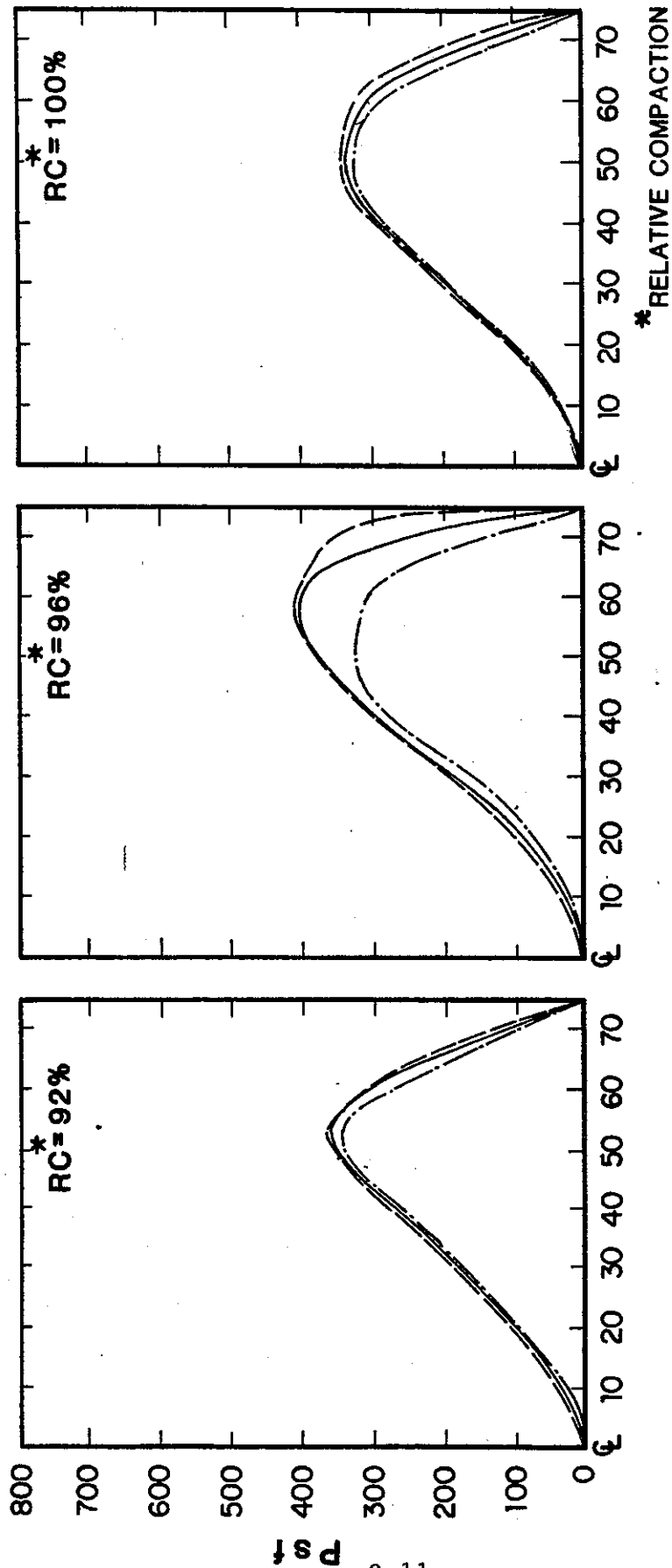


\*RELATIVE COMPACTION

Distance from Centerline (ft.)

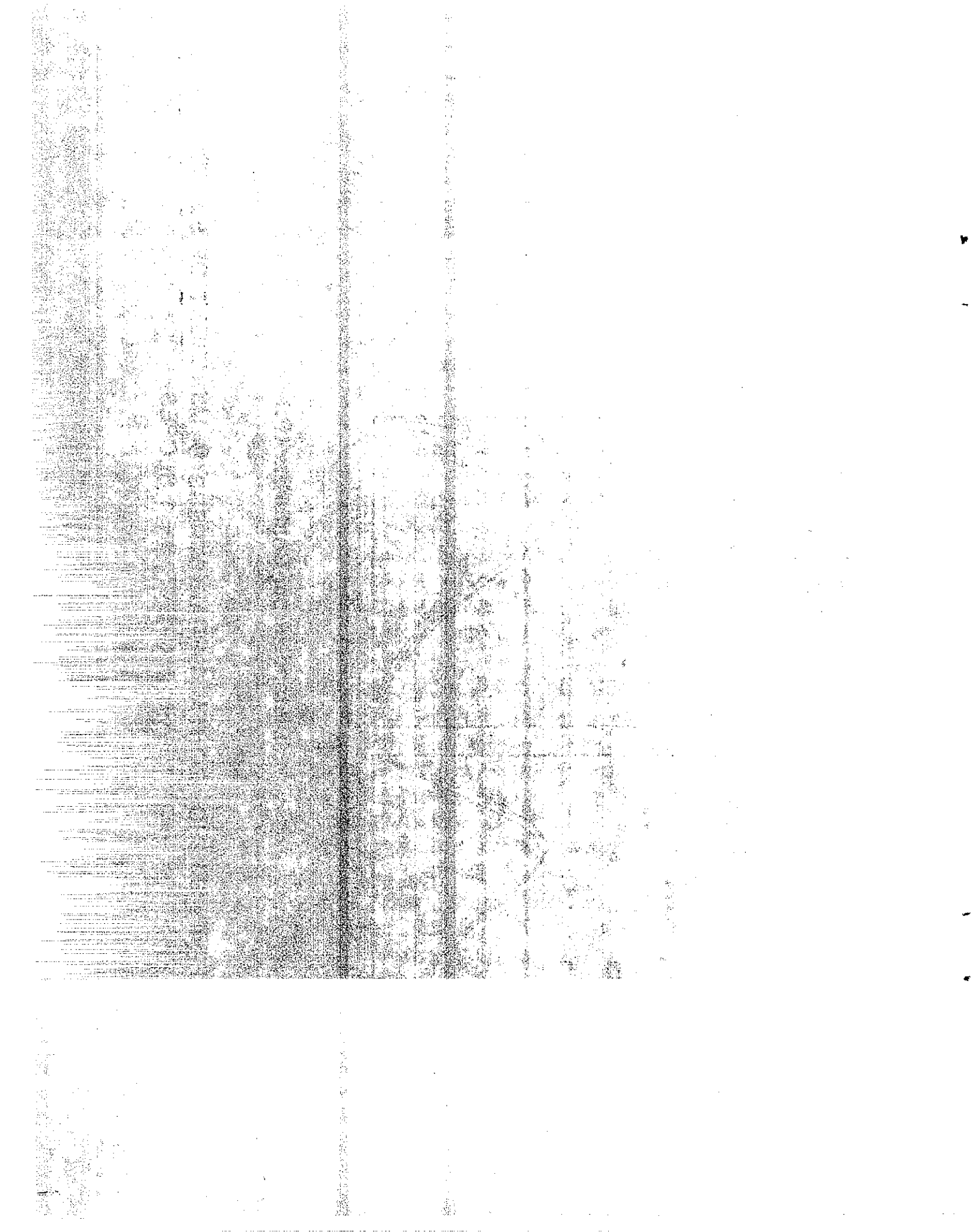
**Figure C8. LATERAL STRESS @ MIDHEIGHT OF 50 FT.  
 EMBANKMENT, 2 : 1 SLOPES**

- - - -2% OF OPTIMUM  
 ——— OPTIMUM  
 - . - . +2% OF OPTIMUM



Distance from Centerline (ft.)

Figure C9. HORIZONTAL SHEAR STRESS @ MIDHEIGHT OF 50 FT.  
 EMBANKMENT, 2 : 1 SLOPES

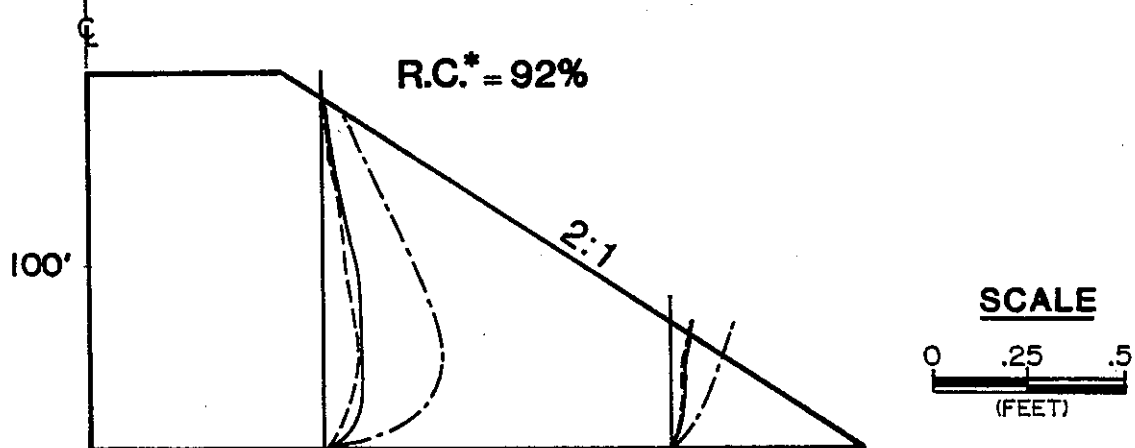
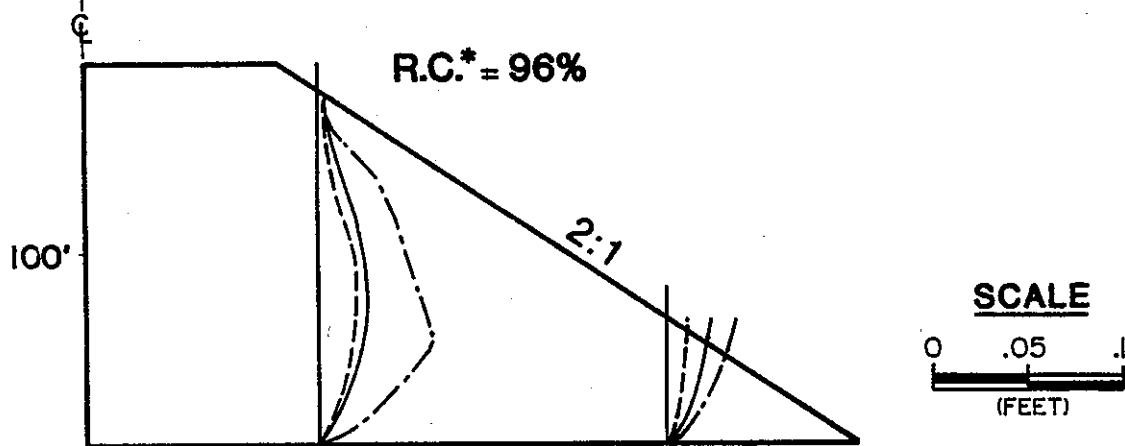
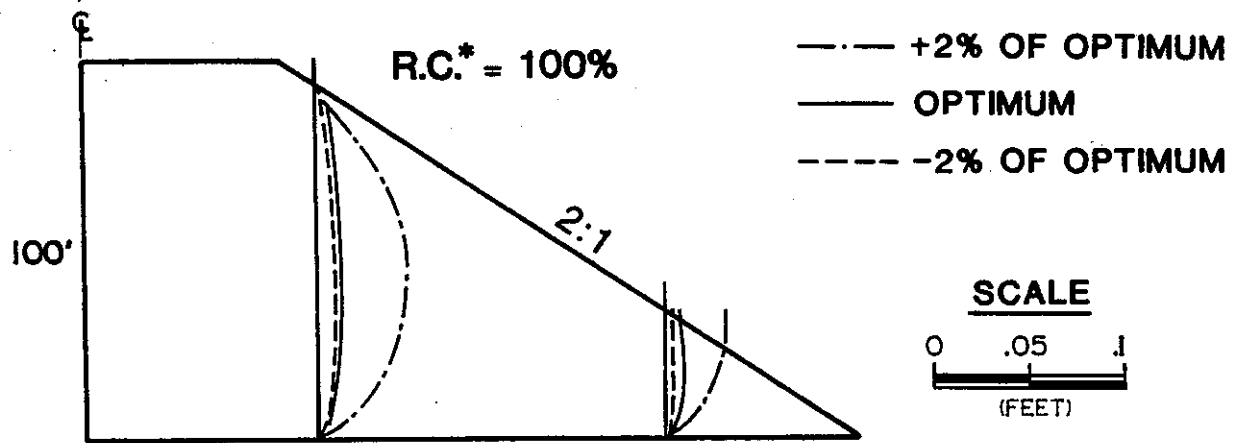


APPENDIX D

Plots of Embankment Movements

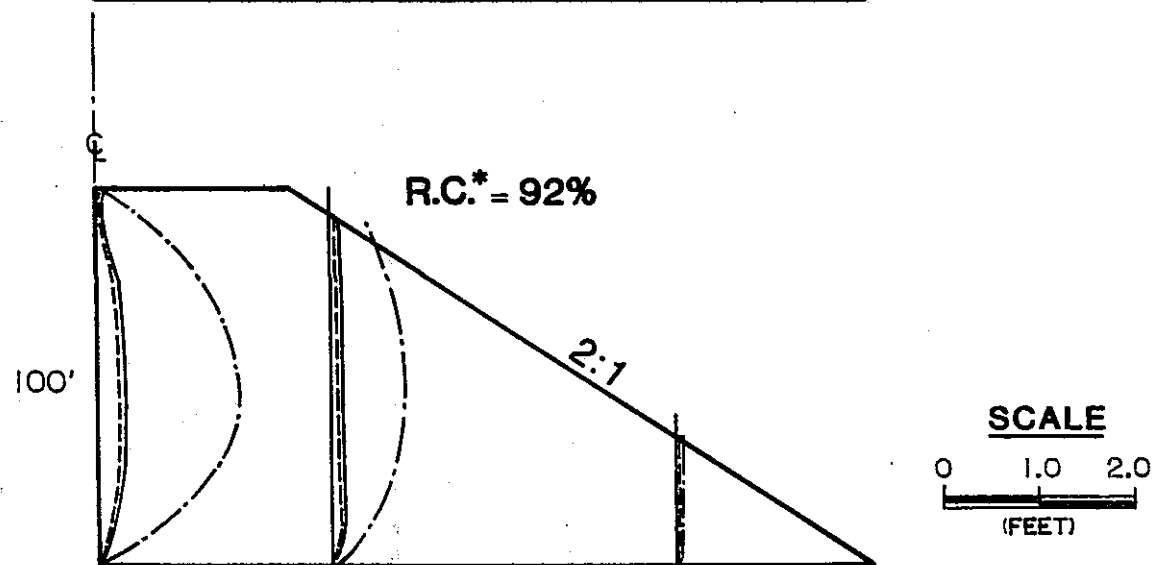
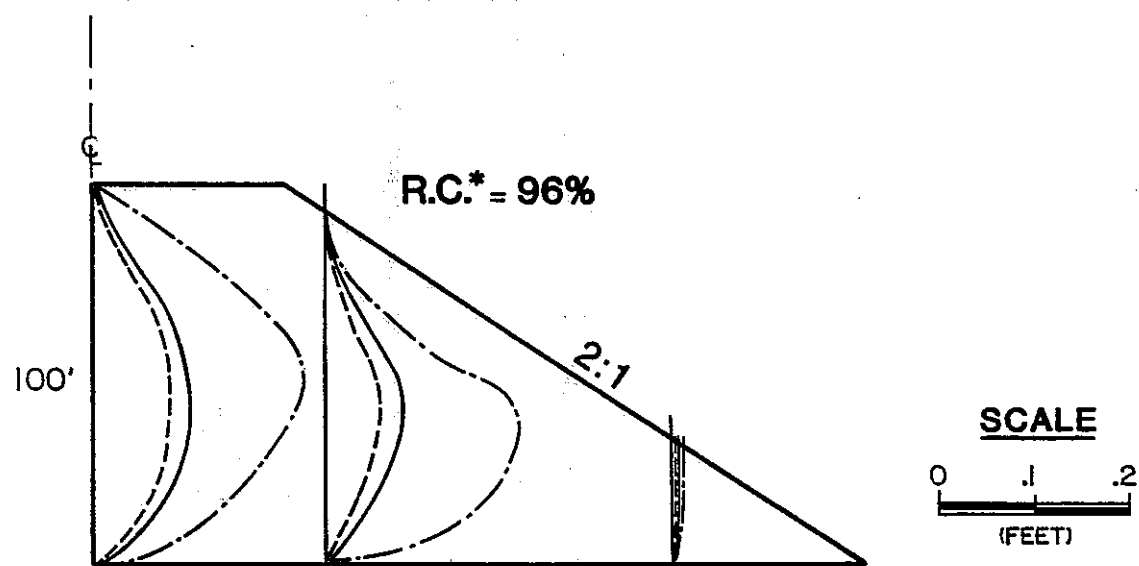
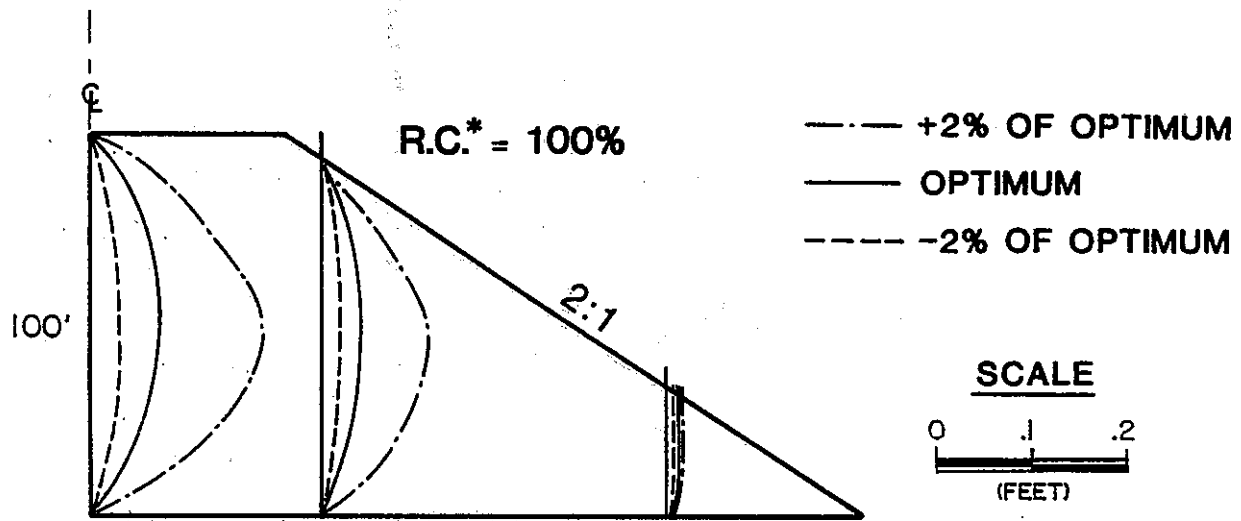
## LIST OF FIGURES

	<u>Page</u>
D.1 Horizontal Movements, 100 ft. Embankment, 2:1 Slopes	D-3
D.2 Vertical Movements, 100 ft. Embankment, 2:1 Slopes	D-4
D.3 Horizontal Movements, 50 ft. Embankment, 1.5:1 Slopes	D-5
D.4 Vertical Movements, 50 ft. Embankment, 1.5:1 Slopes	D-6
D.5 Horizontal Movements, 50 ft. Embankment, 2:1 Slopes	D-7
D.6 Vertical Movements, 50 ft. Embankment, 2:1 Slopes	D-8



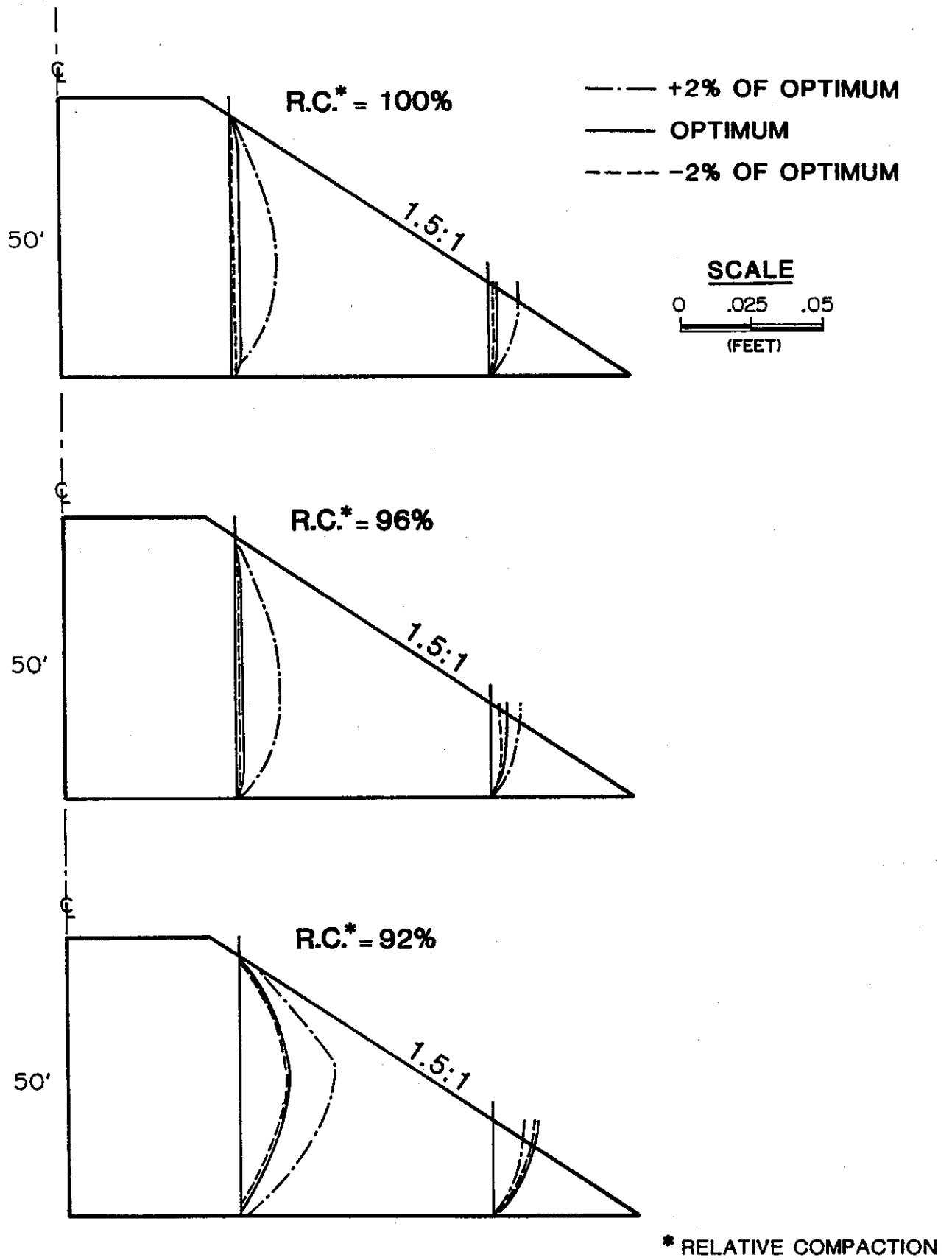
\* RELATIVE COMPACTION

Figure D.1. HORIZONTAL MOVEMENTS, 100ft EMBANKMENT, 2:1 SLOPES

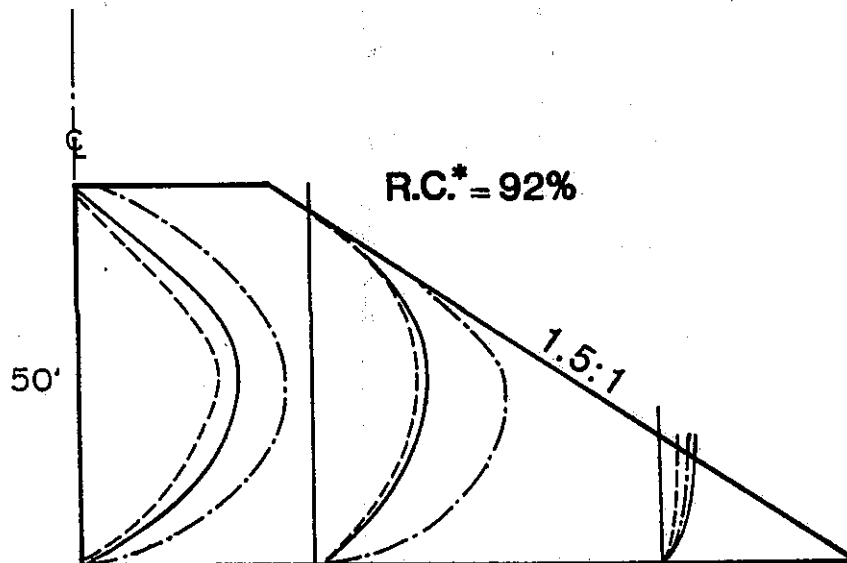
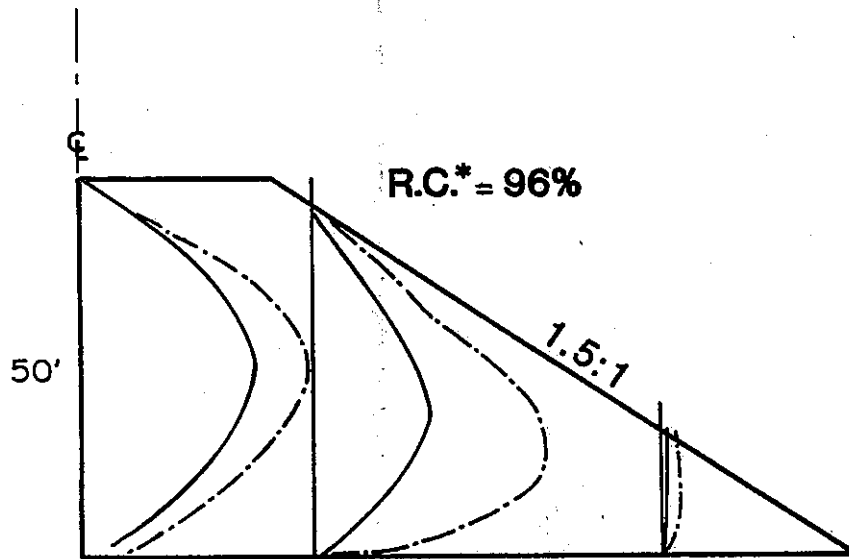
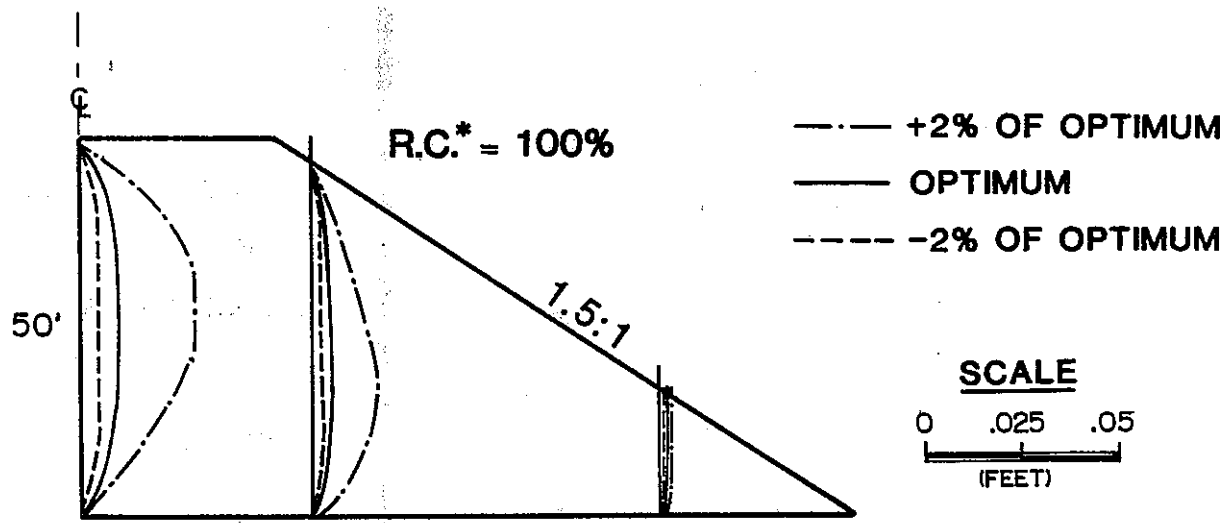


\* RELATIVE COMPACTION

Figure D.2. VERTICAL MOVEMENTS, 100ft EMBANKMENT, 2:1 SLOPES



**Figure D.3. HORIZONTAL MOVEMENTS, 50ft EMBANKMENT, 1.5:1 SLOPES**



\* RELATIVE COMPACTION

**Figure D.4. VERTICAL MOVEMENTS, 50ft EMBANKMENT, 1.5:1 SLOPES**

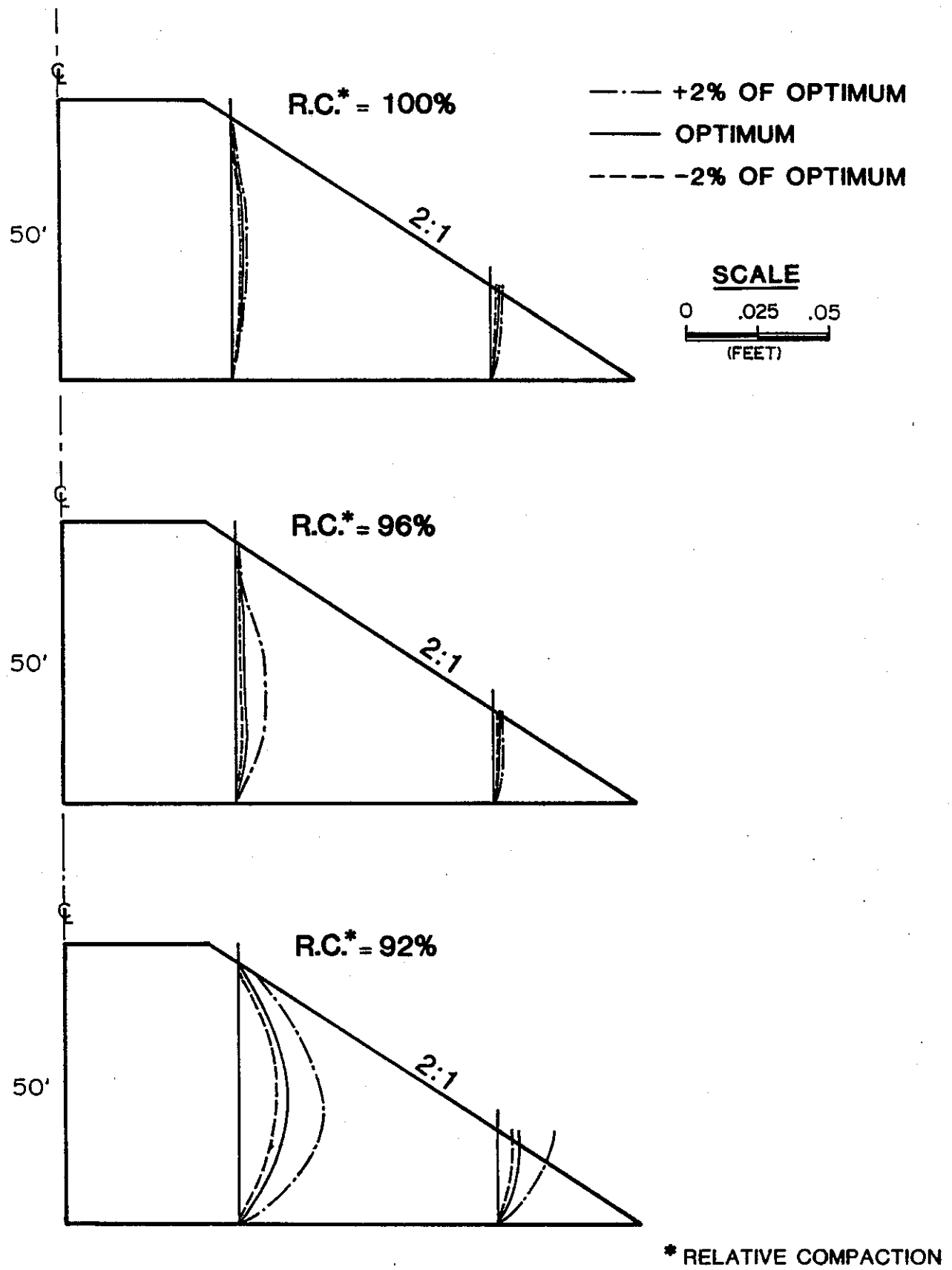
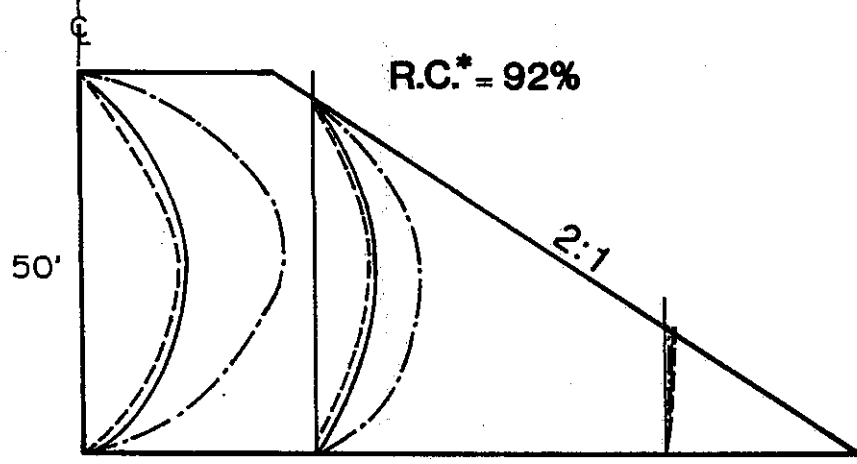
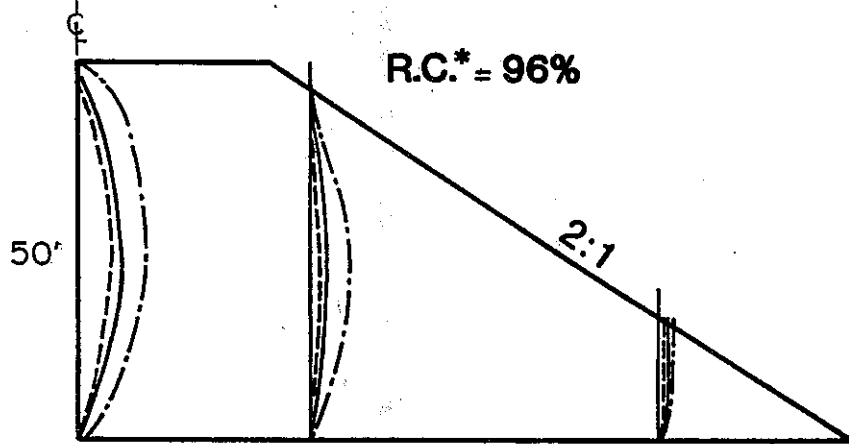
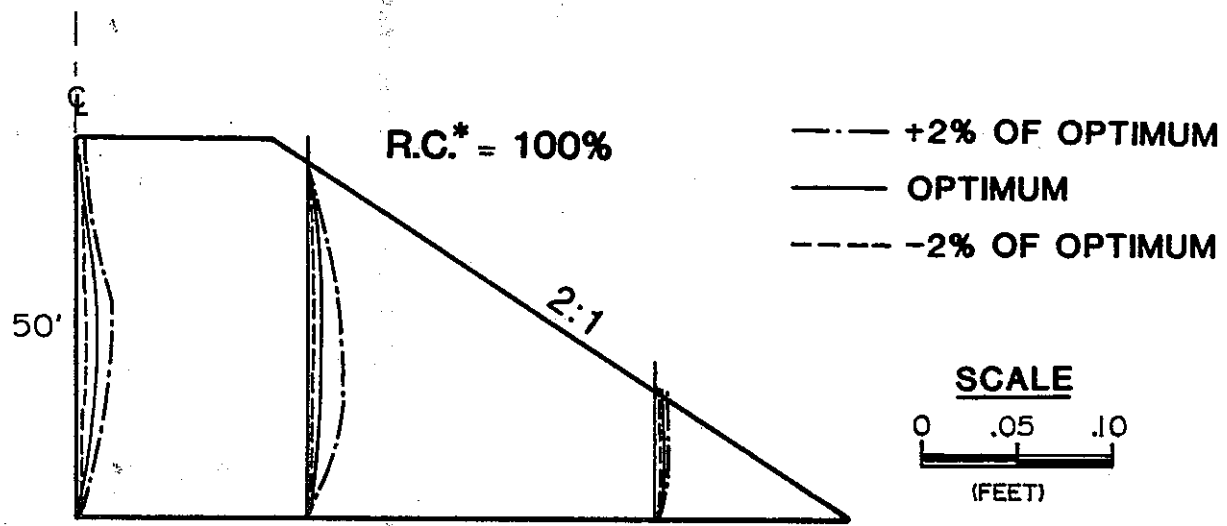


Figure D.5. HORIZONTAL MOVEMENTS, 50ft EMBANKMENT, 2:1 SLOPES



\* RELATIVE COMPACTION

Figure D.6. VERTICAL MOVEMENTS, 50ft EMBANKMENTS, 2:1 SLOPES

APPENDIX E

Instruction Manual for California Resonant  
Footing Apparatus and Testing Procedures

## TABLE OF CONTENTS

	<u>Page</u>
Surface Preparation	E-4
Assembly	E-9
Footing Placement	E-10
Electrical Connections	E-12
Electronic Instrument Settings	E-15
Testing Procedure	E-19
Footing Removal	E-20
Data Reduction	E-21

## LIST OF FIGURES

	<u>Page</u>
E.1 Vaned Footing Plate Attachment	E-5
E.2 Torsional Spring Attachment	E-6
E.3 Beam Adjustment for Magnet and Coil Attachment	E-7
E.4 Top Beam Attachment	E-7
E.5 Top and Bottom Beam Locking Latches	E-8
E.6 Ballast Weight Attachment	E-8
E.7 Locking Latch Test Position	E-11
E.8 Simplified Wiring Diagram	E-13
E.9 Detailed Wiring Diagram	E-14
E.10 Oscilloscope Settings	E-17
E.11 Amplitude Reduction Curves	E-22
E.12 Shear Modulus Curves	E-24
E.13 Rotational Slippage Factor Curves	E-26

## SURFACE PREPARATION

Remove the top unrepresentative soil and clear a level surface somewhat larger (approximately 3 feet square) than the 12 inch diameter footing. There should be enough clearance around the footing at all points such that during testing the footing will at no time contact anything except the soil directly beneath the vared footing base.



**Fig. E.1. VANE FOOTING PLATE ATTACHMENT**

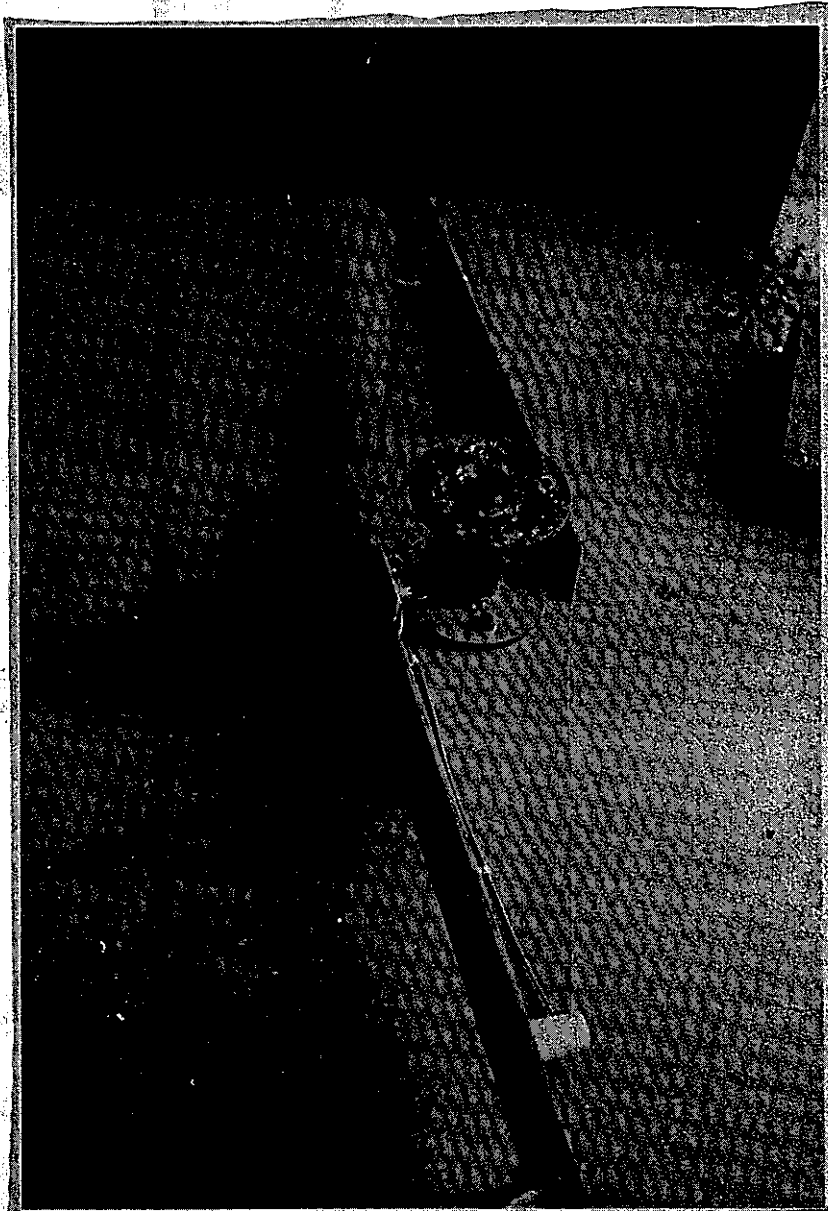


**Fig. E.2. TORSIONAL SPRING ATTACHMENT**

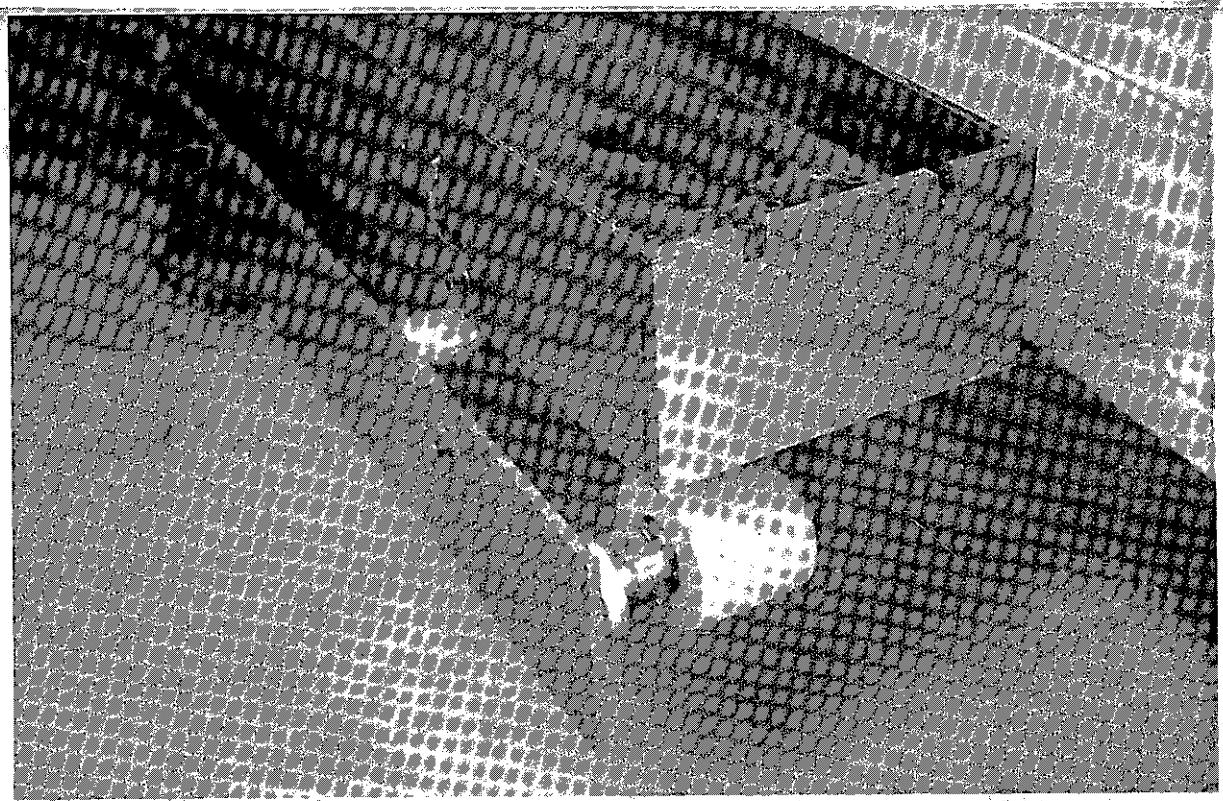


**Fig. E.3. BEAM ADJUSTMENT FOR MAGNET AND COIL ATTACHMENT**

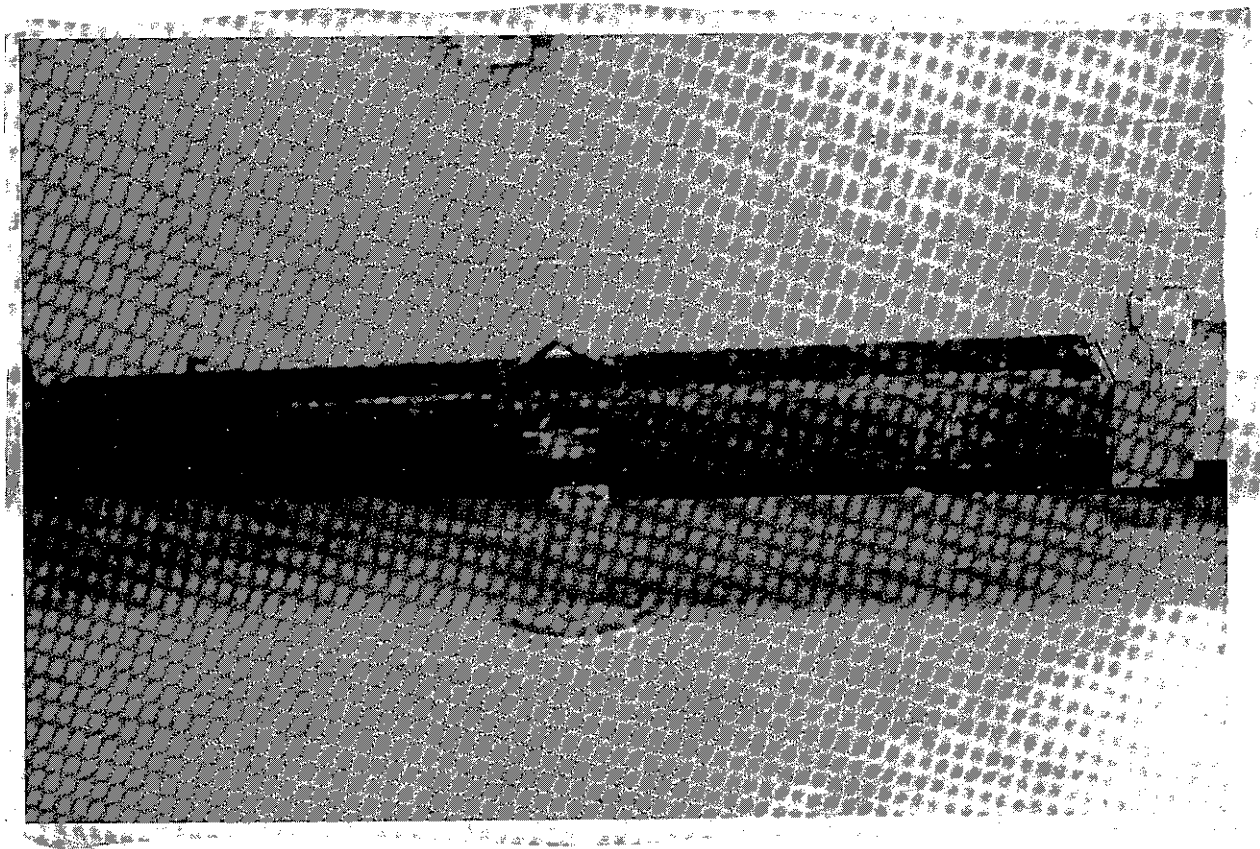


**Fig. E.4. TOP BEAM ATTACHMENT**

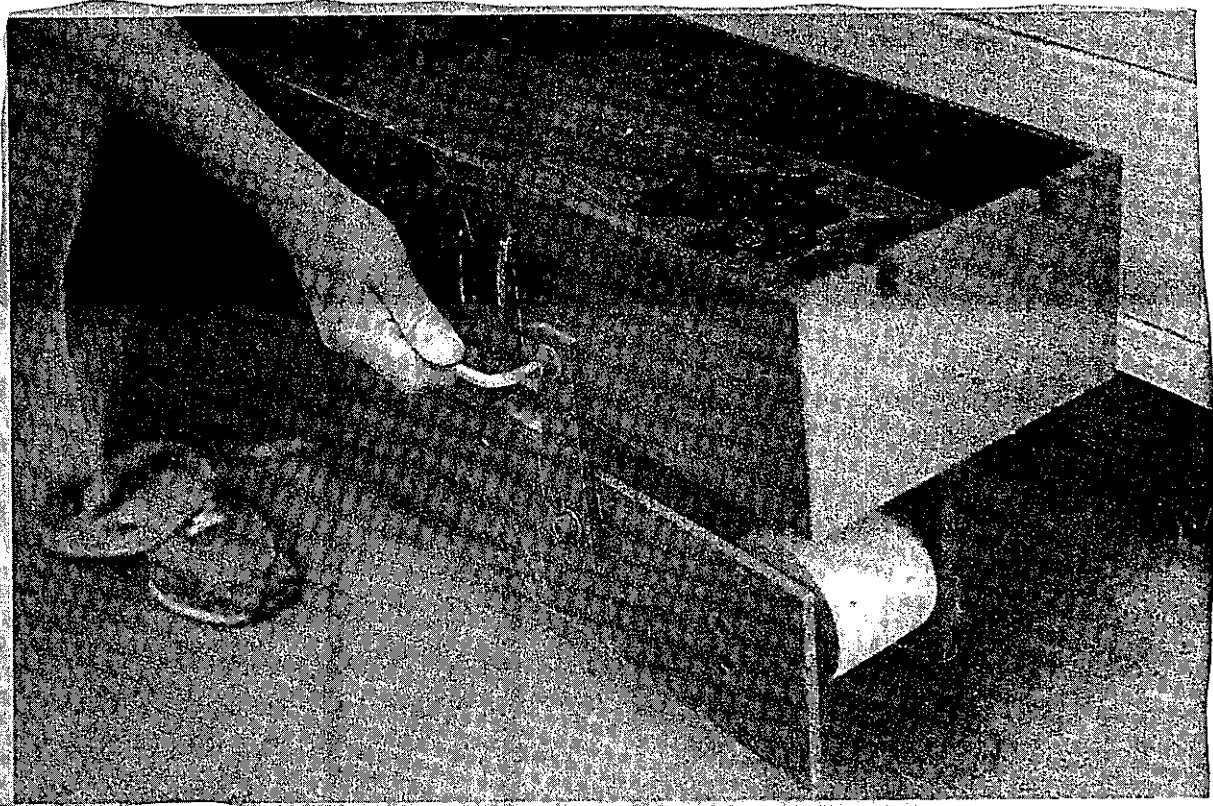


**Fig. E.5. TOP AND BOTTOM BEAM LOCKING LATCHES**



**Fig. E.6. BALLAST WEIGHT ATTACHMENT**

## ASSEMBLY

Bolt the vaned footing plate to the footing mounting plate and bottom beam as shown in Figure E.1. Set the bottom beam on the vaned footing and bolt the torsional (2 inch pipe) spring to the bottom beam as shown in Figure E.2. (In assembly be sure to align the "FRONT" labels on the bottom beam, torsional spring and top beam on the same side.) Set the top beam on the torsional spring with the milled slots in the end plates of the top beam facing up. Rotate the top beam so that sufficient clearance is provided at the ends to attach the magnet plates, magnets and coils at each end as shown in Figure E.3. Attach the magnet plates, magnets and coils according to the "A" and "B" codings on the magnets, coils and beam ends. Carefully rotate the top beam into position such that the coils slide into the magnet gaps. Adjust the coil-magnet alignment at each end by moving magnet, magnet plate and/or coil. Bolt the top beam to the torsional spring as shown in Figure E.4. Check magnet-coil alignment and tighten all bolts. Magnets and coils should not touch each other. Check this condition before testing by the procedure outlined in FOOTING PLACEMENT. Lock the top and bottom beams together with the locking latches as shown in Figure E.5.

NOTE: These locking latches should always be in place except when testing. The ballast weights are simply bolted to the ends of the top beam as shown in Figure E.6, according to the red-orange color code. Support the footing at each end while adding the ballast weights.

## FOOTING PLACEMENT

CAUTION: The locking latches on the sides of the footing should be bolted between the top and bottom beams at all times except when testing.

With the locking latches in place, carefully place the footing on the prepared surface. Check to make sure the vanes on the footing base have penetrated into the soil. If the vanes have not penetrated into the soil, the ballast weights must be bolted to each end of the footing. Support the footing at each end to prevent tipping while adding the weights. The weights are color coded and should always be attached according to the color code. Without the ballast weights in place, the footing applies a bearing pressure of 2.64 psi (0.19 tsf) to the soil. With the ballast weights in place, the footing applies a bearing pressure of 4.43 psi (0.32 tsf). Thus soils may be tested under two different pressures, however, for stiff soils the ballast weights should always be in place to insure coupling with the soil and provide sufficient inertia for the top beam.

When the footing is in its final position for testing, release the locking latches from the bottom beam and bolt the latches securely to the sides of the top beam (see Figure E.7). Check the coils for freedom of movement by striking the top beam with your fist and checking for vibration by placing the thumb and forefinger on the coil adjacent to the magnet. If no movement is detected, adjust the coil-magnet alignment by loosening the mounting bolts and moving the coils and/or magnets until they move freely. If the coils and magnets touch, the electrical signals will be distorted. The footing is now ready to be connected to the electronic measuring system.

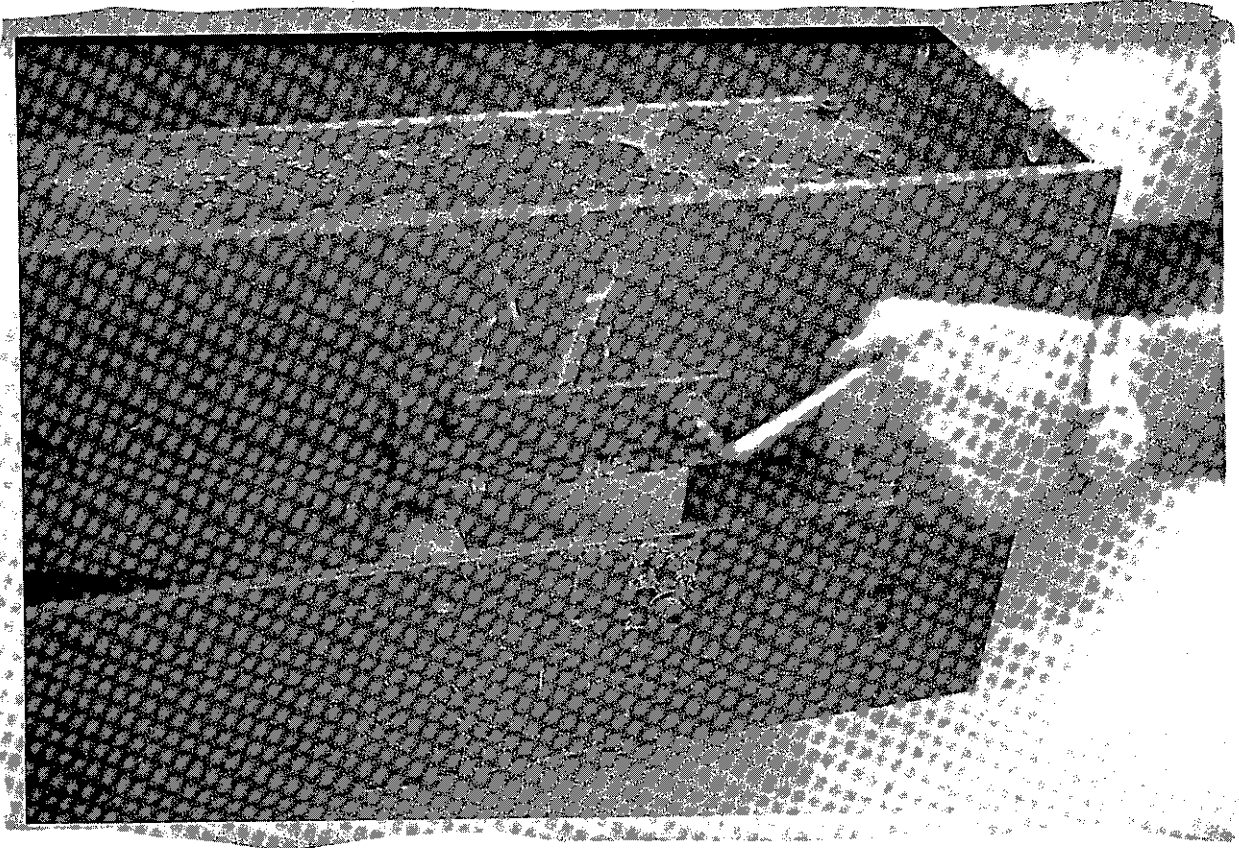


**Fig. E.7. LOCKING TEST POSITION**

## ELECTRICAL CONNECTIONS

A simplified wiring schematic is shown in Figure E.8. Detailed wiring of components is shown in Figure E.9. Referring to Figure E.9, the wiring is as follows: Connect the 204C Oscillator to the 6824A DC Power Supply Amplifier INPUT using a double banana to double banana patch cord provided. (The ground or black wire side of the plugs should always be inserted into the black or COM plug on the instrument.) Connect the DC Power Supply Amplifier INPUT to the Fluke 1900 A Multi Counter using a double banana to BNC patch cord provided. (The double banana plug may be plugged into the back of the double banana plug which was placed in the DC Power Supply Amplifier INPUT in the previous step. Connect the DC Power Supply Amplifier OUTPUT to the EXT TRIGGER OR X-INPUT on the 1220 A Oscilloscope using a double banana to BNC patch cord provided. Connect the DC Power Supply Amplifier OUTPUT to the footing drive coils using the 15 foot double banana to double banana patch cord provided. Plug one end of the patch cord into the red and black terminals at the center of the footing on the bottom beam. The other end may be plugged into the back of the double banana plug already in the DC Power Supply Amplifier OUTPUT from the previous step. Finally, connect the A-Channel INPUT of the 1220 A Oscilloscope to the velocity transducer on the footing using the BNC to Audio Plug patch cord provided. The Audio Plug terminal is located on the footing next to the banana plug terminals for the drive coils.

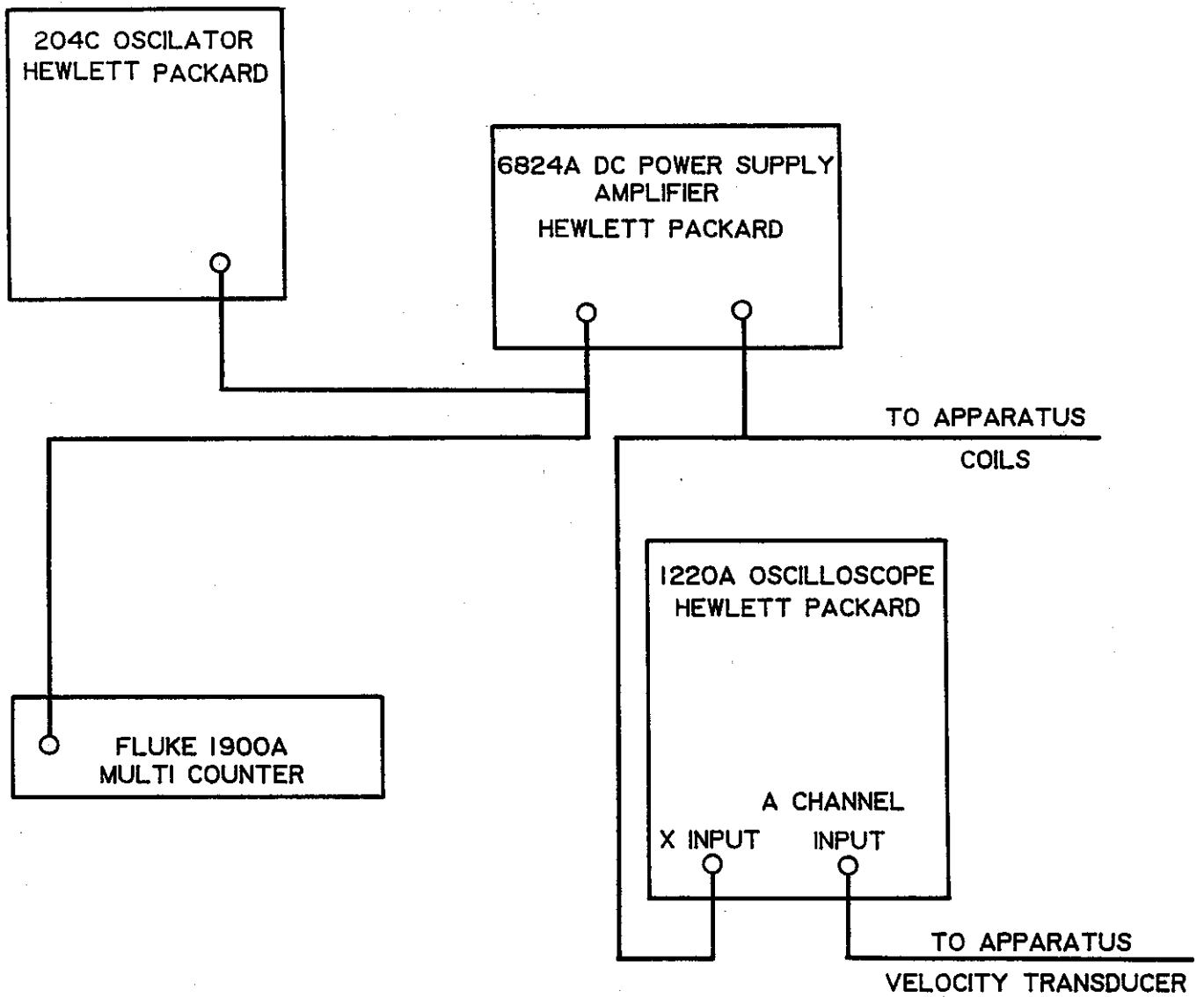
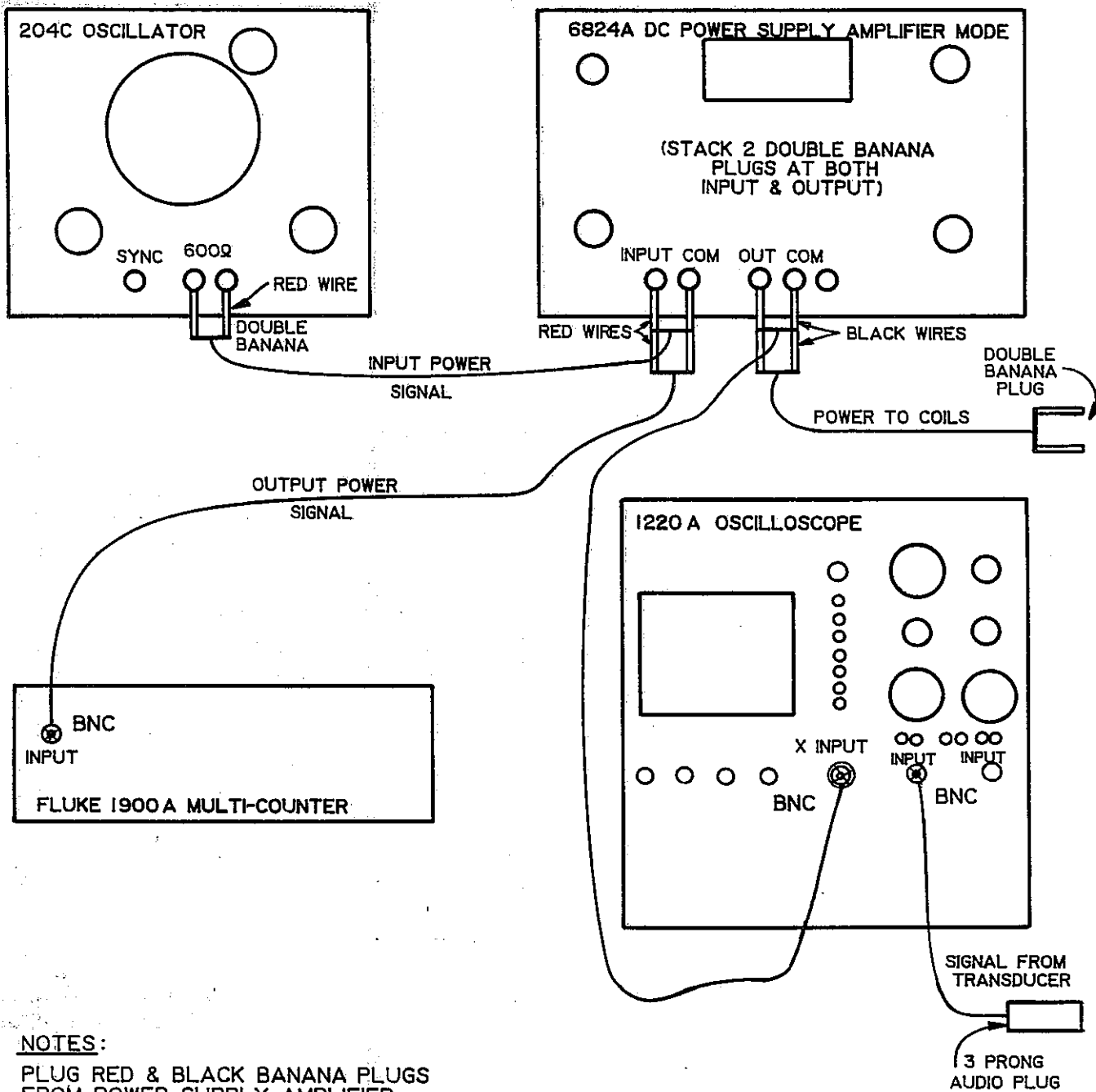


**Fig. E.8. WIRING SCHEMATIC**



**NOTES:**

PLUG RED & BLACK BANANA PLUGS FROM POWER SUPPLY AMPLIFIER OUTPUT INTO RED & BLACK BANANA PLUGS RESPECTIVELY ON FOOTING.  
 PLUG 3 PRONG AUDIO PLUG INTO RECEPTACLE ON FOOTING.

**Fig. E.9. DETAILED WIRING DIAGRAM**

## ELECTRONIC INSTRUMENT SETTINGS

### 204 C Oscillator

Range - X10

Frequency - is variable and must be adjusted to produce resonance. This may be done by the coarse (center) or fine (upper right) adjustment knobs.

Amplitude - is variable and can be adjusted to produce a desired rotational amplitude. (See TESTING PROCEDURE AND DATA REDUCTION)

### 6824A DC Power Supply Amplifier

Mode - Amplifier

Meter - AC Volts

Volts ° Gain - Turn the outer knob fully clockwise. Do not adjust the inner knob.

### Fluke 1900A Multi Counter

ATTEN - IN

FILT - IN

FREQ - OUT

PER - IN

TOT - OUT

CHK - OUT

AUTO - OUT

100 Hz - IN

10 Hz - OUT

1 Hz - OUT

0.1 Hz - OUT

RESET - OUT

If signal is too weak to register on the meter (that is at low amplitudes) set the ATTEN button OUT. If it is desired to measure frequency in KHz instead of period in milliseconds, set the FREQ button IN, PER button OUT, 100 Hz button OUT and 0.1 Hz button IN.

## 1220 A Oscilloscope

Referring to Figure E.10 and using the numbering system shown, position the switches as follows:

- 1 - IN (ON)
- 2 - Approximately mid-position.
- 3 - Adjust as needed to sharpen trace.
- 4 - Push to bring picture to screen and hold in while adjusting 5 and/or 18 to center picture on screen.
- 5 - Horizontal position adjustment for picture.
- 6 - Not needed.
- 7 - Fine adjustment for horizontal width of picture.
- 8 - Not needed.
- 9 - "
- 10 - "
- 11 - "
- 12 - "
- 13 - "
- 14 - "
- 15 - IN
- 16 - Coarse adjustment for picture width. Adjust this and No. 7 to maintain picture width of approximately 2 divisions.
- 17 - Input from DC Power Supply Amplifier OUTPUT.

## ELECTRONIC INSTRUMENT SETTINGS

### 204 C Oscillator

Range - X10

Frequency - is variable and must be adjusted to produce resonance. This may be done by the coarse (center) or fine (upper right) adjustment knobs.

Amplitude - is variable and can be adjusted to produce a desired rotational amplitude. (See TESTING PROCEDURE AND DATA REDUCTION)

### 6824A DC Power Supply Amplifier

Mode - Amplifier

Meter - AC Volts

Volts ° Gain - Turn the outer knob fully clockwise. Do not adjust the inner knob.

### Fluke 1900A Multi Counter

ATTEN - IN

FILT - IN

FREQ - OUT

PER - IN

TOT - OUT

CHK - OUT

AUTO - OUT

100 Hz - IN

10 Hz - OUT

1 Hz - OUT

0.1 Hz - OUT

RESET - OUT

If signal is too weak to register on the meter (that is at low amplitudes) set the ATTEN button OUT. If it is desired to measure frequency in KHz instead of period in milliseconds, set the FREQ button IN, PER button OUT, 100 Hz button OUT and 0.1 Hz button IN.

## 1220 A Oscilloscope

Referring to Figure E.10 and using the numbering system shown, position the switches as follows:

- 1 - IN (ON)
- 2 - Approximately mid-position.
- 3 - Adjust as needed to sharpen trace.
- 4 - Push to bring picture to screen and hold in while adjusting 5 and/or 18 to center picture on screen.
- 5 - Horizontal position adjustment for picture.
- 6 - Not needed.
- 7 - Fine adjustment for horizontal width of picture.
- 8 - Not needed.
- 9 - "
- 10 - "
- 11 - "
- 12 - "
- 13 - "
- 14 - "
- 15 - IN
- 16 - Coarse adjustment for picture width. Adjust this and No. 7 to maintain picture width of approximately 2 divisions.
- 17 - Input from DC Power Supply Amplifier OUTPUT.

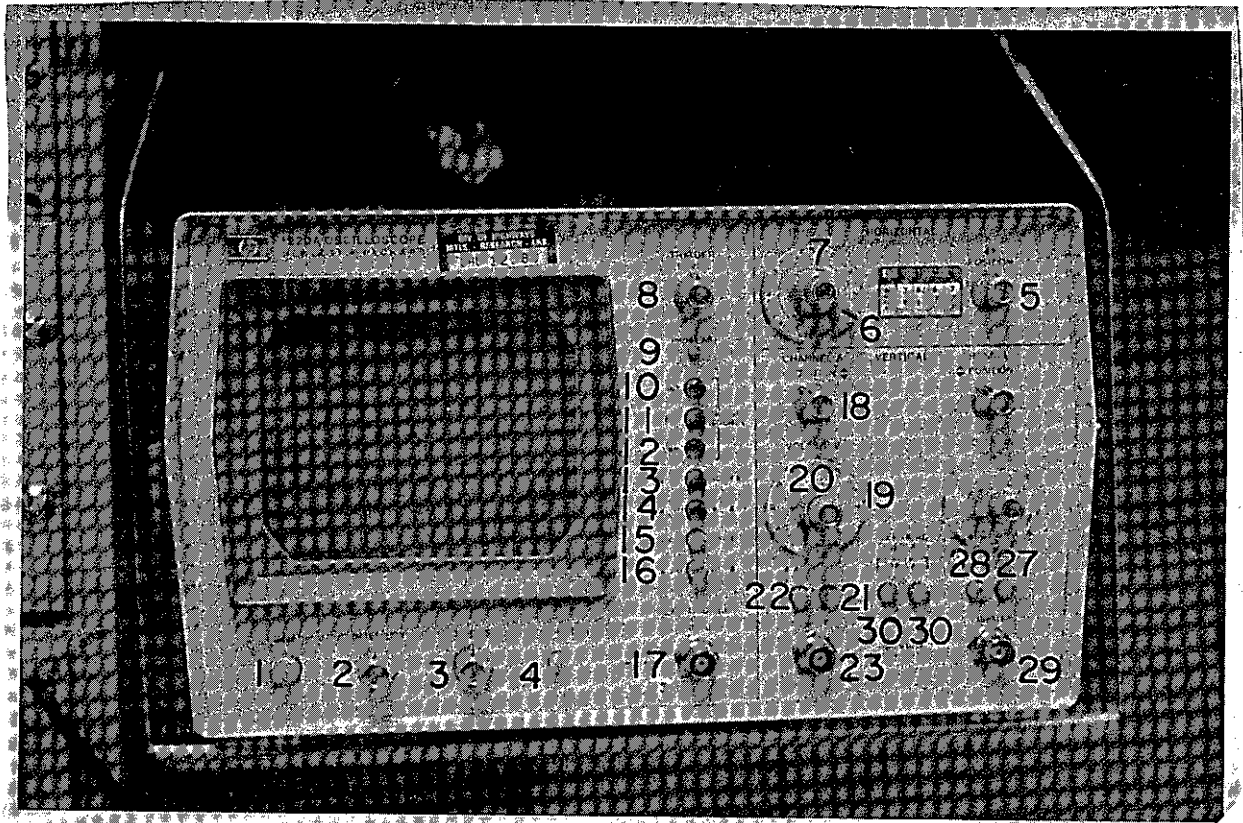


Fig. E.10. OSCILLOSCOPE SETTINGS

- 18 - Position adjustment for vertical position of picture.
- 19 - Vertical scale adjustment. Adjust so that picture covers more than 1/2 height of screen.
- 20 - Fully clockwise.
- 21 - OUT
- 22 - IN
- 23 - Input from velocity transducer on apparatus.
- 24 - Not needed
- 25 - "
- 26 - "
- 27 - "
- 28 - "
- 29 - "
- 30 - Button A - IN    Button B - OUT

## TESTING PROCEDURE

Once all connections have been made and all electronic instruments have been turned on, turn the amplitude knob on the 204C Oscillator clockwise to mid-position. (This may be subsequently adjusted to vary rotational amplitude. See DATA REDUCTION). Locate trace with the beam finder (Button 4 on the 1220 A Oscilloscope) and center the trace on the screen. Adjust the frequency starting at 32 Hz (3.2 on the 204C Oscillator large dial) and gradually increase the frequency until resonance is obtained. (Resonance is denoted by a trace forming a single sloping line.) Adjustments of switches 7, 16 and 19 on the 1220A Oscilloscope may be necessary to keep the trace at least 2 divisions wide and 4 divisions high. If the Fluke 1900A Multi Counter is measuring frequency, wait at least 10 seconds and record the frequency in Hz. (Reading times 1000.) If the Multi Counter is measuring period in milliseconds, record the value directly.

If rotational amplitude is needed, record the trace height in divisions and fractions of a division top to bottom. Multiply this value (peak to peak amplitude) by the volts/div factor shown on knob 19 of the 1220A Oscilloscope and record the result in peak to peak volts. If using a RMS Voltmeter to record the velocity transducer output voltage, multiply this value by  $\sqrt{2}$  to get the peak to peak voltage.

## FOOTING REMOVAL

When testing is completed, turn the power to the footing off by turning the AMPLITUDE knob on the 204C Oscillator fully counterclockwise. Disconnect the double banana plug and audio plug from the footing. Replace the locking latches such that the top and bottom beams are bolted firmly together by the locking latches. If in place, remove the ballast weights. The footing is now ready for transport to the next test site.

## DATA REDUCTION

### Amplitude

To obtain the peak to peak rotational amplitude,  $\theta$ , enter Figure E.11 with the peak to peak voltage reading obtained in TESTING PROCEDURE and read  $\theta$  for the appropriate system resonant frequency,  $f_n$ , curve or interpolate between curves. Alternately rotational amplitude,  $\theta$ , may be obtained from the equation:

$$\theta = \frac{19.89 TV}{f_n} \quad \text{or} \quad \theta = \frac{19.89 V}{f_n}$$

where  $\theta$  = peak to peak rotational amplitude (Radians X  $10^{-3}$ )  
V = peak to peak transducer voltage reading (Volts)  
T = System resonant period (milliseconds)  
 $f_n$  = System resonant frequency (Hz) =  $\frac{1000}{T}$

### Shear Modulus

The expression for the apparent shear modulus,  $G_F$ , as measured by the footing assuming no slippage is given by:

$$G_F = \frac{3}{16} \frac{K_{app}}{r_o^3} \frac{f_n^2}{f_{app}} - 1$$

where  $K_{app}$  = the spring constant of the apparatus (in-lb/rad)  
 $f_{app}$  = the resonant frequency of the apparatus (Hz)  
 $f_n$  = the system resonant frequency (i.e., the resonant frequency as determined in TESTING PROCEDURE) (Hz)  
 $r_o$  = the radius of the footing (inches)

Development of this equation is given by Pang (1).

1. Pang, D., "Resonant Footing Test," Thesis submitted to the University of Kentucky in partial fulfillment of the requirements for the degree of Doctor of Philosophy, November 1972.

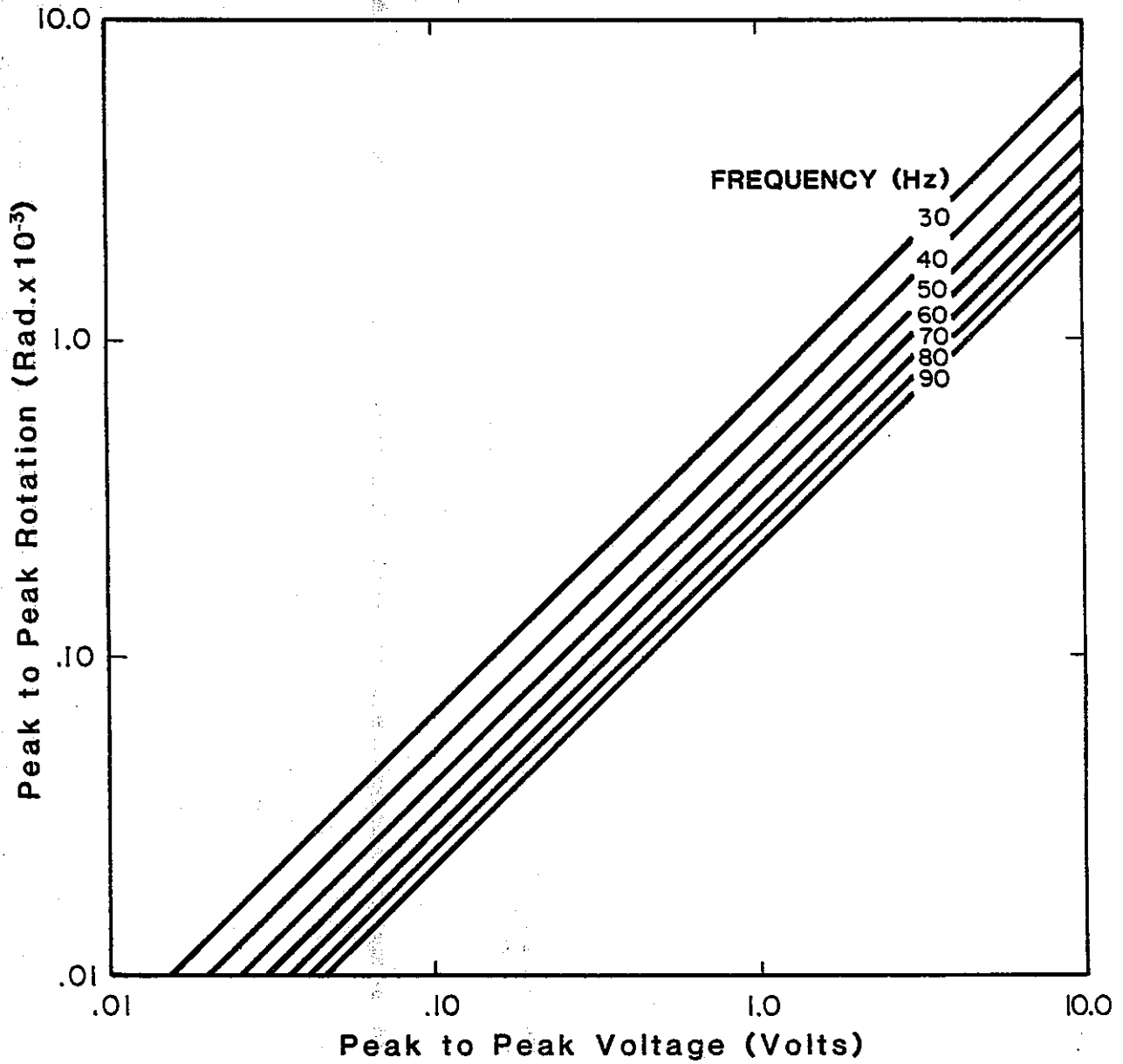


**Fig. E.11. HARDIN RESONANT FOOTING APPARATUS FOR CALIFORNIA DEPARTMENT OF TRANSPORTATION**

For this resonant footing apparatus:

$$K_{app} = 2.315 \times 10^6 \text{ in-lb/rad}$$

$$f_{app} = 32.3 \text{ Hz}$$

$$r_0 = 6.0 \text{ inches}$$

The complete calibration is shown in Appendix I.

The slippage factor, as defined by Pang is given by:

$$SF = \frac{G_F}{G_{real}}, \text{ where } G_{real} \text{ is the actual in situ shear modulus.}$$

$$\text{Rearranging the equation yields: } G_{real} = \frac{G_F}{SF}$$

For cohesive soils, the slippage factor,  $SF = 0.50$ . To obtain the shear modulus,  $G_{real}$ , enter Figure E.12 with the system resonant frequency,  $f_n$ , and read  $G_{real}$  in psi from the cohesive soil curve or use the equation:

$$G_{real} = \frac{3}{8} \frac{K_{app}}{r_0^3} \frac{f_n^2}{f_{app}^2} - 1$$

For cohesionless soils, the slippage factor  $SF$ , is given by:

$$SF = 1 - \frac{0.5 \theta G_F}{p \tan \phi}$$

where  $\theta$  = the peak to peak rotational amplitude for the particular test as obtained previously in DATA REDUCTION. (Radians)

$P$  = the bearing pressure exerted by the footing on the soil (psi) (w/o ballast weights  $P=2.64$  psi w/ballast weights  $P=4.43$  psi)

$\phi$  = the angle of internal friction of the soil

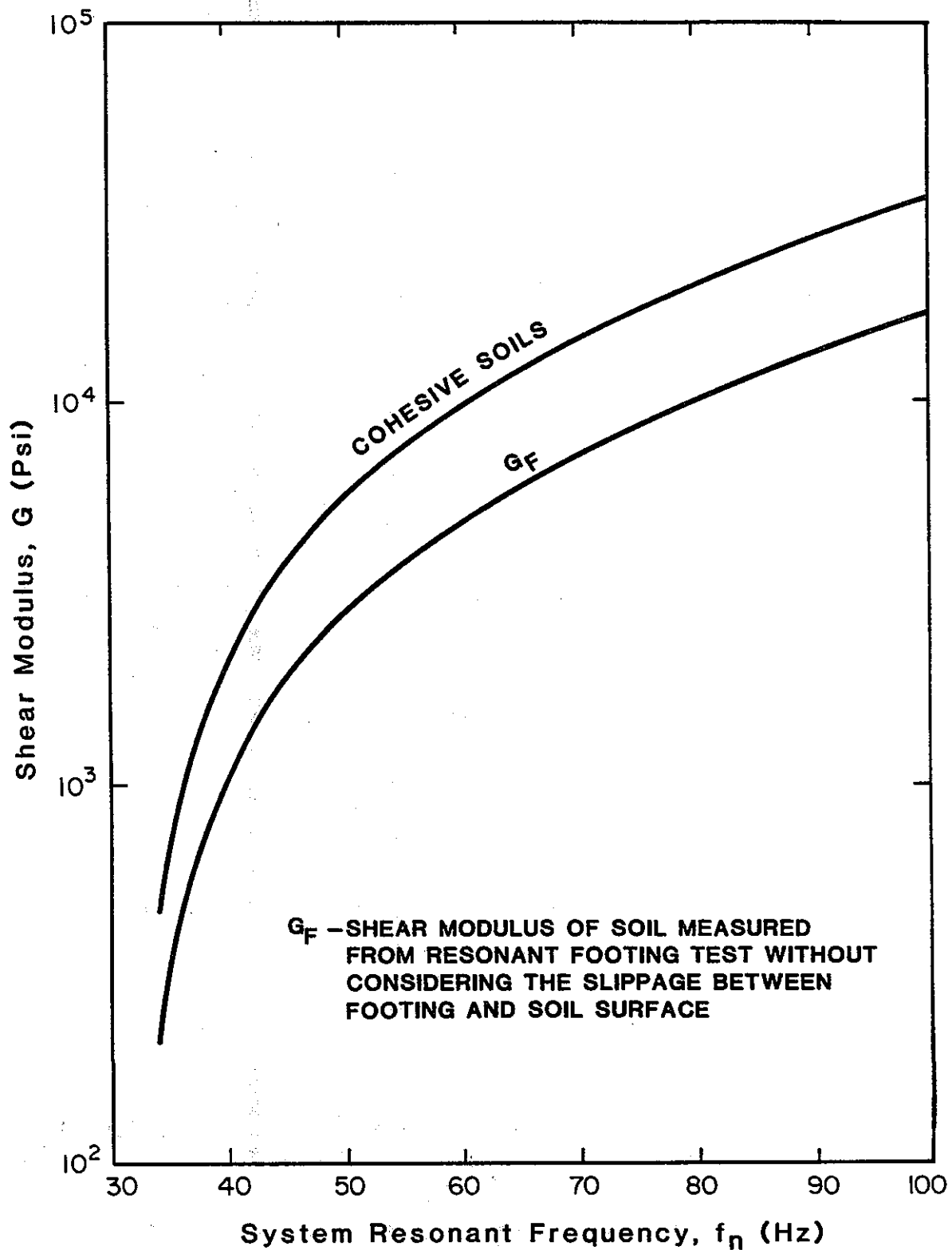


FIGURE E.12

The term  $\frac{0.5 \theta}{p \tan \phi}$  is defined herein as the Rotational Slippage Factor, RSF.

The shear modulus,  $G_{real}$ , may be obtained for cohesive soils as follows:

1. Determine the Rotational Slippage Factor, RSF, from the curves in Figure E.13 or use the equation:

$$RSF = \frac{0.5 \theta}{p \tan \phi}$$

2. With the system resonant frequency,  $f_n$ , enter Figure E.12 and read  $G_F$  from the curve labeled  $G_F$  or use the equation:

$$G_F = \frac{3}{16} \frac{K_{app}}{r_o^3} \frac{f_n^2}{f_{app}} - 1$$

3. Calculate  $G_{real}$  from the equation:

$$G_{real} = G_F / (1 - RSF G_F)$$

Note that in any case, the lower limit for shear modulus is  $G_F$ .

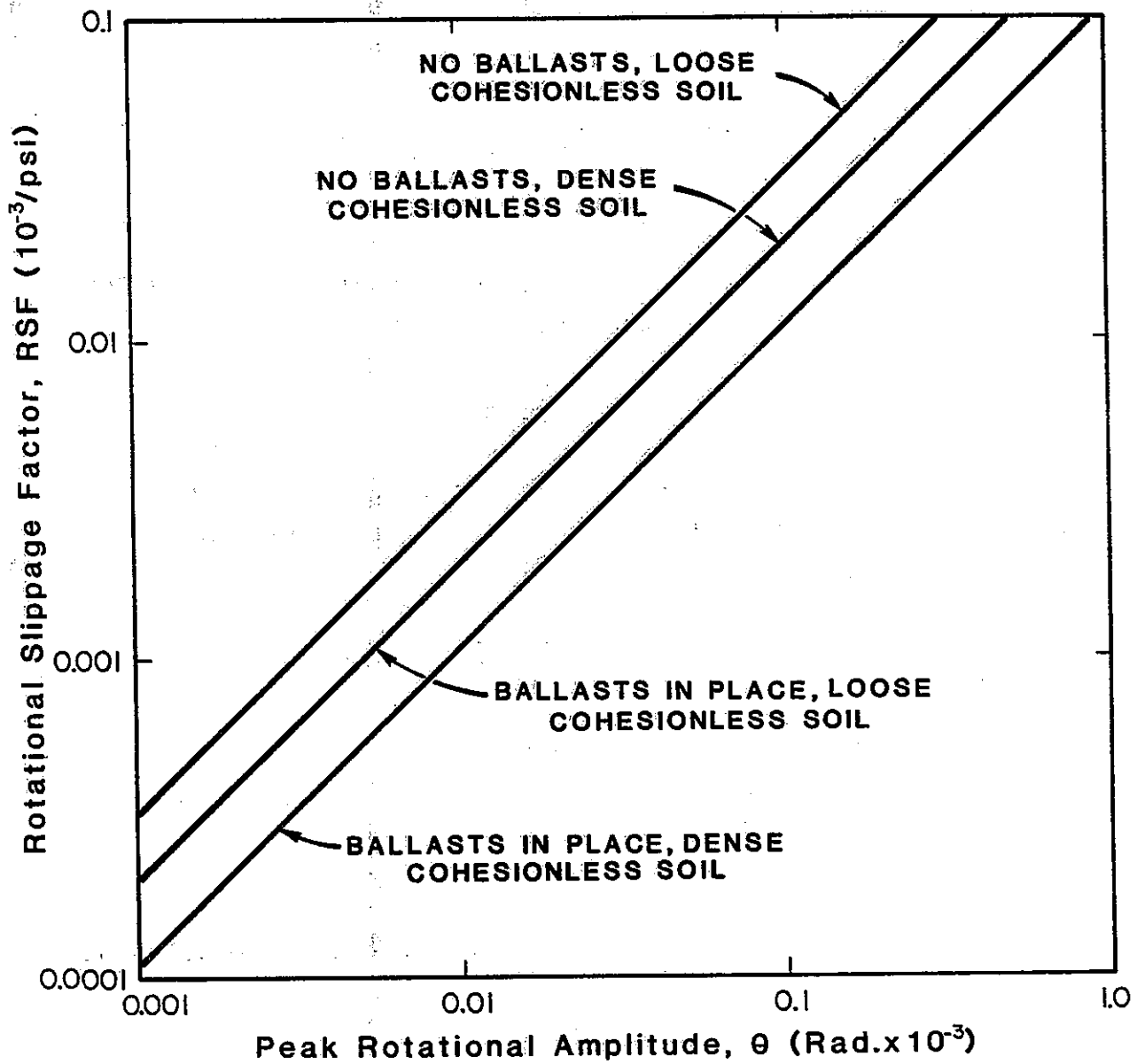


**FIGURE E. 13**

APPENDIX F

California Resonant Column Apparatus  
and Testing Procedures

PROCEDURES FOR TESTING SHEAR MODULUS AND DAMPING  
CONSTANTS OF SOIL BY RESONANT COLUMN APPARATUS

I. Major Components of the Test System

- A. Hardin Oscillator
- B. Audio Oscillator, Hewlett Packard 200 AB
- C. Oscilloscope, Tektronix 5103N
- D. Switch Box
- E. A.C. Voltmeter, Hewlett Packard 400E
- F. Bridge Amplifier, Statham SC1103
- G. Digital Multimeter, Systron Donner 7050
- H. Frequency Measuring Counter, Hewlett Packard 5300/5304A

II. General Description of Each Instrument

- A. Hardin Oscillator - The Hardin Oscillator is a device for applying a forcing torque to the vibration end of the soil specimen about its axis. It consists of a center mass which connects to an outer ring by four leaf springs. A force is produced between the center mass and outer ring by the coils and permanent magnets that rotate to produce a torque about the axis of the specimen.

A Columbia Research Labs accelerometer is attached to and becomes a part of the specimen top cap of the Hardin Oscillator which will produce a calibrated electrical output that is a measure of the angular acceleration of the vibration end of the specimen. The output of the accelerometer is amplified by the charge amplifiers and converted to voltage reading with the Hewlett Packard A.C. Voltmeter. A summary of the calibration data for the accelerometer is listed below:

Acceleration Range:	0.01 to 10kg
Voltage Sensitivity:	59.3 pk mv/pk-g
Charge Sensitivity:	22.2 pk pcmb/pk-g
Resonant Frequency:	30 KC
Frequency Range:	1 cps to 5kc

- B. Audio Oscillator, Hewlett Packard 200 AB - This instrument is capable of producing a sinusoidal voltage with means of varying the voltage amplitude and its frequency. This instrument is used to drive the forcing coils of the Hardin Oscillator.
- C. Oscilloscope - The oscilloscope is an instrument used for voltage measurement and analysis of wave forms. The oscilloscope is used as a means to determine the resonant frequency of the B.O. Hardin Oscillating System. The voltage drop across a precision resistor in series with the driving coils and is connected to the horizontal input displayed on the X-axis. This voltage is in phase with and has the same frequency as the forcing torque applied to the system. The output of the accelerometer is connected to vertical input and displayed on the Y-axis.

The figure traced on the screen is a measure of the phase between the two voltages. The frequency of the audio oscillator should be adjusted until a vertical axis ellipse or circle is displayed on the oscilloscope. The vertical and horizontal settings on the oscilloscope may have to be adjusted to achieve the ellipse.

- D. A.C. Voltmeter, Hewlett Packard 400E - The A.C. Voltmeter is used to read the voltage drop across precision resistor and the output of the charge amplifier. Selection of the voltage to be read by the meter is made by the toggle switch on the switch box.
- E. Bridge Amplifier - The Bridge Amplifier is a signal conditioning unit for the load cell that supports the mass of the Hardin Oscillator. This unit provides the circuit to "null out or zero" any output voltage of a transducer due to unbalanced resistance of the bridge circuit. It also has a sensitivity adjustment to allow the output voltage to correspond to definite load applied to the transducer. The Bridge Amplifier unit is used here to show the amount of vertical force exerted on the soil sample test.

- F. Frequency Measuring System - The Hewlett-Packard model 5304A/Time Counter, when plugged onto an HP model 5300A Measuring System, is capable of: measuring frequencies up to 10 MHz, Time Interval Measurements from 500 NSEC to 10,000 seconds period average over a range of 10 Hz to 1 MHz, and totalizing.

This unit provides an accurate reading of the generating frequencies from the audio oscillator applied to the torque generating coils of the Hardin Oscillator Resonant Column.

III. Cable Connection (See Interconnection Diagram Figure F.1)

1. Connect cable No. 1 between the output terminals of the Hewlett Packard 200 AB audio oscillator and the power terminal of the Hardin Oscillator.
2. Connect cable No. 2 between the torque voltage terminals of the Hardin Oscillator and the horizontal input of the Tektronix Oscilloscope.
3. Connect cable No. 3 between the accelerometer of the Hardin Oscillator and the input terminals of the Columbia Research Labs Charge Amplifier.
4. Connect cable No. 4 between the output terminals of the Columbia Research Labs Charge Amplifier and the vertical input of the Tektronix Oscilloscope.
5. Connect cable No. 5 between the output terminal of the Columbia Research Labs Charge Amplifier and the side of the switch box marked "accelerometer".
6. Connect cable No. 6 between the load cell terminal on the steel plate of the Hardin Oscillator and the connector H1 in the top plate of the Hardin Cell.
7. Connect cable No. 7 between connector H2 on the wire from the top of the Hardin Cell and Statham Bridge Amplifier (connection at Bridge Amplifier has been made permanent).

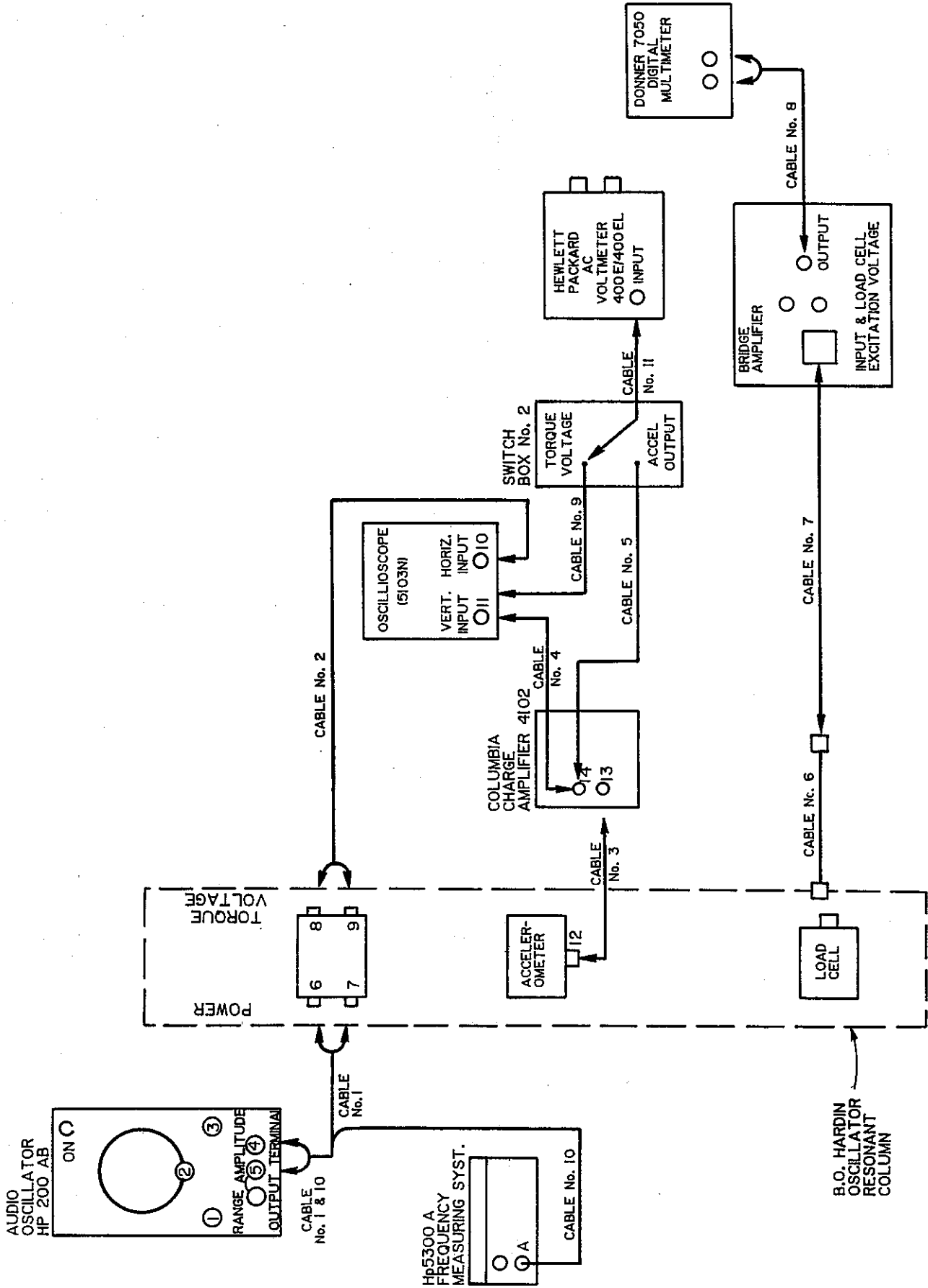
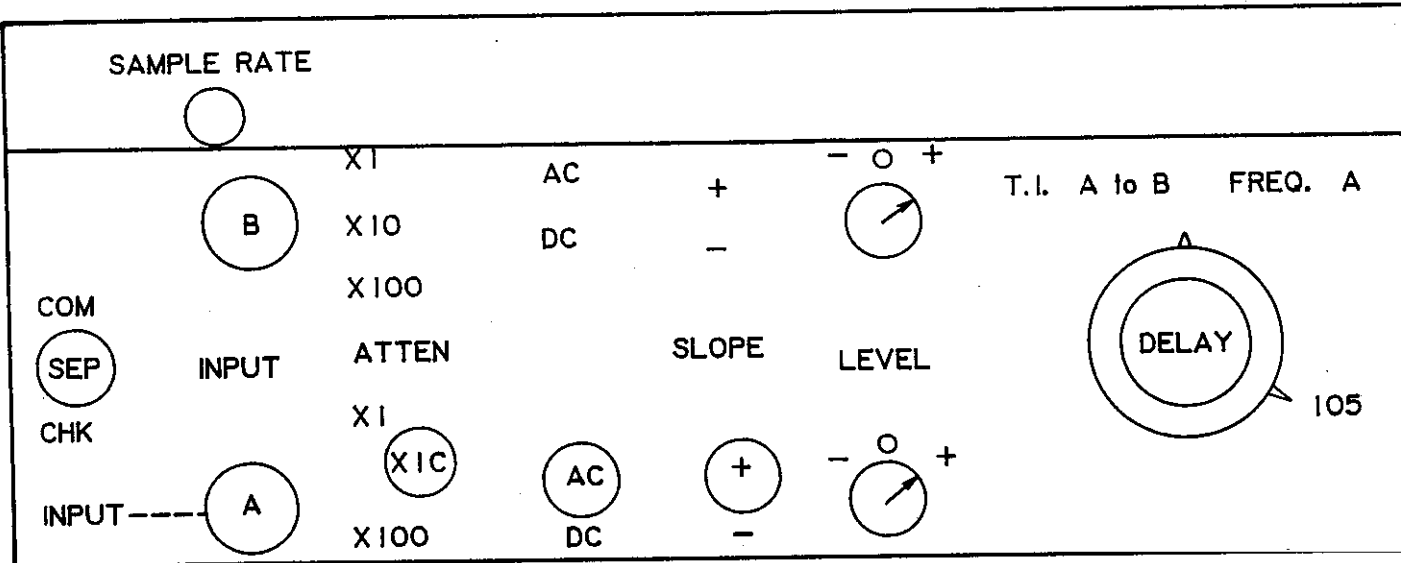


Fig. F.1. INTERCONNECTION DIAGRAM FOR THE B.O. HARDIN OSCILLATOR RESONANT COLUMN TESTING SYSTEM

8. Connect cable No. 8 between the Bridge Amplifier output terminals and the Systron Donner 7050 Digital Multimeter.
9. Connect cable No. 9 from the side of the switch box marked torque voltage mode to the same horizontal input terminal of the oscilloscope to which cable No. 2 is connected.
10. Connect cable No. 10 between the "A" input terminal of the Hewlett-Packard 5300A frequency measuring system and the output terminal of the Hewlett-Packard 200 AB Audio Oscillator.
11. Connect cable No. 11 from the switch box to the input terminal of the Hewlett-Packard A.C. Voltmeter.

#### IV. Instrument Range Settings

- A. Audio Oscillator
  1. Set frequency to 160 Hz.
  2. Set voltage amplitude to near zero.
- B. Tektronix 5103N Oscilloscope
  1. The 5B13N Time Base, depress the following buttons:
    - a. Auto trig
    - b. EXT
    - c. 100 mV
  2. The 5A23N Vertical Amplifier  
Depress the 100 mV button
- C. Switch Box  
Set toggle switch of box to torque voltage position
- D. A.C. Voltmeter, Hp 400E  
Set range selector switch to 0.03 position.
- E. D.C. Digital Multimeter, Systron Donner 7050  
Set D.C. range switch to 1.5 volt position.
- F. Charge Amplifier
  1. Set "Transducer Sensitivity Dial" to accelerometer charge sensitivity of 22.2 pk-pcmb/pk-g.
  2. Depress left button.
- G. Frequency counter, Hp 5300A  
Set switches on the front panel of the frequency counter as shown: Set "ATTEN" to "X1".



## V. Power Setting

- A. Plug the "Master power plug" to 115 V. AC sources from the wall outlets.
- B. Turn all instruments of the test system "on".
- C. Warm-up Time  
Allow approximately 15 minutes warm-up time for all the instruments except the Bridge Amplifier which takes longer period for it to stabilize, therefore, it is essential for the operator to have the bridge amplifier energized maybe one or two hours ahead of the test.

## VI. Axial Load Calibration and Measurement

### A. Calibration

1. Suspend the Hardin Oscillator from the axial loading piston (top cap must be in place but it must not touch anything). Adjust the "balance knob" of the Bridge Amplifier until the D.C. Voltmeter display "0.000".
2. Insert 14.88K calibration resistor into the red and black terminals of the Statham Bridge Amplifier.
3. Adjust the sensitivity of the Statham Bridge Amplifier until + 1.000 volt display on the Digital Voltmeter.

4. Remove the "14.88K Calibration Resistor" from the Bridge Amplifier and check the D.C. Voltmeter for "0.000" display. If display of the D.C. Voltmeter is other than "0.000", repeat steps 1 to 3 until the values are obtained. The calibration factor is then 100 lb/volt.

## VII. Oscilloscope Operational Procedure

### A. General Setup and Precaution

1. Pull power button out.
2. Adjust intensity to mid-range.
3. Use focus knob to clear trace as necessary.

### B. The 5A23N Vertical Amplifier

1. Depress display and GND buttons if they are not already depressed.
2. Position the electronic beam to the center position of the oscilloscope screen by turning the vertical position switch (Adjust "Intensity" control to prevent screen damage caused by electron beam).
3. Release the GND button.
4. Depress the A.C. button.
5. Depress the 100 mV button for the signal from the charge amplifier to be displayed.

### C. The 5B13N Time Base

1. Depress the 50 mV EXT button of the SEC/DIV or VOLTS/DIV switch.
2. Depress the AUTO TRIG button.
3. Depress the EXT button.

## VIII. Specimen Preparation Procedures

Specimen preparation procedures are identical to those used for conventional triaxial specimen preparation. Specimen weight in grams, specimen diameter and specimen length, both in centimeters must be determined. For soils that aren't too soft, filter paper strips may be used to decrease consolidation times.

## XI. Placement of the Specimens in the Apparatus

For tests where volume changes of the specimen are to be made by observing burette volume changes or where the specimen is to be saturated by use of back pressures, it is

important that the pore water lines and porous stone in the base pedestal be saturated with deaired water in the conventional manner. After doing this, close the pore valve at the base of the specimen. The sides of the base pedestal and top cap should have a light coating of vacuum grease.

Place a trimmed, weighed and measured specimen on the base pedestal. Place the top cap on the specimen. Place the membrane over the specimen and end caps with a membrane expander. Use the membrane expander to put two O-rings over the membrane at the base pedestal.

It is sometimes convenient to remove the air entrapped between the membrane and the sample by inserting a very small diameter tube into the space between the top cap and the membrane. The other end of the tube is connected to a vacuum source. Vacuum grease can be used to form a seal between the tube, top cap, and membrane. It takes just a few seconds to have the vacuum pull the membrane to the specimen. The small diameter tube is then gently withdrawn. Complete the sealing process by using the membrane expander to place two O-rings over the membrane at the top cap.

#### X. Assembly of the Apparatus for the Test

Place and level the lower half of the pneumatic cylinder support device on the triaxial chamber base, surrounding the specimen and connect the pneumatic cylinders to the outlet in the base. Apply an air pressure of at least 50 psi to the pneumatic cylinders causing the pistons to extend approximately 1/2 inch.

Place the upper part of the pneumatic support device on the lower half and adjust the three cylindrical nuts until the top of the platform is level and at an elevation 1 cm (3/8") above the top of the top cap.

Place the Hardin Oscillator on the support platform and align the clamping collar with the top cap. Gently lower the Hardin Oscillator onto the top cap by adjusting the three cylindrical nuts. Tighten the two cap screws on the Hardin Oscillator specimen cap clamp equally, thus attaching the vibration excitation device rigidly to the specimen cap, with its weight being supported by the pneumatic cylinders.

Place the cast acrylic cylinder of the triaxial chamber over the Hardin Oscillator. Make sure that it is centered with respect to the base and that the O-ring is in the groove.

Hold the triaxial chamber lid above the triaxial cell and connect the accelerometer, load cell and power cables. (The power cable can be distinguished from the load cell cable by the fact that it has only two pins in the connector.)

Check to see that the O-ring is in place in the triaxial chamber lid and with the air inlet facing forward gently lower it onto the chamber. Be careful to arrange the wires connecting the Hardin Oscillator to the chamber lid so that they do not obstruct the lid from seating or cause stress on the Hardin Oscillator. Complete the seal by firmly tightening the three knurled nuts atop the chamber lid.

Clean and lubricate the piston and insert it into the top of the chamber. Screw it into the load cell located in the top of the Hardin Oscillator. Put the length measuring dial gage into place and adjust it to read 0.100 inch.

Fasten the counterbalance system to the piston and apply about 17 lbs. of weight (including hanger weight) to counterbalance the weight of the oscillator. The entire chamber may have to be moved to align it with the counterbalance system. The output of the Systron Donner Multi-meter should read near "0.000" when the proper amount of weight is added.

Remove the pressure to the Hardin Oscillator support system. The system should retract and the load cell reading (Systron Donner Multimeter) should read zero. If it does not, add counterbalance weights to reduce the reading or vice versa.

If a liquid confining media is desired, introduce it into the chamber through the valve port on the chamber base that is located closest to the cast acrylic tube. ONLY FILL THE LIQUID TO COVER THE O-RINGS ON THE SPECIMEN TOP CAP. LIQUIDS CONTACTING THE HARDIN OSCILLATOR COULD DAMAGE IT. Close the valved port after filling.

Connect the regulated air supply to the top of the chamber by use of the quick disconnect fitting. Complete the assembly by connecting any of the electrical cables to the chamber top that might have been disconnected.

## XI. Consolidation of Test Specimens

The procedure for back pressuring and consolidating test specimens is identical to the procedure used in conventional triaxial testing except that slight adjustment must be made to the counterbalance weights to account for pressure in the chamber acting on the loading pistons. For isotropic stresses, adjust the weights to maintain the load cell reading (Systron Donner Multimeter) at 0.00  $\pm$ 0.005 volt.

For anisotropic stresses, the load cell reading should be maintained at the value calculated from the following equation:

$$\text{Load Cell Reg. (volts)} = \frac{\text{Force (lb)}}{\text{LCF (lb/volt)}}$$

Where:

LCF = Load Calibration Factor  
= 100 lb/volt

Force =  $\sigma_3 \pi D^2/4$  (PSR-1)

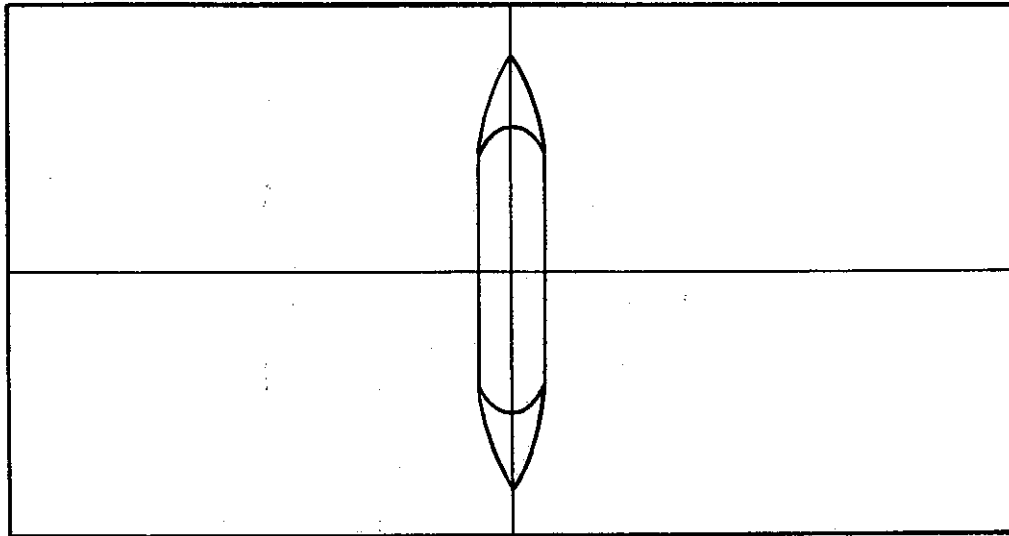
$\sigma_3$  = cell pressure (psi)

D = specimen dia. (in)

PSR = principal stress ratio,  $\frac{\sigma_1}{\sigma_3}$

## XII. Measurements of Low Amplitude Shear Modulus, Gmax, and Low Amplitude Damping

- A. Set the switch to Torque Voltage
- B. Set the Hewlett-Packard 400E to the .03 scale (30 mVRMS full scale)
- C. Adjust the amplitude control on the Hewlett-Packard 200 AB to get a Torque Voltage reading between 20 mVRMS and 30 mVRMS.
- D. Adjust the frequency control on the Hewlett-Packard 200 AB to establish resonance. Resonance occurs when the ellipse on the oscilloscope has its major and minor axes vertical and horizontal (X and Y gains on the oscilloscope may have to be adjusted to obtain an ellipse that fills the screen vertically and looks as follows:



- E. With resonance established, read and record the following items:

Elapsed time in minutes  
Cell pressure in psi  
Back pressure or pore pressure in psi  
Axial load reading in volts  
Length reading in inches  
Burette reading in cubic centimeters and torque reading in mVRMS

- F. Switch the toggle switch on the switch box to "Accelerometer Voltage", check oscilloscope to see that resonance is being maintained (adjust frequency on HP 200 AB if necessary) and read and record accelerometer voltage from HP 400 E. (Left button on CRL Charge Amplifier should remain depressed for all of these readings.)

- G. Read and record the resonant frequency from the HP 5300 A Frequency Monitoring Center.

### XIII. Check on Vibratory System Calibrations

It is good practice to make this check before and after a series of resonance measurements are made at each confining pressure.

- A. Determine the resonant frequency for low amplitude vibration using the method just previously outlined.
- B. Multiply the value of resonant frequency by 1.414 and set the resulting value on the frequency dial of the HP 200 AB.
- C. Set the switch on the switch box to "Torque Voltage" and set the HP 400 E to the 0.10 scale.
- D. Adjust the "Amplitude" control on the HP 200 AB until the needle on the HP 400 E points to 1 (Full Scale).
- E. Position the switch on the switch box to "Accelerometer Voltage". The needle on the HP 400 E should move from one to 0.6 (60 mVRMS) plus or minus 0.05 unit (+ 5 mVRMS). If it does not, the system is out of calibration and needs to be checked. Be sure to note the value of Accelerometer Voltage reading at  $\sqrt{2}$  X resonant frequency in the "Remarks" area at the bottom of the data sheet.

#### XIV. Measurement of Shear Modulus and Shear Damping as a Function of Shear Strain Amplitude

The procedure is quite similar to that for measurement at low strain amplitude that was outlined earlier except that the Torque Voltage Readings are increased over the previous value. Resonance should be established and a set of readings (time, cell press, back press, etc.) should be taken at the following Torque Voltage settings; 25, 50, 100, 200, 400, 800, and 1500 mVRMS. If more data points are desired, the torque voltage settings can be made at closer spaced values. For the larger values, the associated Accelerometer Voltage readings may exceed 3000 mVRMS, in which case the center button on the CRL Charge Amplifier must be depressed and the readings of Acceleration Voltage from the HP 400 E must then be multiplied by a factor of 10.

After making the above readings, it is good practice to make several low amplitude readings to evaluate the effect of high amplitude straining on specimen modulus and damping (see Section XII).

## XV. Measurement of Damping by the Amplitude Decay Method

This method is not ordinarily used because it is somewhat more cumbersome than the magnification factor method. It may be used occasionally to check the system operation and the damping calculations.

The system must be vibrating at the resonant frequency. Output from the CRL Charge Amplifier is connected to an oscilloscope having a single sweep control and a method of trace recording (Storage and/or camera). Triggering is adjusted to have continuous sweeping and the Y-gain is adjusted so that the wave form fills at least half of the screen. (The value of the gain setting is unimportant.) The sweep rate should be set so that at least 20 cycles appear on the screen. Reset the trigger for single sweep and prepare to record the single sweep (on Tektronix 564, set both storage switches to "ERASE" then to "STORE"). Simultaneously, start the sweep and cut the power to the drive coils by pulling the double banana plug on cable #1 from the front of the HP 200 AB Audio Oscillator. Check the recorded trace to see that the power cut off occurred during the sweep and at least 10 cycles of decaying vibration were recorded. Label the photograph\* with the date, test name and the elapsed time and put it with the data records for the test.

\*If a Polaroid camera with film having an ASA rating of 3000 is used, the camera settings should be f-stop = 5.6, shutter speed - 1/10 second.

## XVI. Switch "OFF" the Following Apparatus Components if no Additional Tests are to be Performed

- A. Audio Oscillator
- B. Oscilloscope
- C. A.C. Voltmeter
- D. Charge Amplifier
- E. D.C. Voltmeter
- F. Bridge Amplifier
- G. Frequency Measuring Counter HP 5300
- H. Remove the "master power plug" from wall socket.

